THE UNIVERSITY OF MICHIGAN

8077-4-T

MEASURED BACK SCATTERING CROSS SECTION OF THIN WIRES

Technical Report

May 1967

Prepared by

Seichoong Chang and Valdis V. Liepa*

Contract No. AF 33(615)-5170
Project 5546, Task 554601

Air Force Avionics Laboratory, AVWE
Research and Technology Division, AFSC
Wright-Patterson Air Force Base, Ohio

*Presently a Postdoctoral Research Associate at the Institute for Telecommunication Sciences and Aeronomy, Environmental Science Services Administration, Boulder, Colorado.

onSn

UMR1165

ABSTRACT

A set of measured back scattering patterns is presented for a thin wire ($a/\lambda = 6.27 \times 10^{-3}$) for $\ell/\lambda \simeq 0.3\ (0.025)\ 0.55 (0.05) 1.60 (0.10) 5.42$, where a is the radius of the wire, ℓ is the length, and λ is the wavelength. The measurements were performed in an anechoic chamber at 2.370 GHz. From this set of patterns a number of curves has been extracted showing the amplitude and position of each back scattering lobe as a function of the wire length. These curves provide a convenient means of cross section estimation and may be used to reconstruct with reasonable accuracy the back scattering pattern for any value of ℓ/λ, $\ell/\lambda \leq 5.42$.

TABLE OF CONTENTS

I

INTRODUCTION

In studies of electromagnetic scattering, a circular cylinder has probably received more attention than any other geometric shape. As early as 1877 Lord Rayleigh (Strutt, 1945) carried out the analysis explicitly for the case of a plane sound wave incident upon a thin column of gas of given compressibility and density. Hallén (1938) was the first to obtain an approximate solution for a thin cylindrical antenna by deriving an integral equation for the unknown current distribution and then solving it approximately by an iteration technique. This paved the way in a new field of research, and since then many authors have introduced modification for the integral equation, or used techniques such as Wiener-Hopf (Williams, 1956) or variational methods (Tai, 1951) to arrive at the solution. King (1956) has treated extensively the subject in a book Linear Antennas, and recently Einarsson, et al (1965) have published a survey report on electromagnetic and acoustic scattering by circular cylinders.

In studies dealing with scattering from composite geometric shapes it is often helpful to compare the back scattering patterns with those of a thin wire, especially in the resonance region. A search through the literature produced only isolated cases of back scattering data from thin wires, and a set was therefore obtained by measuring the return from a thin wire ($a/\lambda = 6.27 \times 10^{-3}$) for $\ell/\lambda \simeq 0.3(0.025)0.55(0.05)1.6(0.1)5.42$ at 2.370 GHz. These patterns constitute the body of this report. Also included is a set of curves showing the amplitudes and angular position of various back scattering lobes as a function of the length of the wire.

II

EXPERIMENTAL PROCEDURES

The data presented here were taken at the Radiation Laboratory Willow Run Facility of The University of Michigan. A conventional C.W. back scattering system whose block diagram is shown in Fig. 2-1 was used. The frequency was 2.370 GHz, the polarization horizonal, and the distance from the transmit-receive antenna to the model was about 30 feet. To assist in choosing a model, the back scattering patterns of aluminum and silver-plated stainless steel rods of 1/16 inch diameter were compared for $\ell/\lambda \simeq 0.477$ and 3.815. There were no distinguishable differences between two sets of patterns, implying that for the rod of this radius at the frequency used the lesser conductivity of aluminum has a negligible effect on the back scattering behavior. Therefore, for convenience, an aluminum rod of 1/32 inch radius was used for a model.

In all, 81 back scattering patterns were measured, starting with a 27 inch ($\ell \simeq 5.422\lambda$) long rod and then, after each measurement, shortening the rod by 1/2 inch ($\simeq 0.100\lambda$). The increment was changed to 1/4 inch at $\ell = 8.0$ inches ($\simeq 1.606\lambda$) and then to 1/8 inch at $\ell = 2.75$ inches ($\simeq 0.552\lambda$) down to the shortest length measured, 1.5 inches ($\simeq 0.3\lambda$). For calibration a 3.935 inch diameter sphere was used, and for each pattern both the wire at normal incidence and the sphere were rocked to compensate for the errors introduced by back-ground reflections (Blacksmith et al, 1965).

From these patterns a broadside return versus length of the rod was then plotted. However, the data points were slightly erratic; some values deviated as much as 1 db from the mean. An additional experiment in the anechoic chamber indicated that this erratic behavior was compositely due to:

(a) interaction of the model with the pedestal,

(b) diffraction of the incident wave by the upper edge of the absorber that was placed in front of the pedestral to shield its metallic turntable from the incident

wave, and

(c) room reflections.

To correct the errors introduced by (a) and (b) the regular pedestal was removed. The model was then supported by nylon strings as shown in Fig. 2-2. With this type of support only broadside returns could be measured and such measurements were performed for the same wire lengths as in the previous run. This time a 1.980 inch diameter sphere, suspended in a fine nylon hair net by a string from the ceiling, was used for calibration. Again, both the sphere and the wire were rocked to compensate for the errors resulting from back-ground reflections.

Using the last set of data as reference for calibration, 0 db λ^2 was determined for each pattern obtained previously by rotating the wire on the pedestal. These patterns are reproduced in this report, and for the most part they are self - explanatory. The broadside incidence is at $\theta = 0^o$ and the end-on incidence at $\theta = \pm 90^o$. For some patterns there may, however, be a slight overall displacement of the pattern, due to inaccurate centering of the pattern on the recording paper.

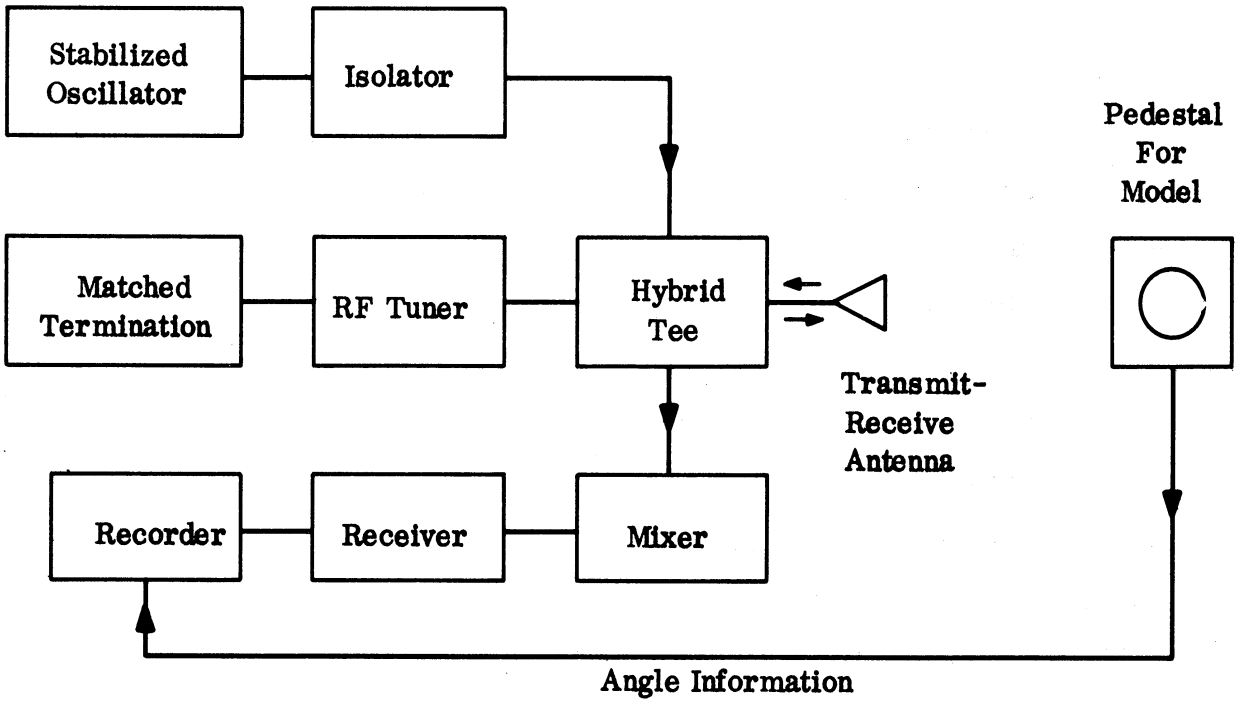

FIG. 2-1: BLOCK DIAGRAM OF CW SYSTEM USED FOR MEASURING BACK SCATTERING.

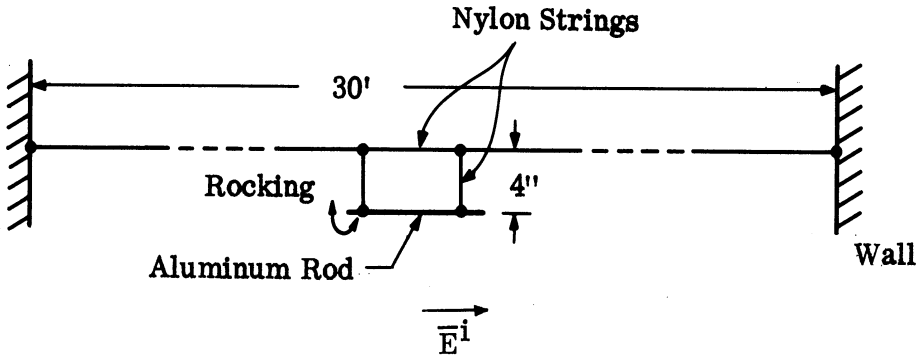

FIG. 2-2: SUPPORTING THE WIRE BY NYLON STRINGS.

III

SUMMARY OF THE RESULTS

Once a set of patterns is available, it is of interest to examine the characteristic behavior of the back scattering lobes as a function of the length of the rod. For an electrically short rod, only a single (broadside) lobe appears. At $\ell/\lambda \simeq 0.8$ a pair of adjacent lobes emerges, and as the length increases further, additional lobes appear. A closer examination of the back scattering patterns reveals that these lobes move in a definite manner. Consider, for example, the pattern for $\ell/\lambda = 5.221$ as well as patterns adjacent to it. We see that as ℓ/λ increases, the large lobes move toward the side of the pattern, and the small lobes that appear between the large lobes actually move toward the center. The motion of the lobes is depicted by arrows for increasing ℓ/λ in Fig. 3-1, where the pattern for $\ell/\lambda = 5.221$ has been reproduced. For reference purposes the lobes are numbered by the sequence of their appearance as ℓ/λ increases, starting with the near end-on lobe. It is observed that as ℓ/λ increases, the nth lobe generally appears first near the side of the pattern with a small amplitude, and as ℓ/λ increases further, it moves toward the center, and after reaching a certain angular position it moves back toward the side. Except possibly when it is near the broadside lobe, the nth lobe always lies between the $(n-1)$th and the $(n+1)$th lobes and its amplitude is always less than that of the $(n-1)$th lobe for the same ℓ/λ.

As we have already seen, the important features of these back scattering patterns are the amplitudes and dispacements of various lobes as a function of wire length. In Fig. 3-2 a familiar curve for broadside back scattering cross section versus ℓ/λ is shown. In part (a) the cross section scale is linear, and in (b) it is in dB. The same applies to other relavant figures. The data points are quite smooth and the values agree reasonably well with those measured by Ås and Schmitt (1957). Unfortunately, a direct comparison of the results cannot be made, since the measurements are not for the same value of a/λ.

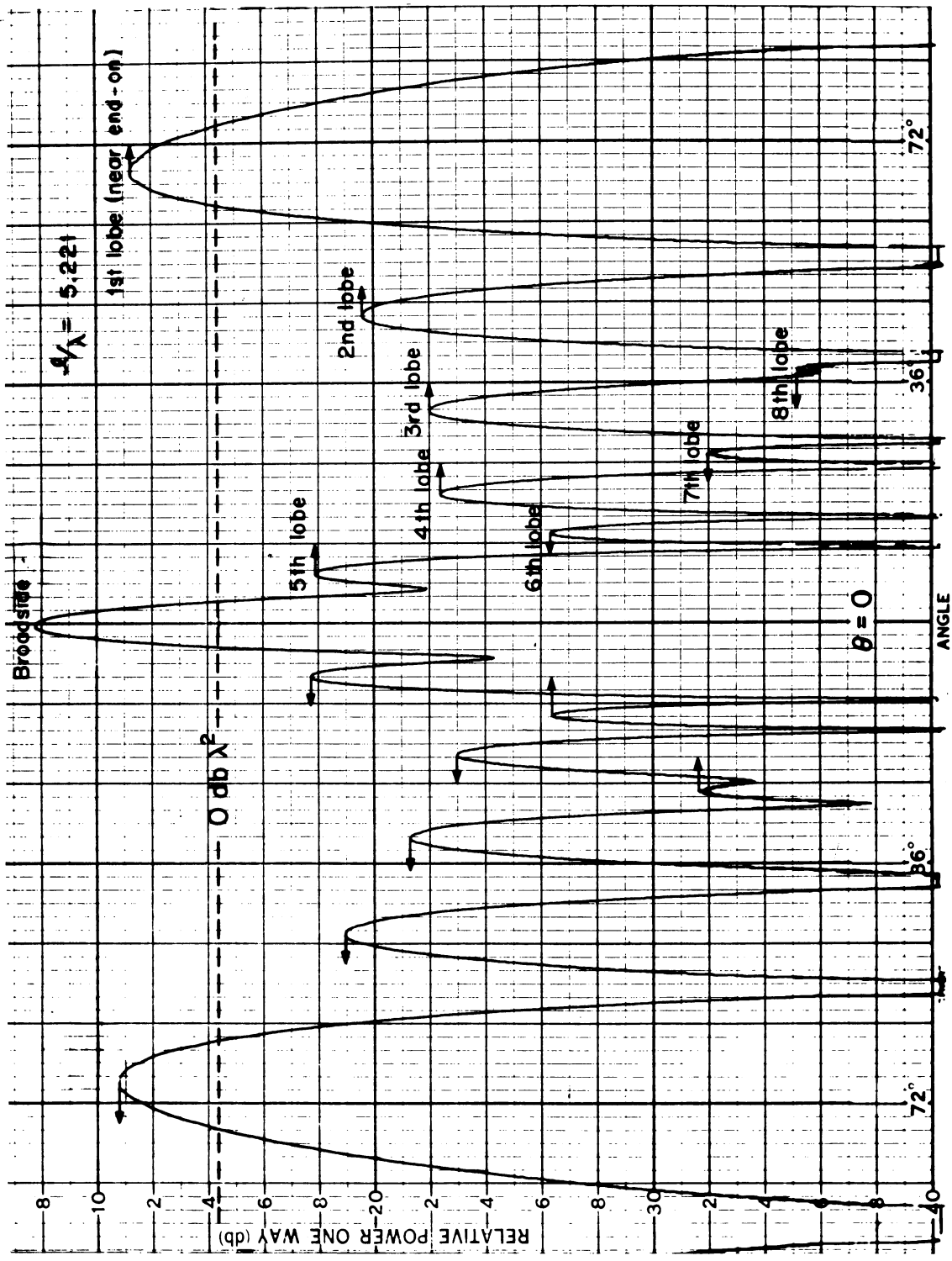

FIG. 3-1: DIRECTION (⟶) OF THE DISPLACEMENT OF VARIOUS LOBES AS ℓ/λ INCREASES; $\ell/\lambda = 5.221$, $a/\lambda = 6.27 \times 10^{-3}$.

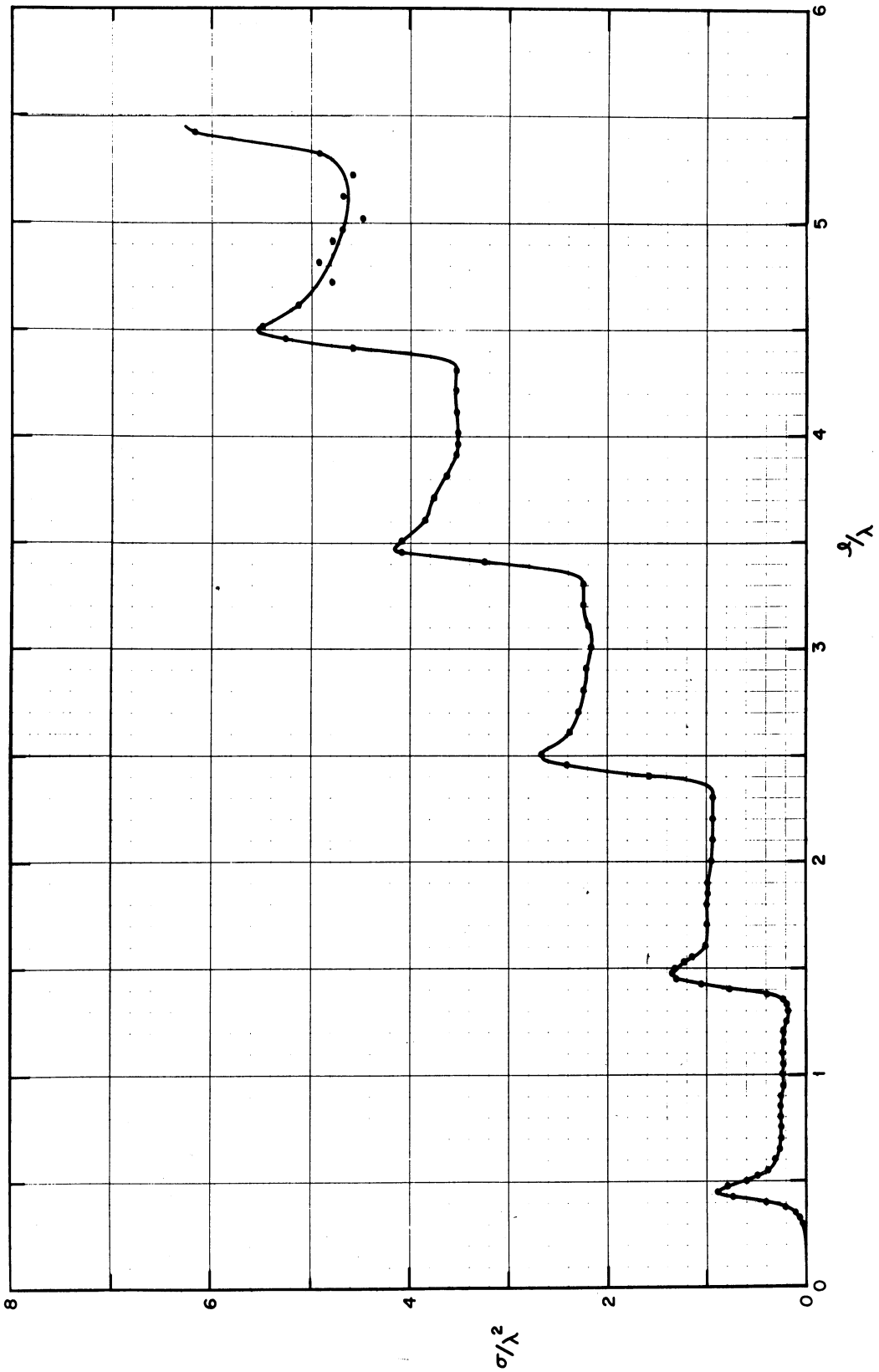

FIG. 3-2a: MEASURED BACK SCATTERING CROSS SECTION OF THE BROADSIDE LOBE; $a/\lambda = 6.27 \times 10^{-3}$ (Linear Scale).

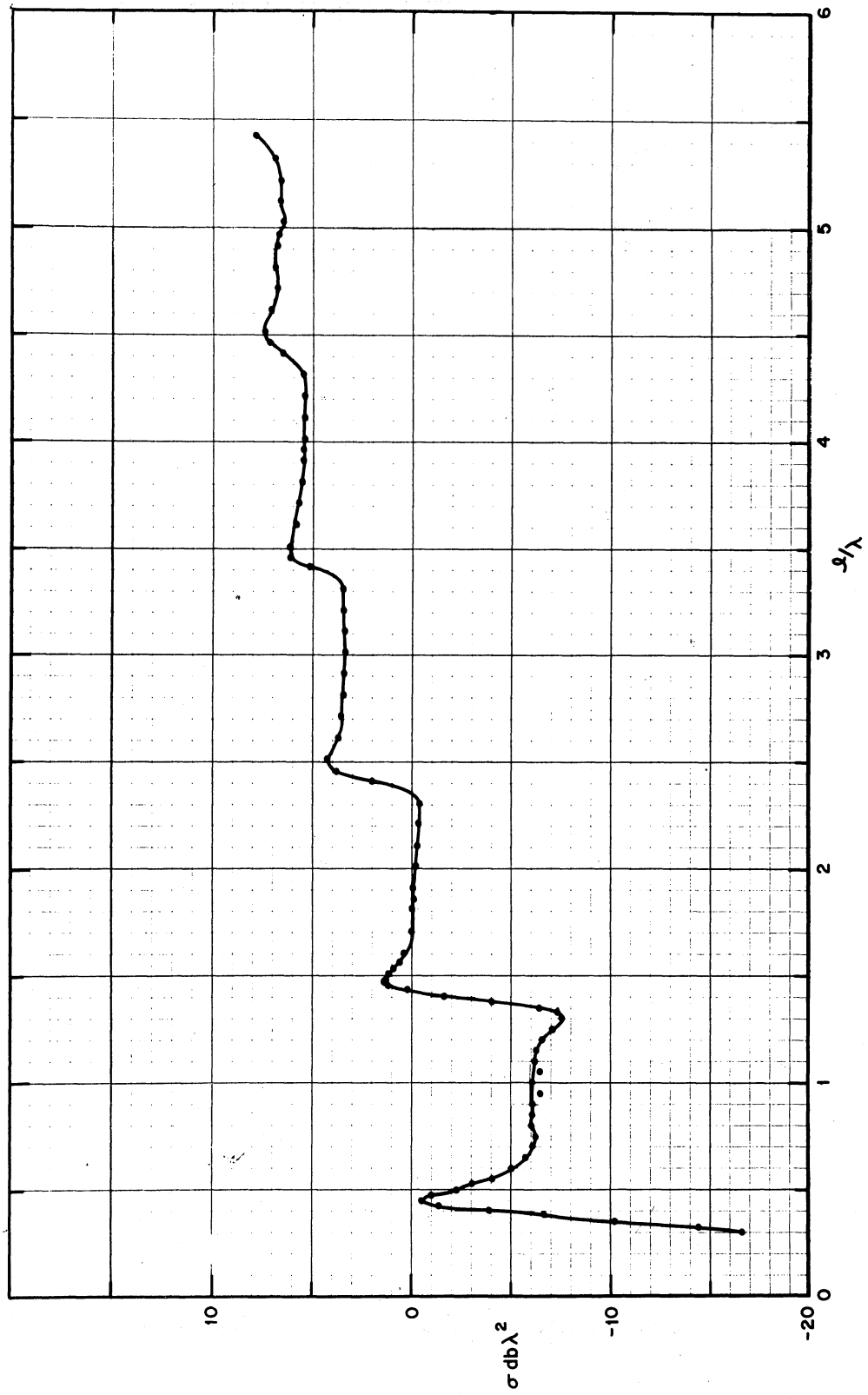

FIG. 3-2b: MEASURED BACK SCATTERING CROSS SECTION OF THE BROADSIDE LOBE; $a/\lambda = 6.27 \times 10^{-3}$ (db Scale).

In the next figure, Fig. 3-3, the back scattering cross section of the first lobe (near end-on) is shown. The lobe does not appear until $\ell/\lambda \simeq 0.8$. Then, as ℓ/λ increases, its amplitude increases in a rapidly oscillating manner with a period of $\ell/\lambda \simeq 0.5$, with peaks having higher values than those of the broadside return for the same ℓ/λ. For determining the side lobe cross section level from the patterns, an average value of the corresponding left-side and right-side lobes has been used.

In Fig. 3-4 the cross sections for the second and third lobes are shown. The oscillations are similar to those for the first lobe shown in Fig. 3-3, but the amplitudes are only about a tenth. On the left side (Fig. 3-4) the curves loose their regular pattern. This is a result of an overlapping of the lobe in the pattern with one of much larger amplitude. Dotted lines are used to give continuous curves wherever the lobe in the pattern disappears or becomes non-detectable due to this overlapping. The cross sections for the remaining lobes, fourth, fifth and sixth are shown in Figs. 3-5 and 3-6. Their amplitudes are again relatively small and give somewhat similar curves as shown in the left-side of Fig. 3-4. It is expected that as ℓ/λ increases further, they would also oscillate similarly as seen in Figs. 3-3 and 3-4.

The angular displacement of the various side lobes as a function of the rod length is shown in Fig. 3-7. The broadside lobe is always at $\theta = 0^{\circ}$ and is not shown. When $\ell/\lambda \simeq 0.8$ the first lobe emerges at $\theta \simeq 24^{\circ}$ and then is gradually displaced toward 90° as ℓ/λ increases. The other lobes first emerge at a higher value of θ, go through a minimum and then are gradually displaced toward the side as ℓ/λ increases. The negative slope of the curves indicates that the corresponding lobe moves toward the center as ℓ/λ increases (cf Fig. 3-1).

In addition, as a convenient means of cross section estimation, Figs. 3-2 through 3-7 may be used to provide an approximate reconstruction of the back scattering pattern for any value of ℓ/λ within the range considered here. For example, consider the case $\ell/\lambda = 3.5$. From Fig. 3-7 we find the peaks located

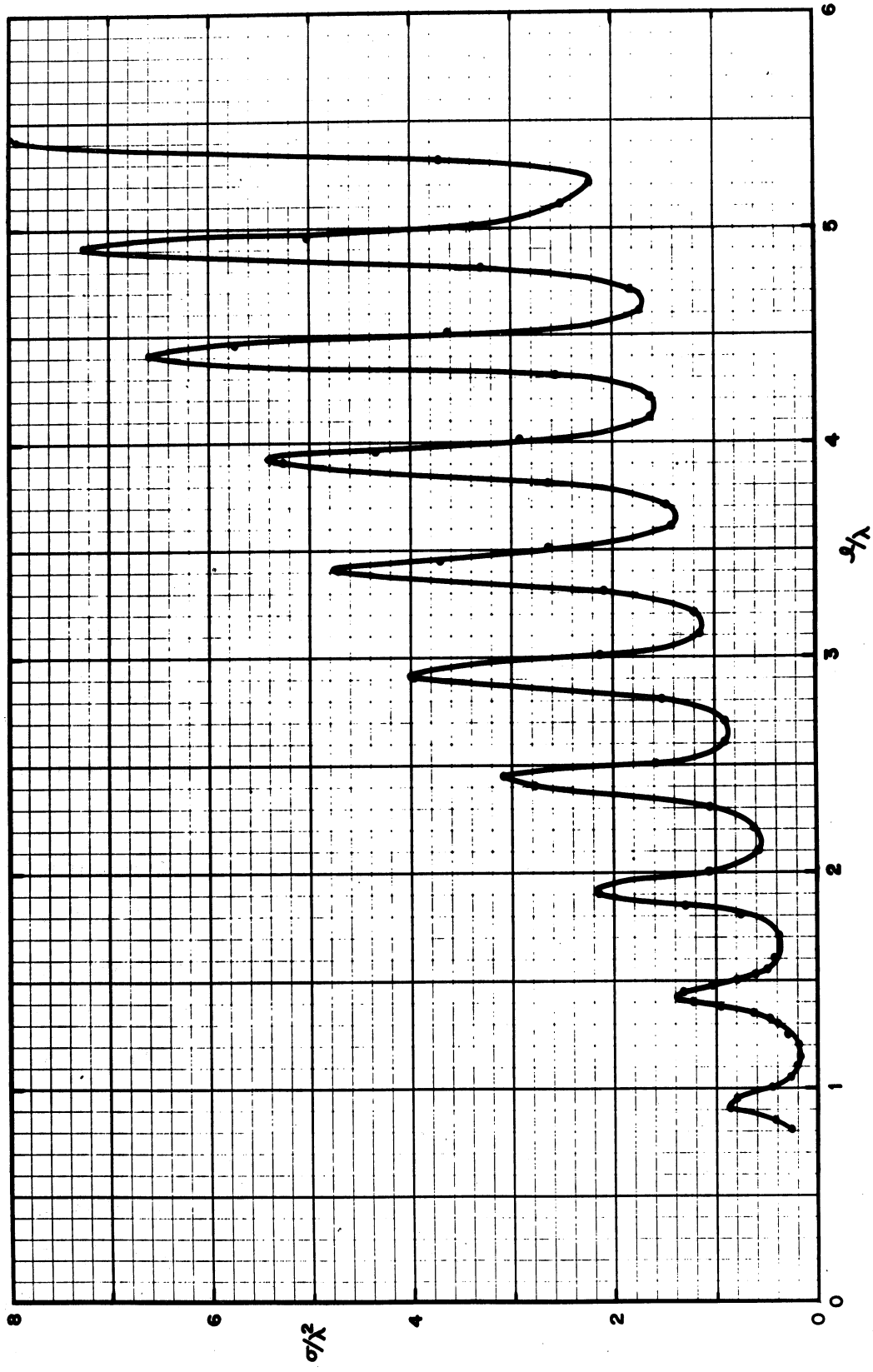

FIG. 3-3a: MEASURED BACK SCATTERING CROSS SECTION OF THE FIRST LOBE (Near End-on); $a/\lambda = 6.27 \times 10^{-3}$ (Linear Scale).

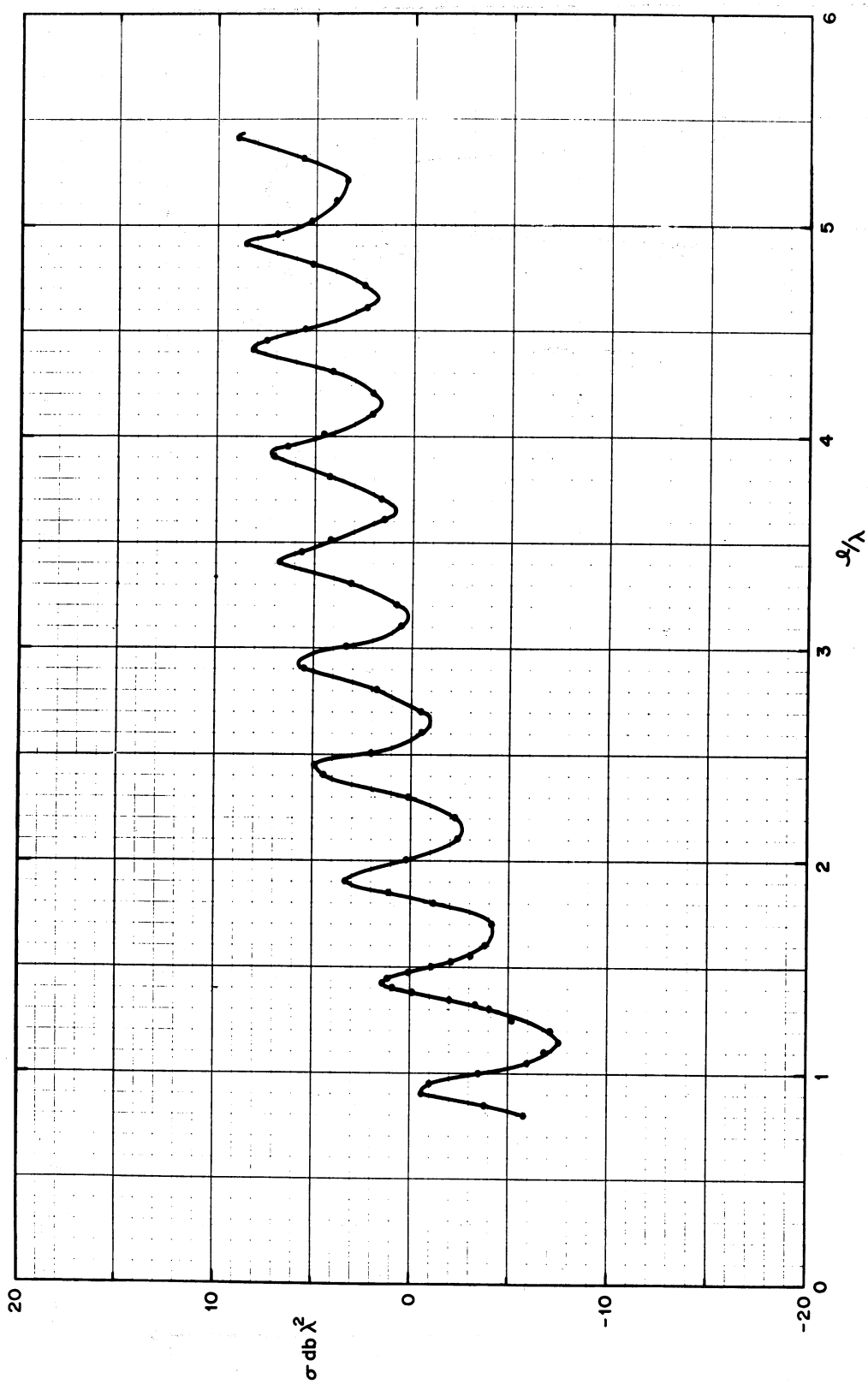

FIG. 3-3b: MEASURED BACK SCATTERING CROSS SECTION OF THE FIRST LOBE (Near End-on); $a/\lambda = 6.27 \times 10^{-3}$ (db Scale).

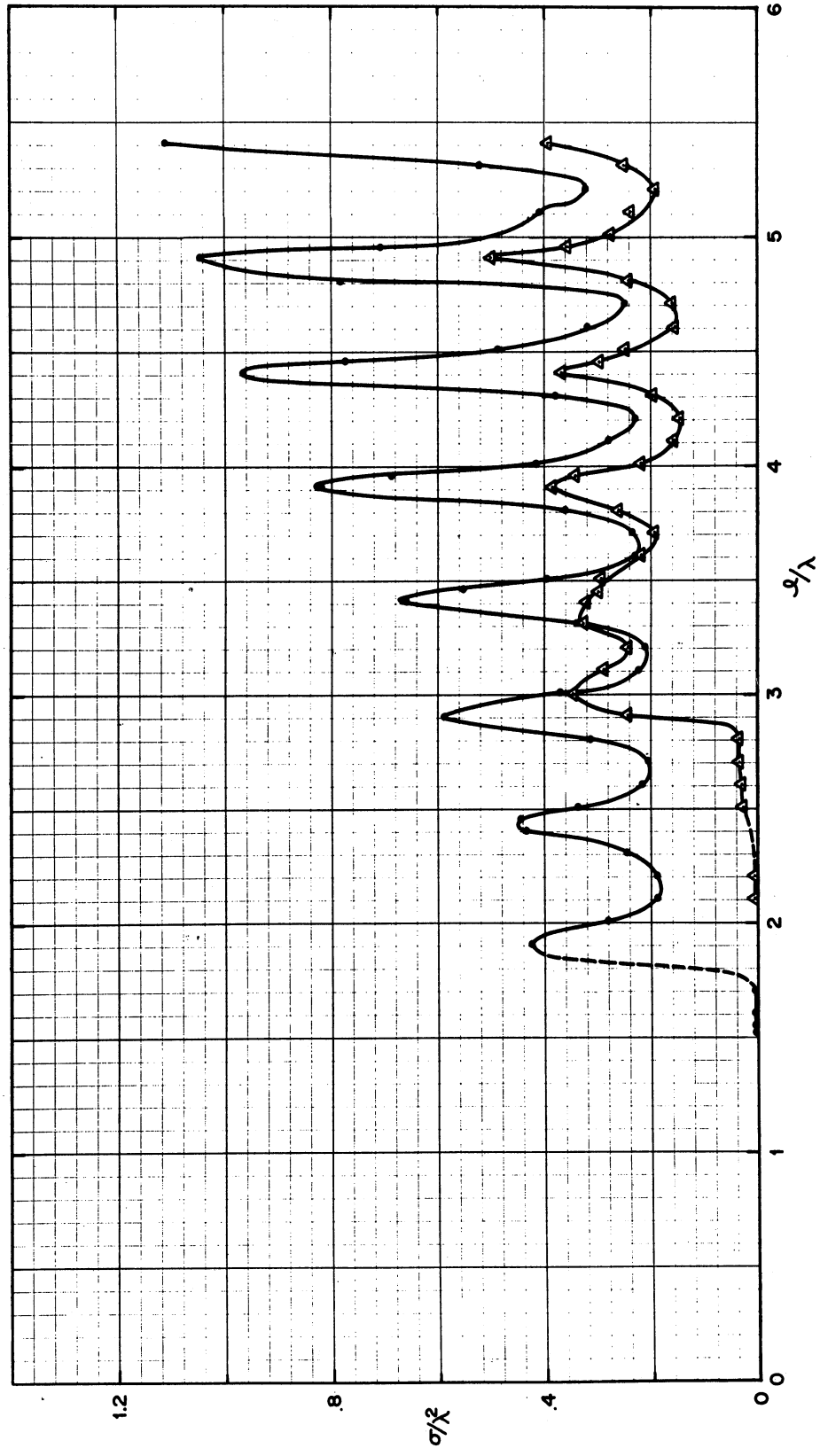

FIG. 3-4a: MEASURED BACK SCATTERING CROSS SECTIONS OF THE SECOND (•••) AND THIRD (ΔΔΔ) LOBES; $a/\lambda = 6.27 \times 10^{-3}$ (Linear Scale).

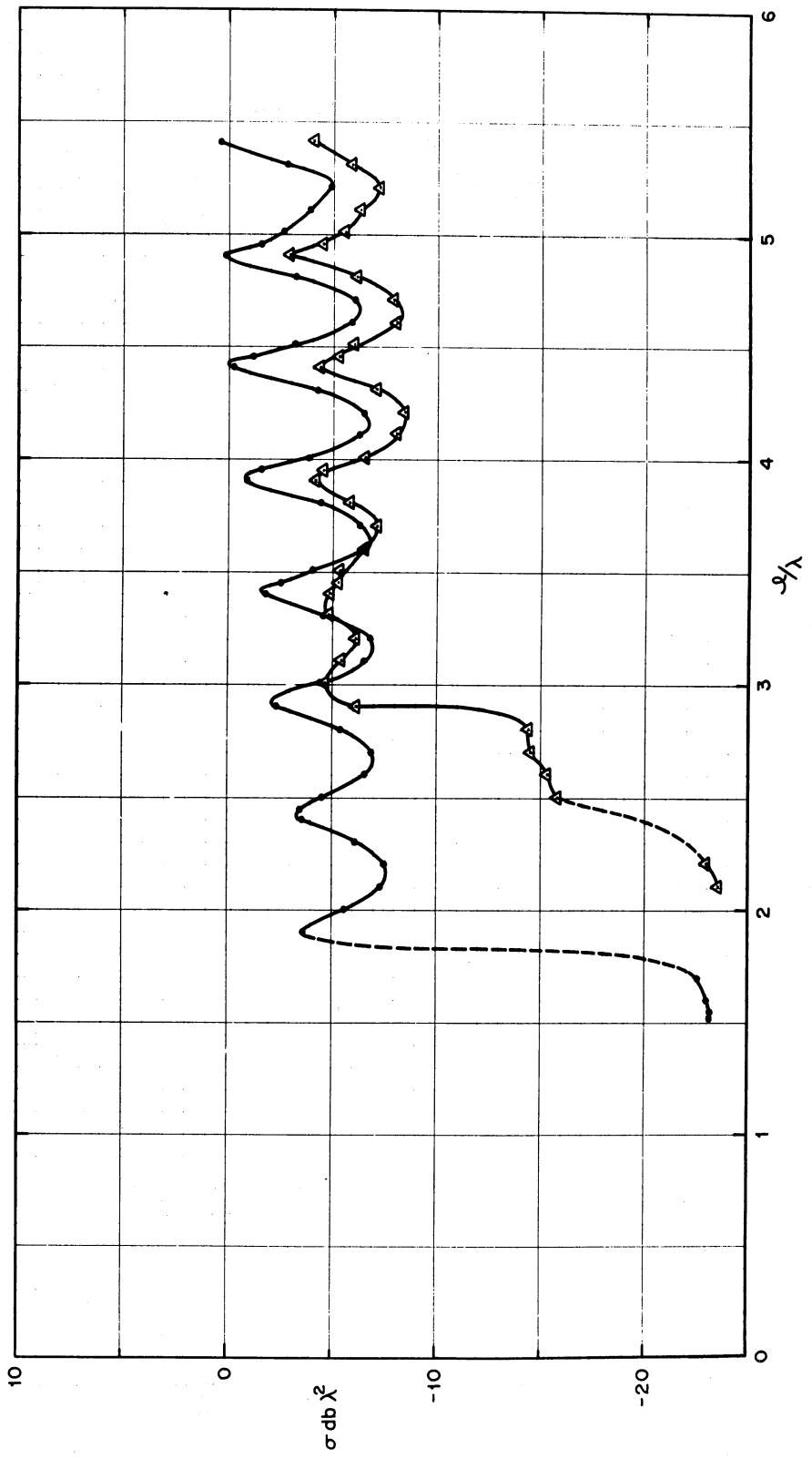

FIG. 3-4b: MEASURED BACK SCATTERING CROSS SECTIONS OF THE SECOND (•••) AND THIRD (ΔΔΔ) LOBES; $a/\lambda = 6.27 \times 10^{-3}$ (db Scale).

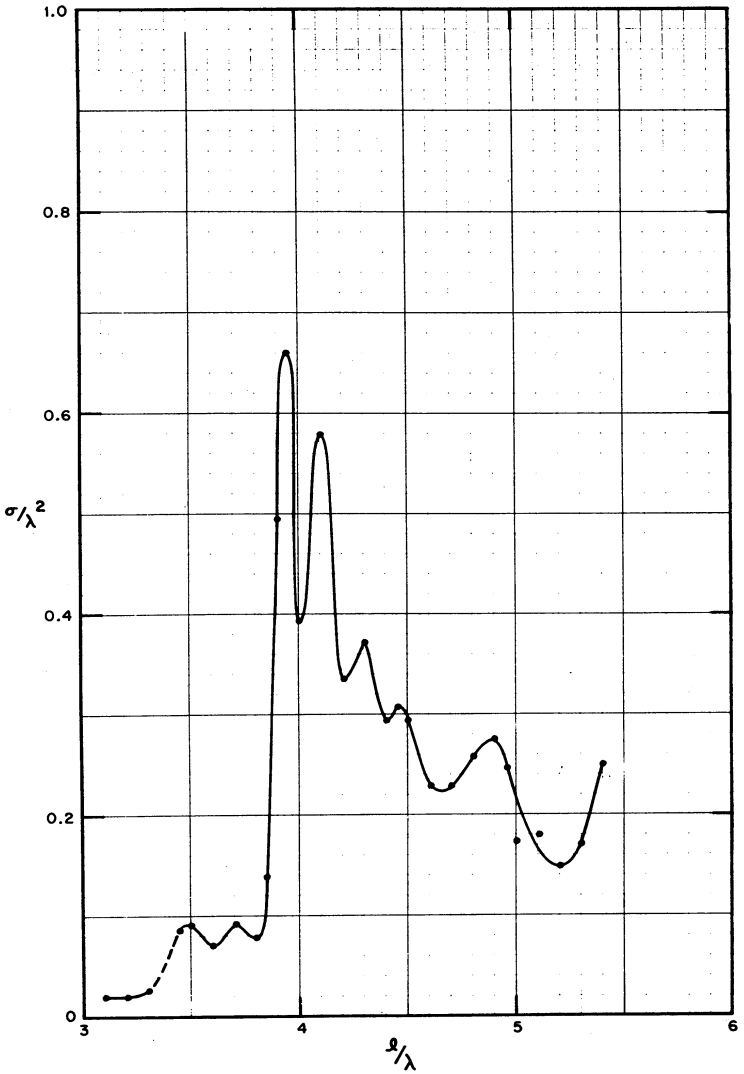

FIG. 3-5a: MEASURED BACK SCATTERING CROSS SECTION OF THE FOURTH LOBE ; $a/\lambda = 6.27 \times 10^{-3}$ (Linear Scale).

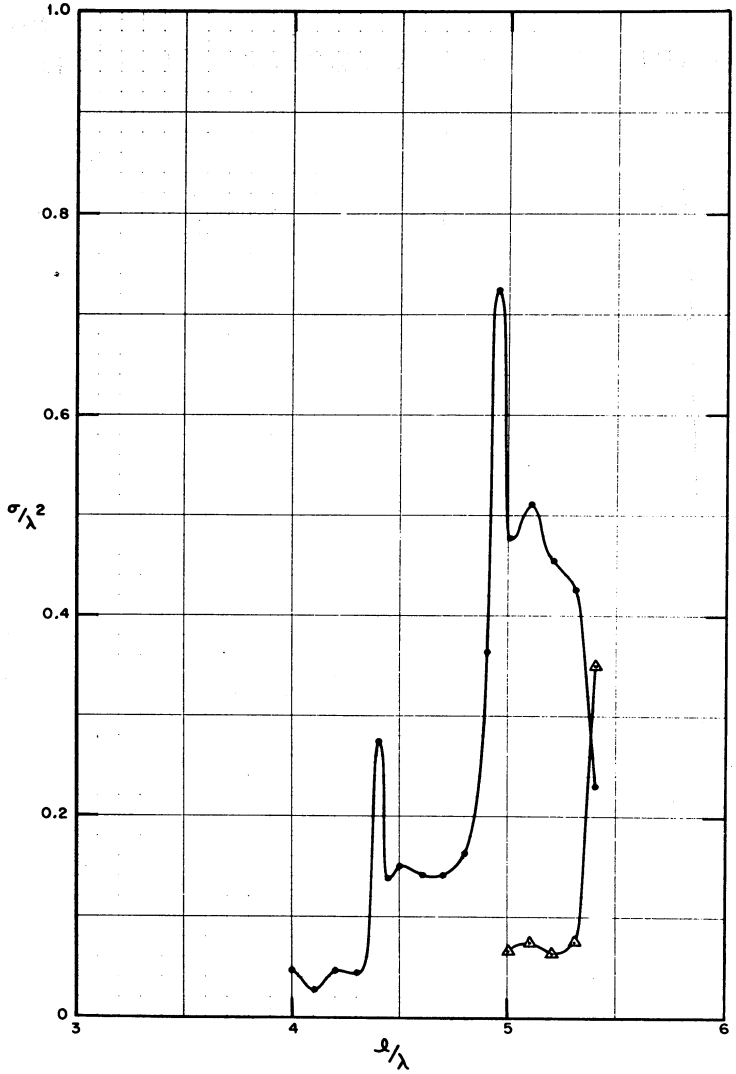

FIG. 3-6a: MEASURED BACK SCATTERING CROSS SECTIONS OF THE FIFTH (●●●) AND SIXTH (ΔΔΔ) LOBES; $a/\lambda = 6.27 \times 10^{-3}$ (Linear Scale).

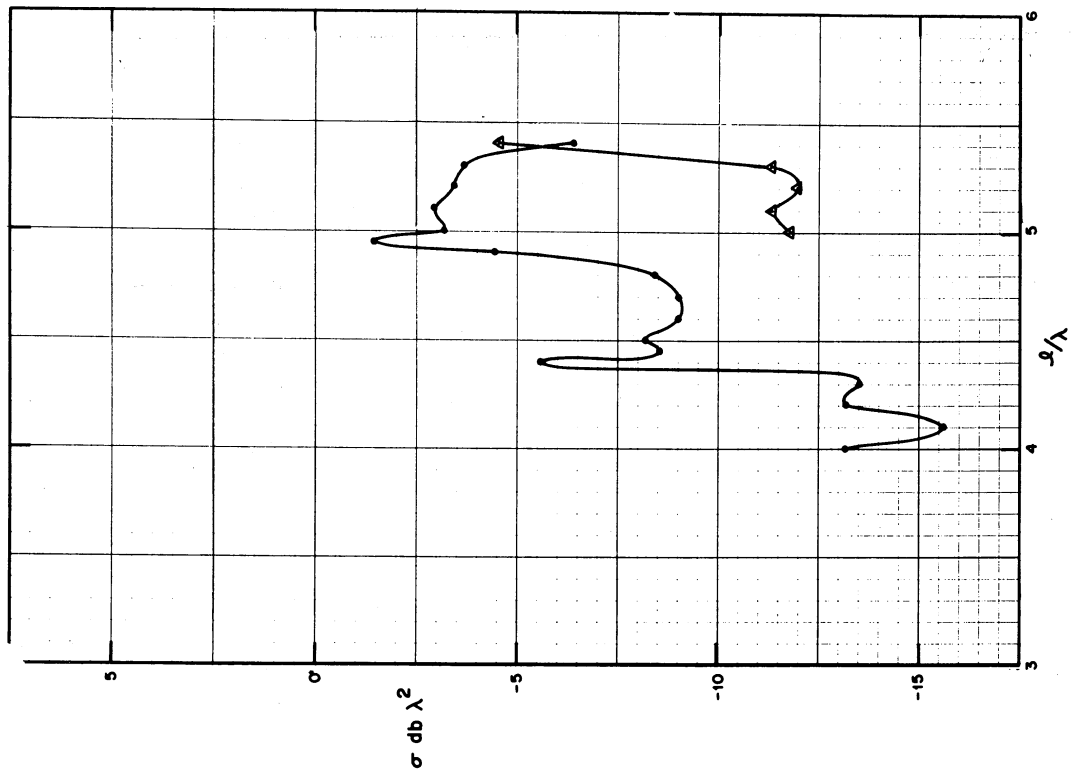

FIG. 3-6b: MEASURED BACK SCATTERING CROSS SECTIONS OF THE FIFTH (●●●) AND SIXTH (△△△) LOBES; $a/\lambda = 6.27 \times 10^{-3}$ (db Scale).

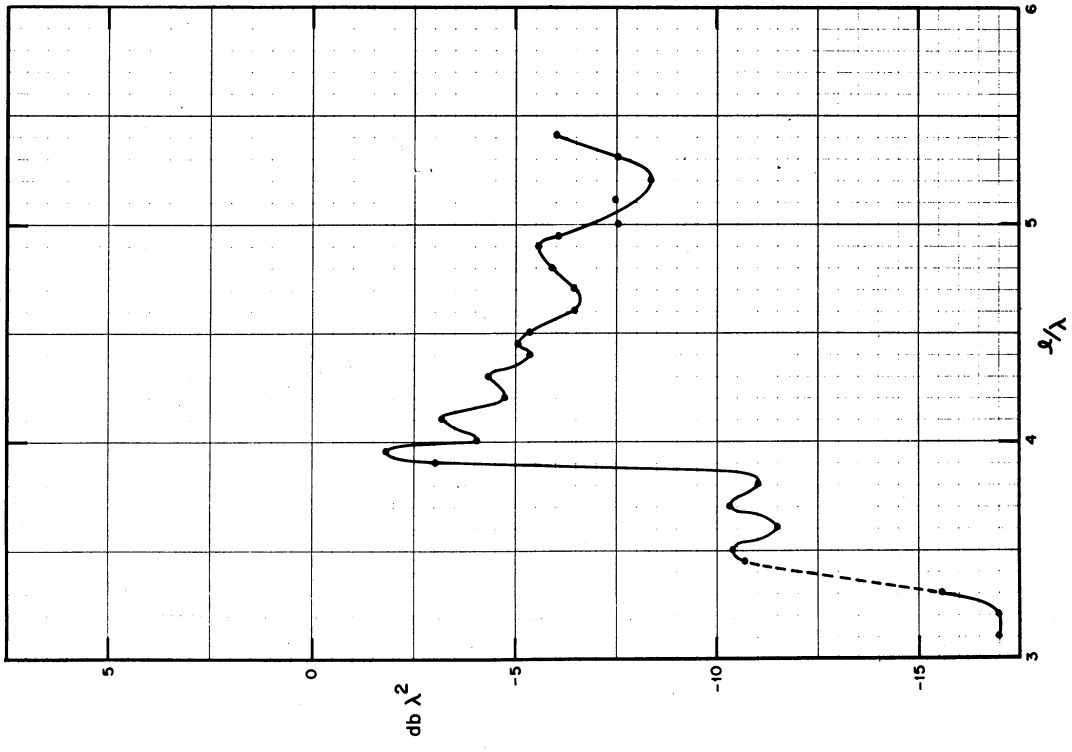

FIG. 3-5b: MEASURED BACK SCATTERING CROSS SECTION OF THE FOURTH LOBE; $a/\lambda = 6.27 \times 10^{-3}$ (db Scale).

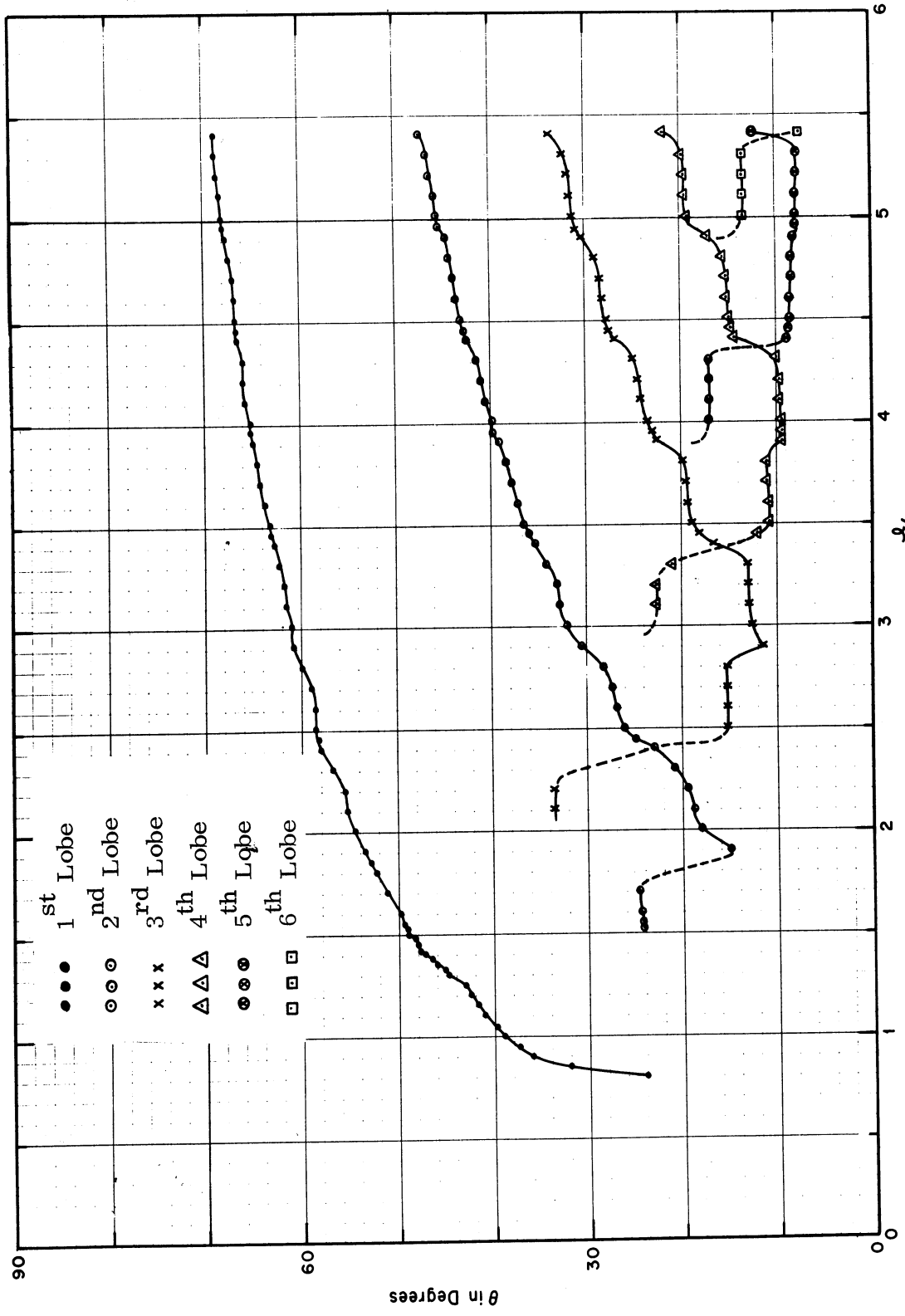

FIG. 3-7: MEASURED DISPLACEMENT OF VARIOUS LOBES; $a/\lambda = 6.27 \times 10^{-3}$.

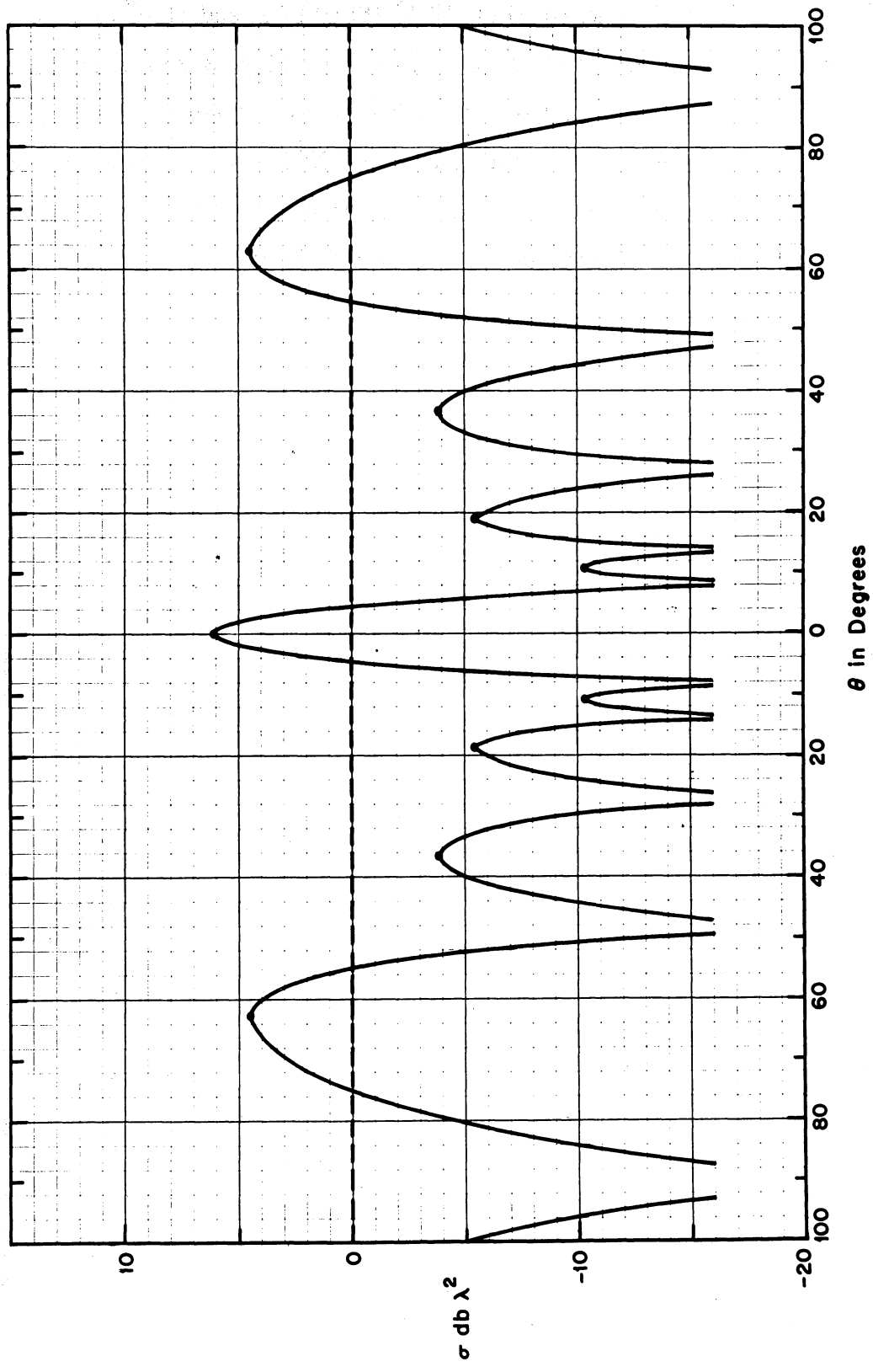

FIG. 3-8: A RECONSTRUCTED BACK SCATTERING CROSS SECTION PATTERN FOR $\ell/\lambda = 3.5$, $a/\lambda = 6.27 \times 10^{-3}$.

at $\theta = 63.0^{\circ}$ (first lobe), 36.5° (second lobe), 18.8° (third lobe) and 11.0° (fourth lobe). The broadside peak is located at $\theta = 0^{\circ}$. Then from Figs. 3-2 through 3-6 (use part (b) for reconstruction on a dB scale) we find the amplitudes for the corresponding peaks. Assuming that the return at end-on ($\theta = 90^{\circ}$) is zero, a pattern now can be sketched, as shown in Fig. 3-8. For reconstruction of patterns with a linear cross section scale, part (a) of Figs. 3-2 through 3-6 should be used.

ACKNOWLEDGMENTS

The authors are greatly indebted to Dr. T.B.A. Senior for his helpful suggestions, and to Messrs. August Antones and Richard Leland for preparing the illustrations.

REFERENCES

Ås, B.-O. and H J Schmitt (1958), "Back-Scattering Cross Sections of Reactively Loaded Cylindrical Antennas," Harvard University, Cruft Laboratory Scientific Report No. 18, Cambridge, Massachusetts.

Blacksmith, P., R.E. Hiatt and R.B. Mack (1965), "Introduction to Radar Cross Section Measurements," Proc. IEEE, 53, pp. 901-919.

Cassedy, E.S. and J. Feinberg (1960), "Back Scattering Cross Sections of Cylindrical Wires of Finite Conductivity," IRE Trans., AP-8, pp. 1-7.

Einarsson, O., R.E. Kleinman, P. Laurin, P.L. E. Uslenghi, (1966), "Studies in Radar Cross Section L-Diffraction and Scattering by Regular Bodies IV: The Circular Cylinder," The University of Michigan Radiation Laboratory Report No. 07133-3-T, Ann Arbor, Michigan.

Hallén, E. (1938), "Theoretical Investigations into the Transmitting and Receiving Qualities of Antennas," Nova Acta Regiae Societatis Scientiarum Upsaliensis, Ser. IV, II, No. 4.

King, R.W.P. (1956), The Theory of Linear Antennas, (Harvard University Press, Cambridge, Massachusetts).

Schindler, J.K., R.B. Mack, P. Blacksmith (1965), "The Control of Electromagnetic Scattering by Impedance Loading," Proc. IEEE, 53, pp. 993-1003.

Strutt, J.W., Lord Rayleigh (1945), The Theory of Sound (Dover Publications, New York).

Tai, C-T (1951), "Radar Response from Thin Wires," Stanford Research Institute Technical Report No. 18, Stanford, California.

Williams, W.E. (1956), "Diffraction by a Cylinder of Finite Length," Proc. Cambridge Phil. Soc., 52, Pt. 2, pp. 322-335.

BACK SCATTERING CROSS SECTION PATTERNS OF A THIN ROD OF DIAMETER 2a = 1/16 INCH AS A FUNCTION OF THE ANGULAR POSITION, θ FOR VARIOUS VALUES OF ℓ/λ WITH $\lambda = 4.98$ INCHES (frequency f = 2.37 GHz).

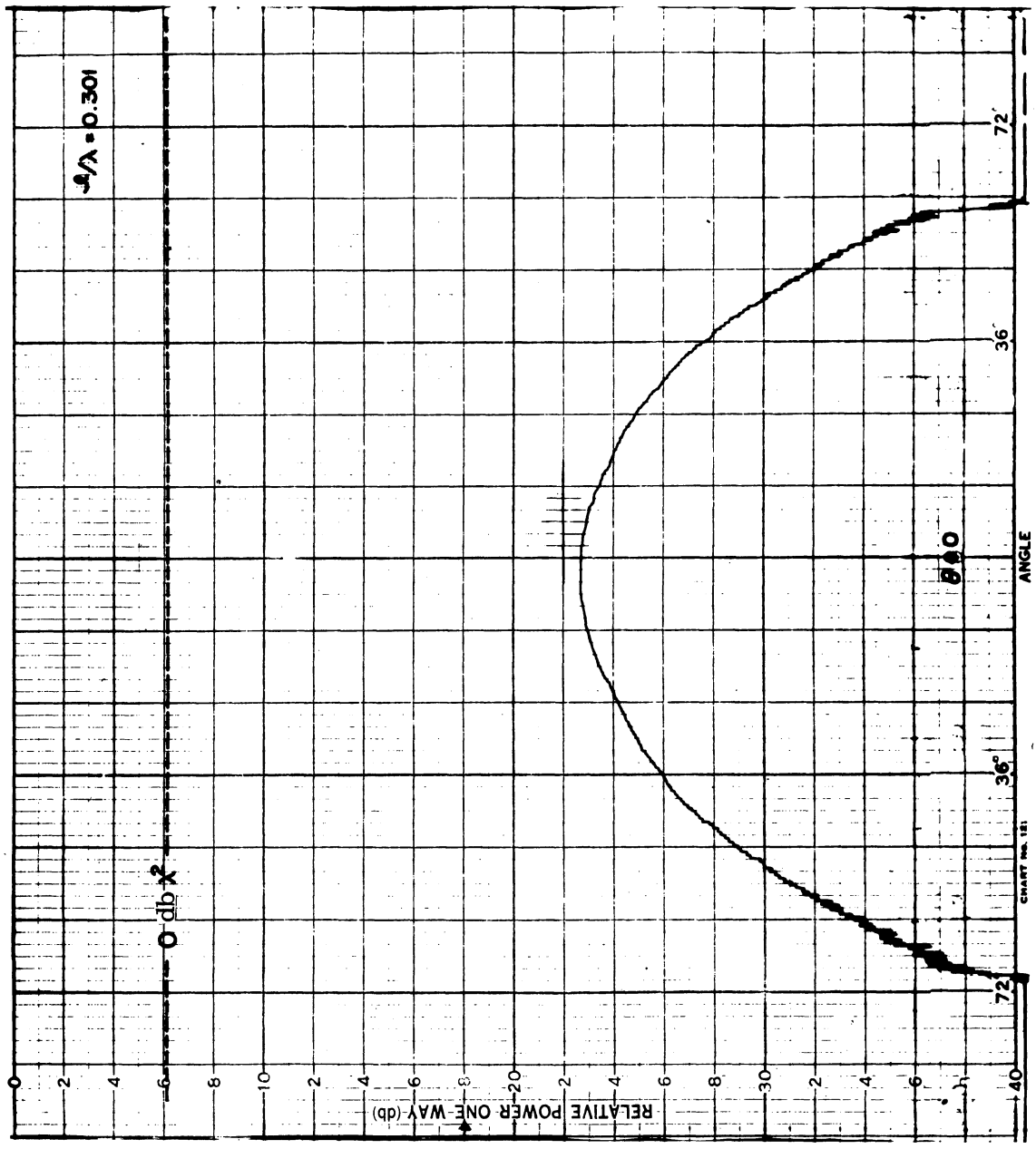
d/λ = 0.301
0 db
RELATIVE POWER ONE WAY (db)
ANGLE
0
2
4
6
8
10
20
30
40
72
36
36
72

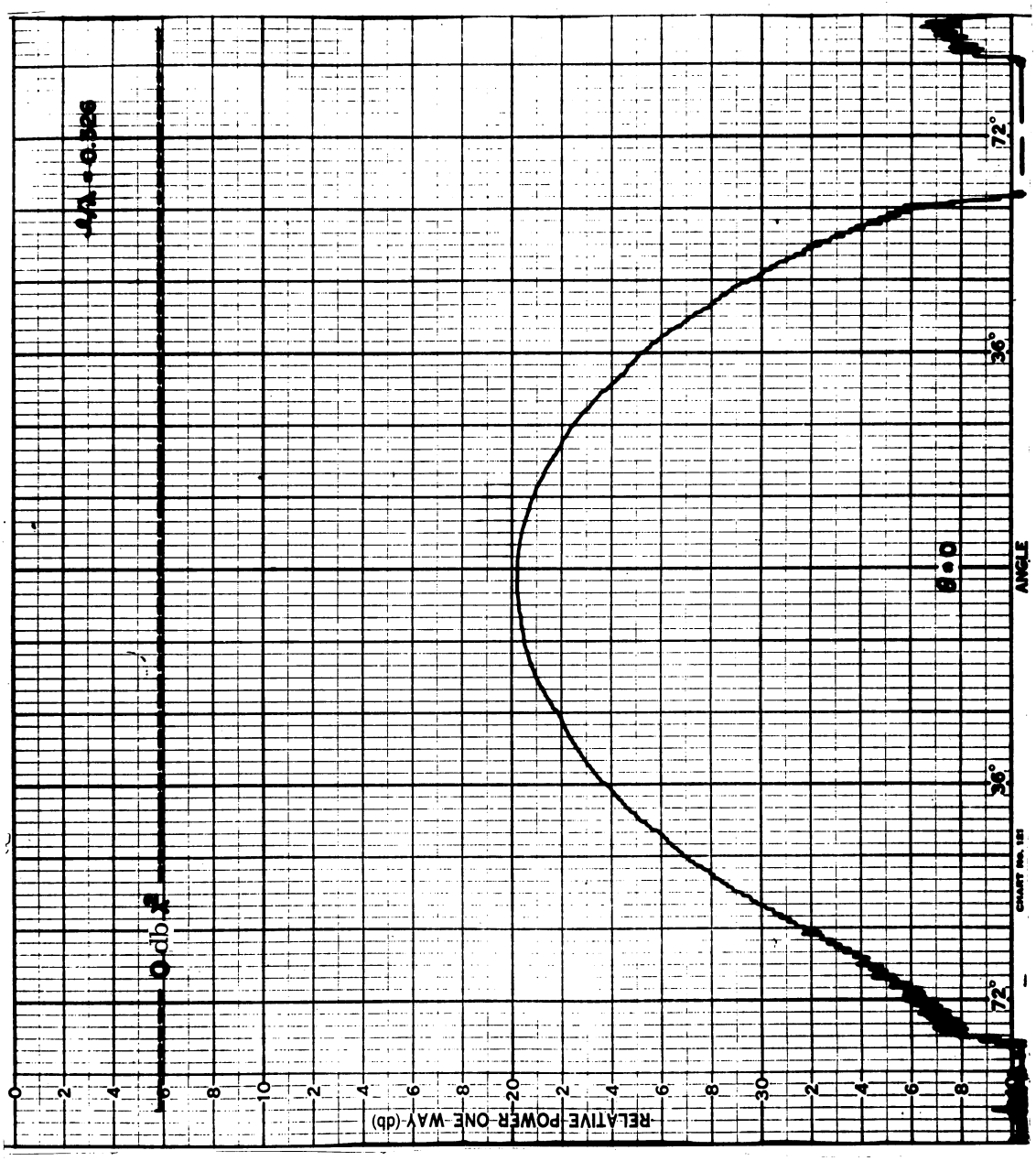
RELATIVE POWER ONE WAY (db)
0 db
0.0
ANGLE
72°
36°
36°
72°

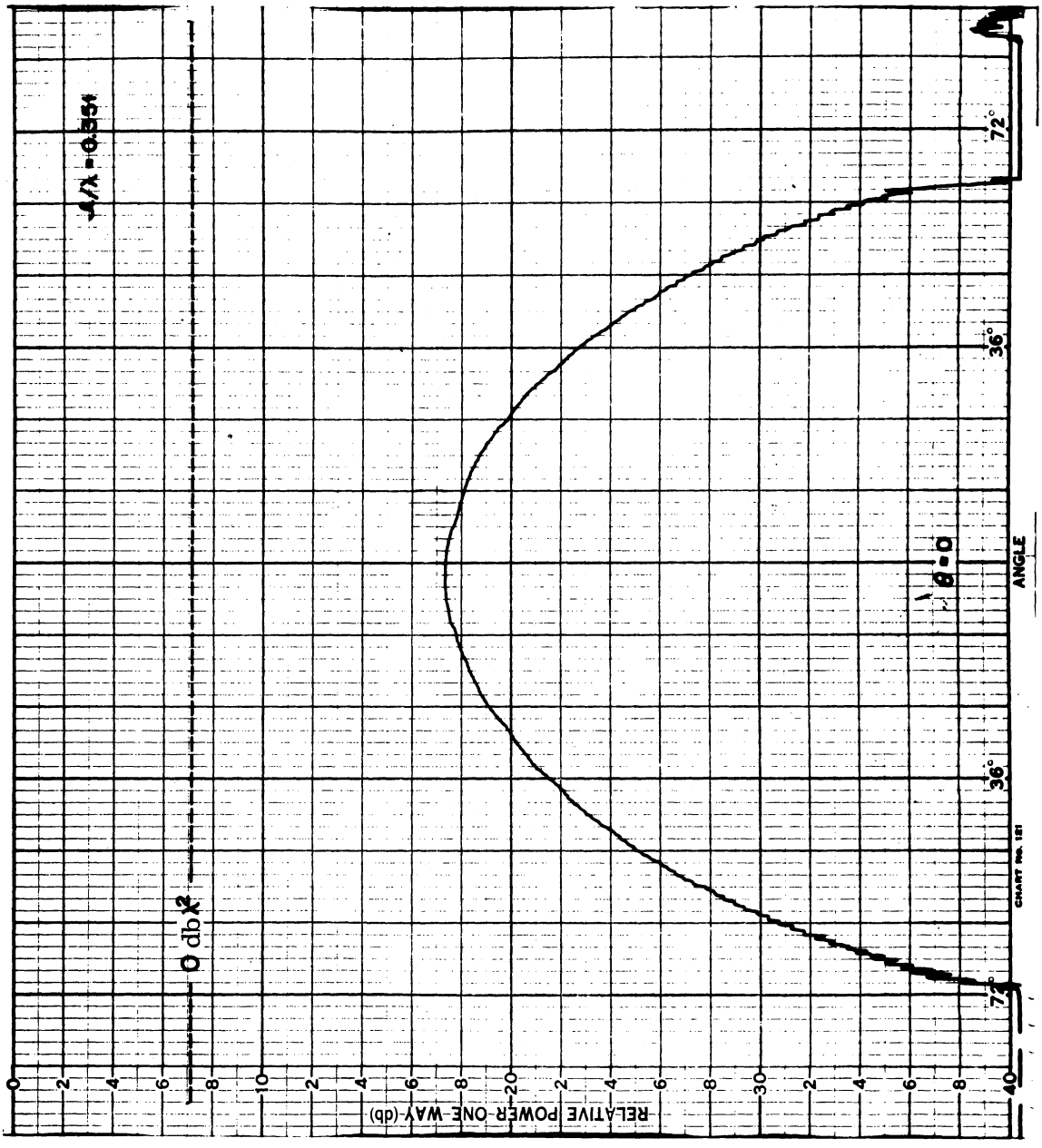
d/λ = 0.35
0 db
θ = 0
72°
36°
36°
72°
ANGLE
RELATIVE POWER-ONE-WAY-(db)
0
2
4
6
8
10
2
4
6
8
20
2
4
6
8
30
2
4
6
8
40

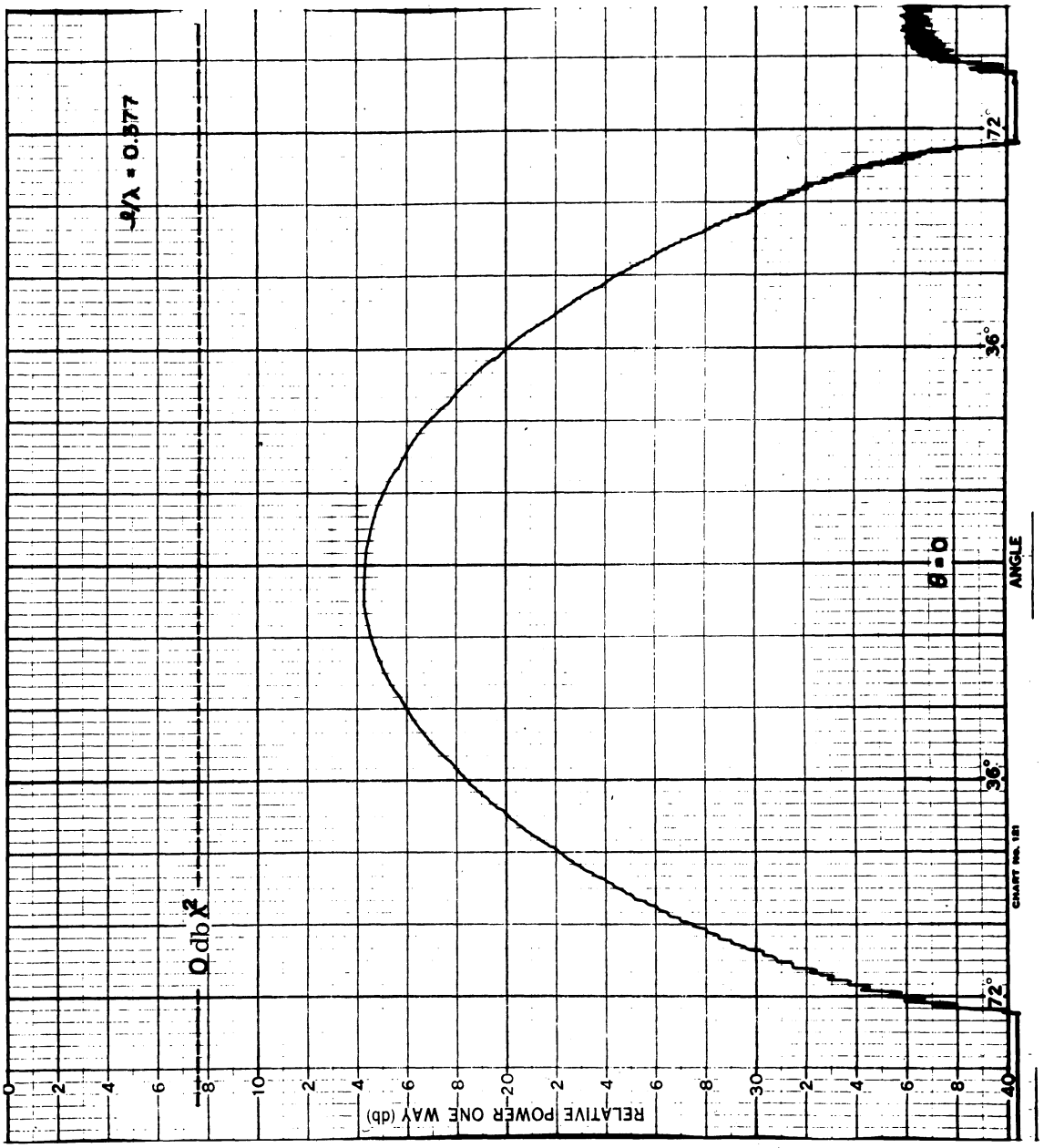
ℓ/λ = 0.577
0 db
RELATIVE POWER ONE WAY (db)
θ = 0
ANGLE
72°
36°
36°
72°

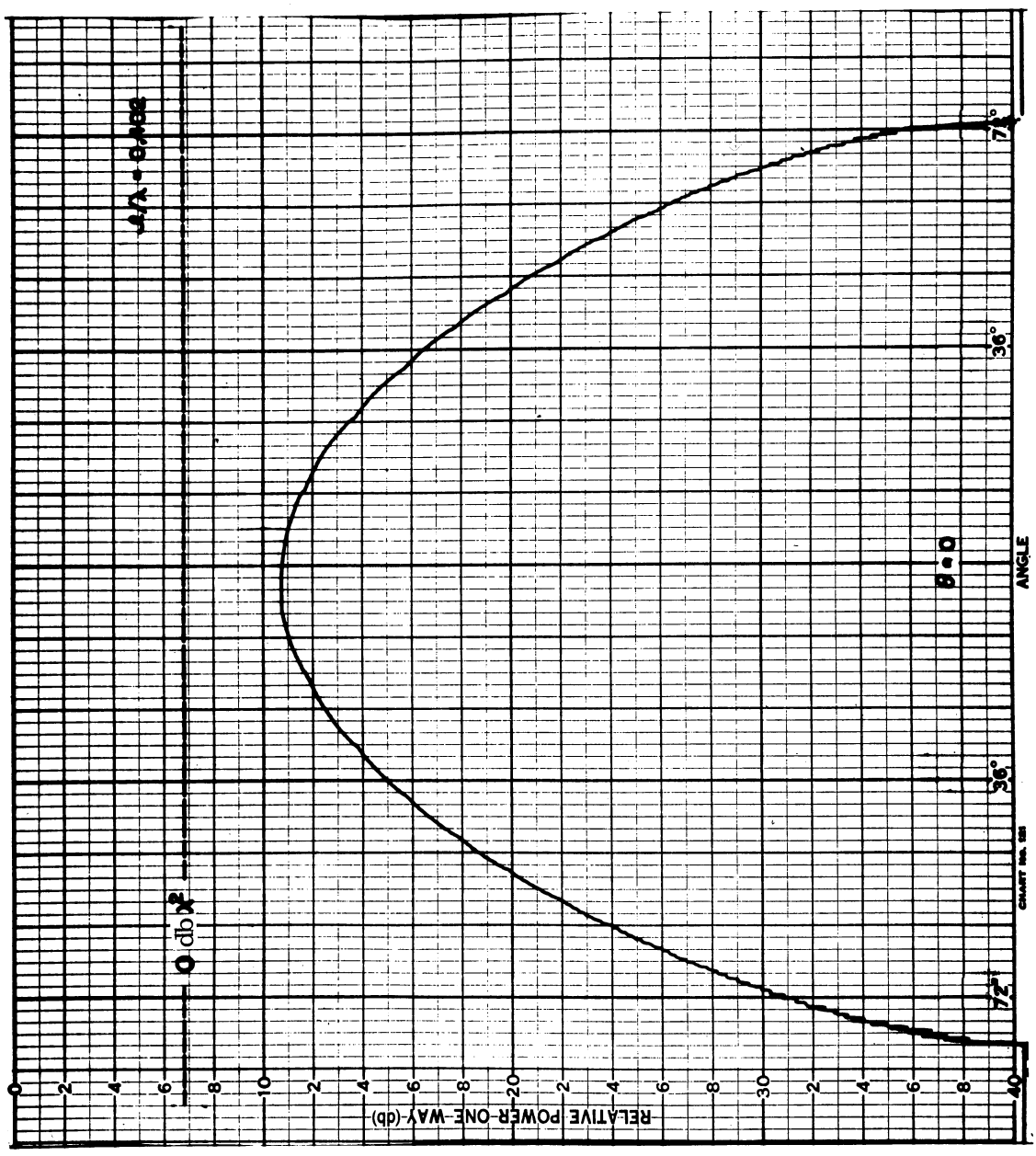
RELATIVE POWER ONE WAY (db)
0 db
ANGLE
72°
36°
0°
36°
72°

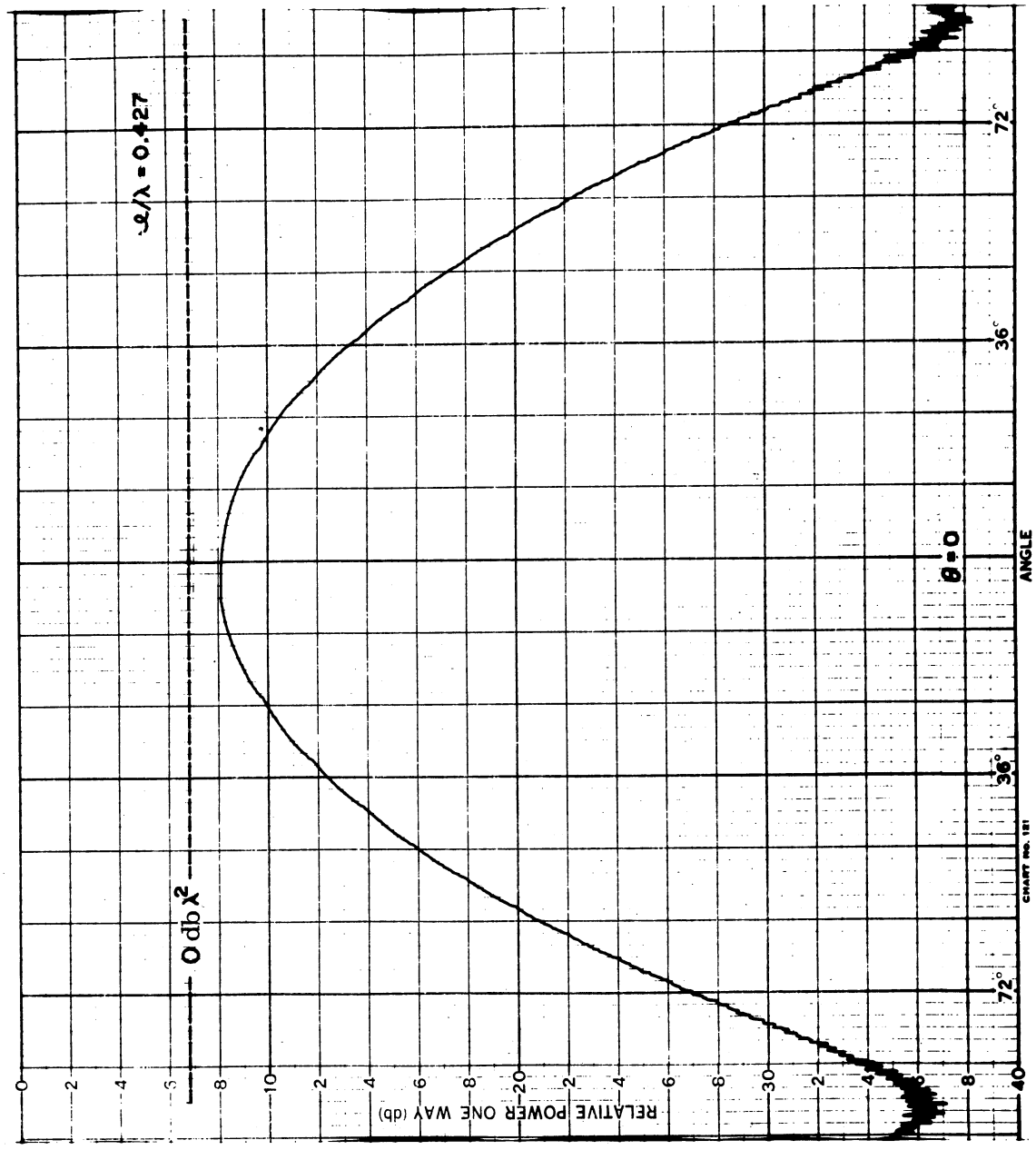
ℓ/λ = 0.427
0 db λ²
RELATIVE POWER ONE WAY (db)
0
2
4
6
8
10
2
4
6
8
20
2
4
6
30
2
4
6
8
40
72°
36°
θ = 0
36°
72°
ANGLE
CHART No. 181

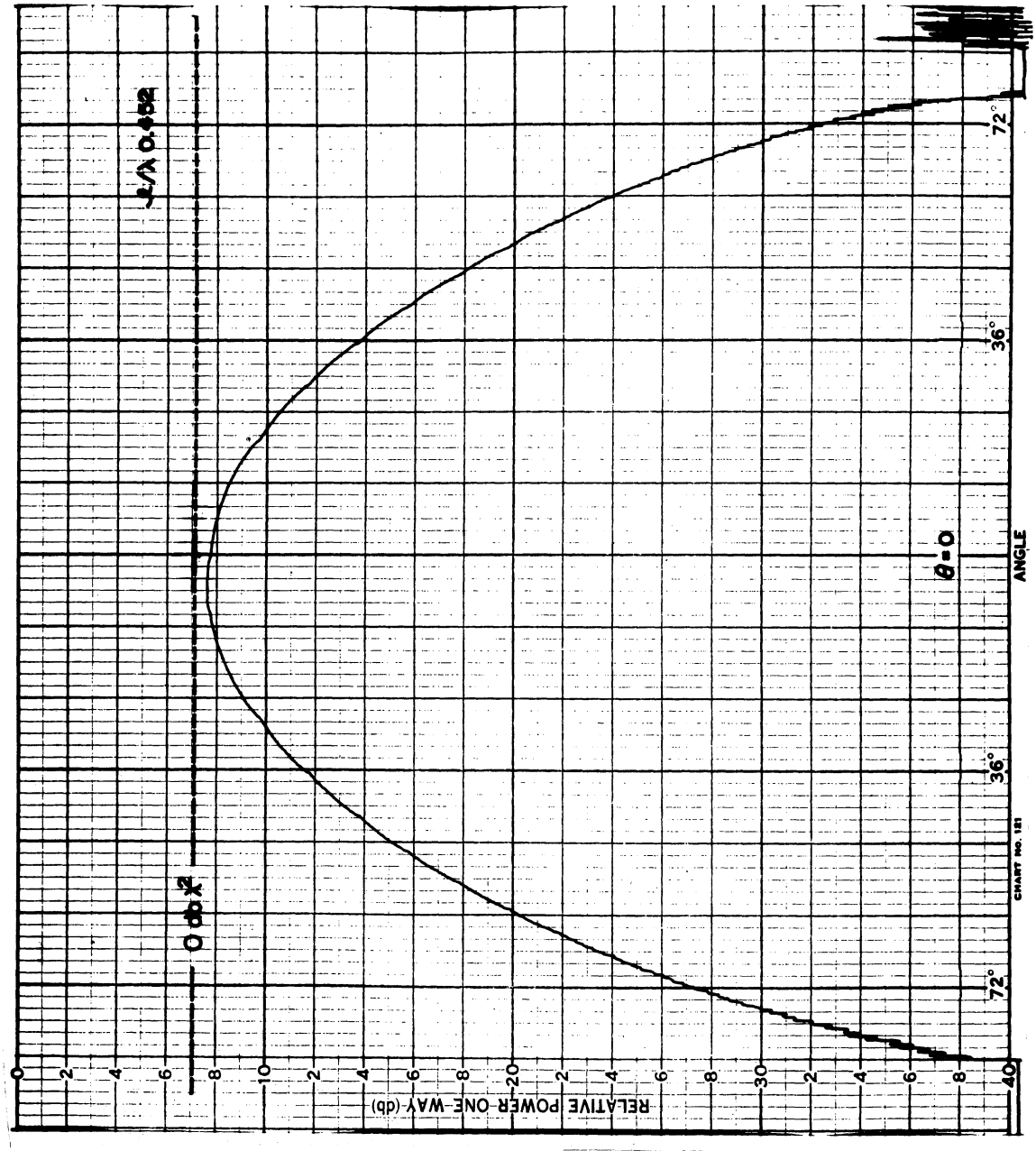
0 db
θ=0
72°
36°
36°
72°
ANGLE
RELATIVE POWER ONE-WAY (db)
0
2
4
6
8
10
2
4
6
8
20
2
4
6
8
30
2
4
6
8
40

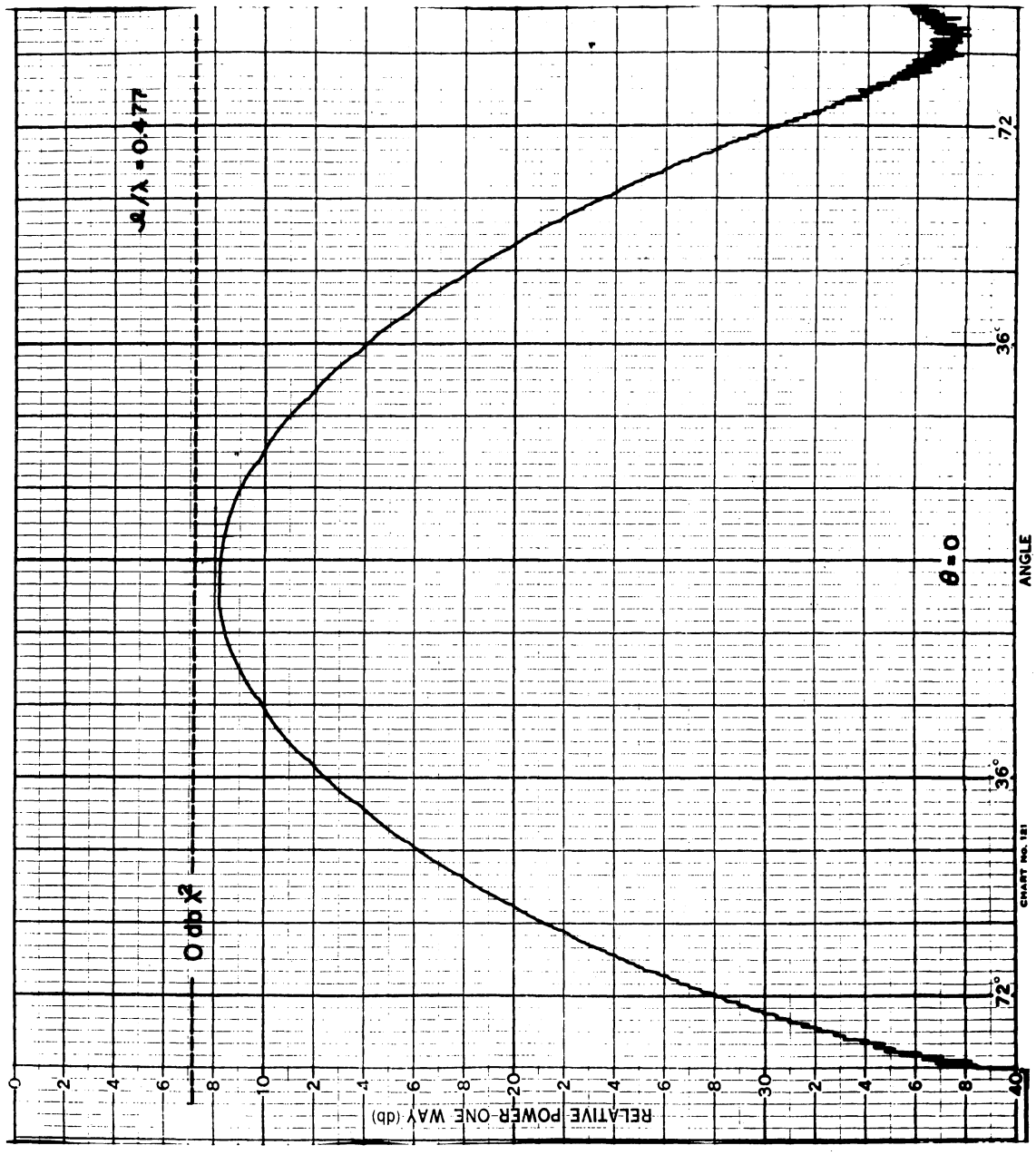
d/λ = 0.477
0 db
RELATIVE POWER ONE WAY (db)
θ = 0
ANGLE
72°
36°
36°
72
CHART NO. 121

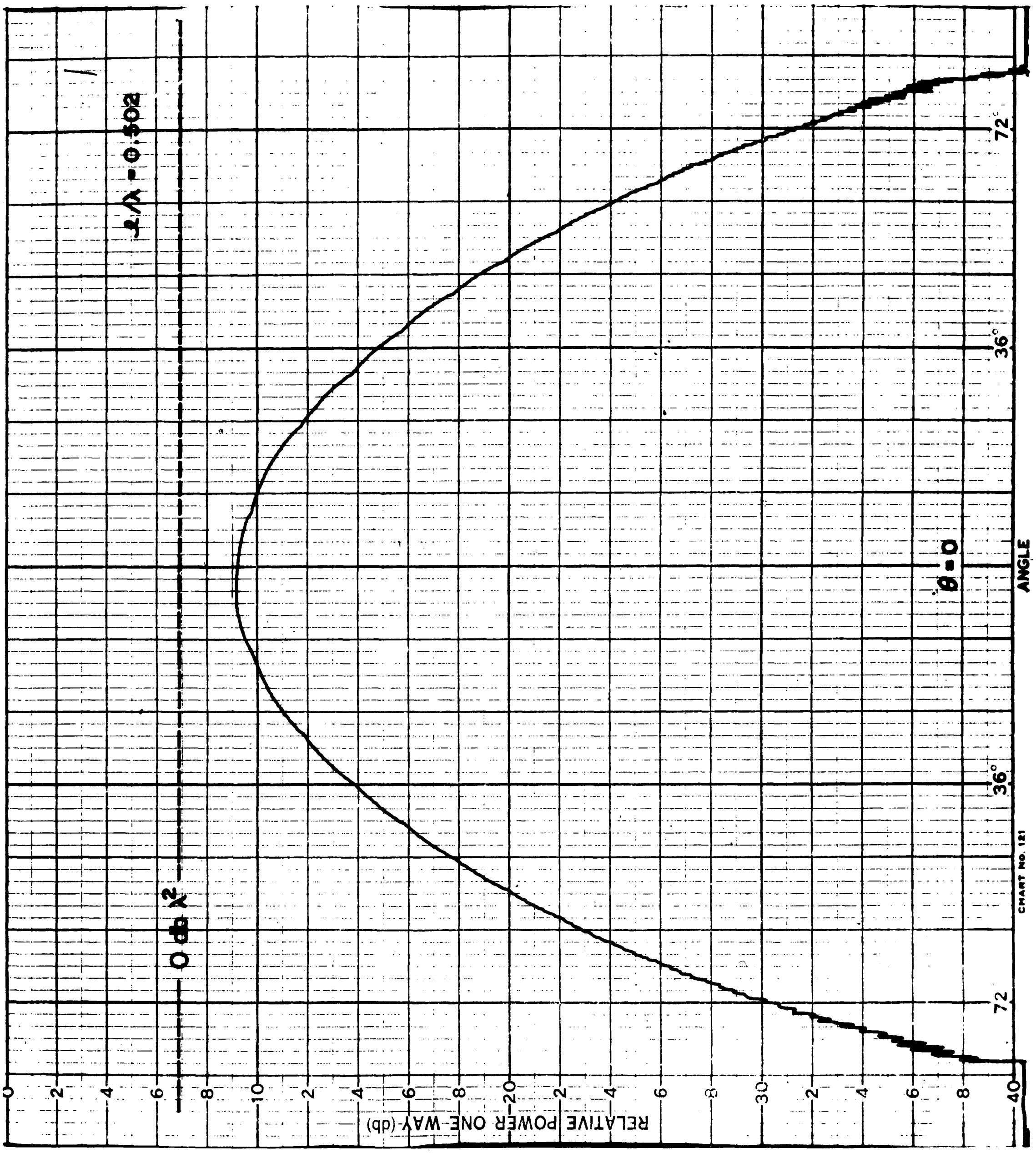
RELATIVE POWER ONE-WAY-(db)
ANGLE
CHART NO. 121
72°
36°
0
72
36°
θ = 0
0 db λ²
ℓ/λ = 0.502

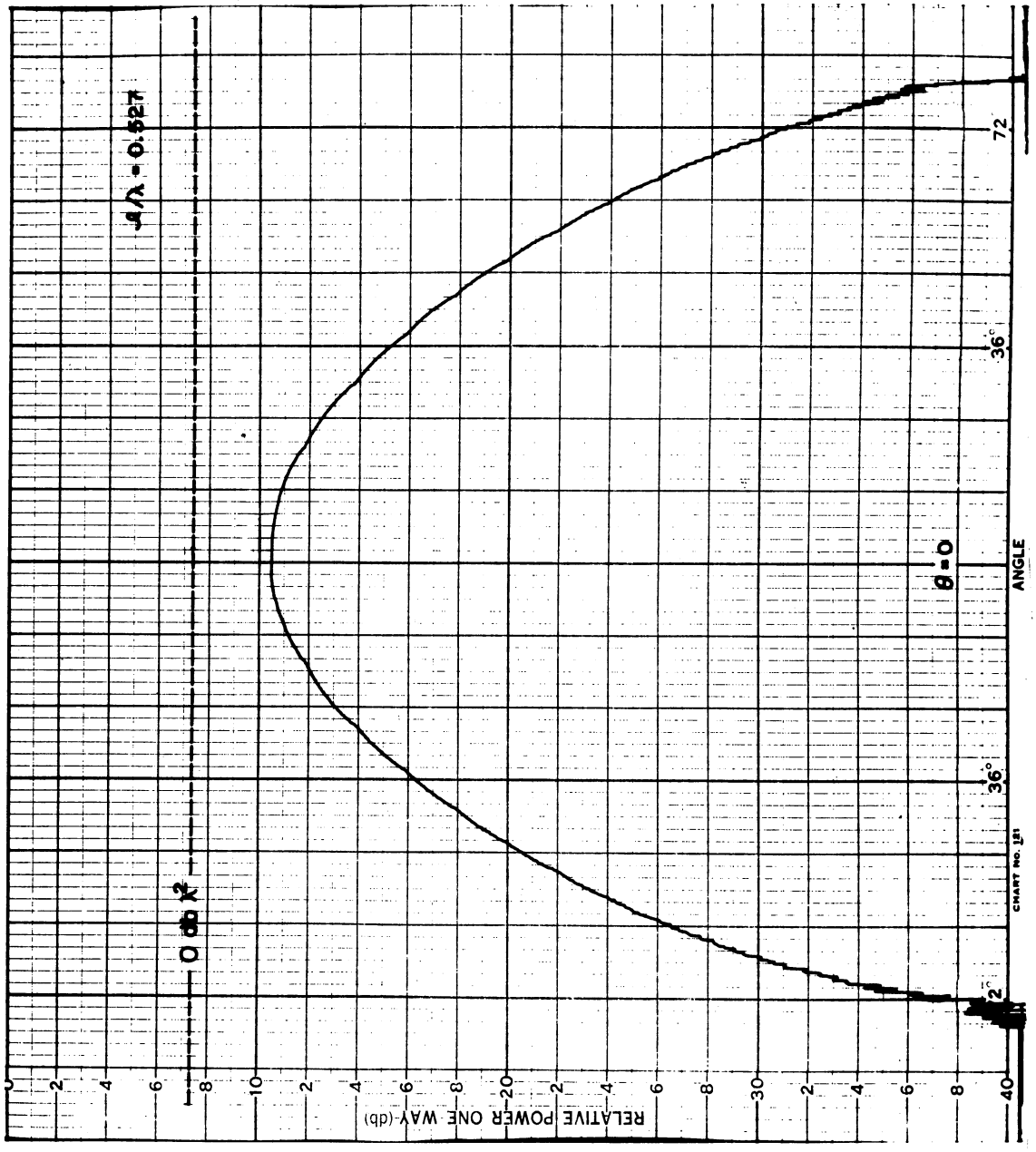
d/λ = 0.527
θ = 0
72
36°
36°
2°
ANGLE
RELATIVE POWER ONE WAY-(db)
CHART NO. 121

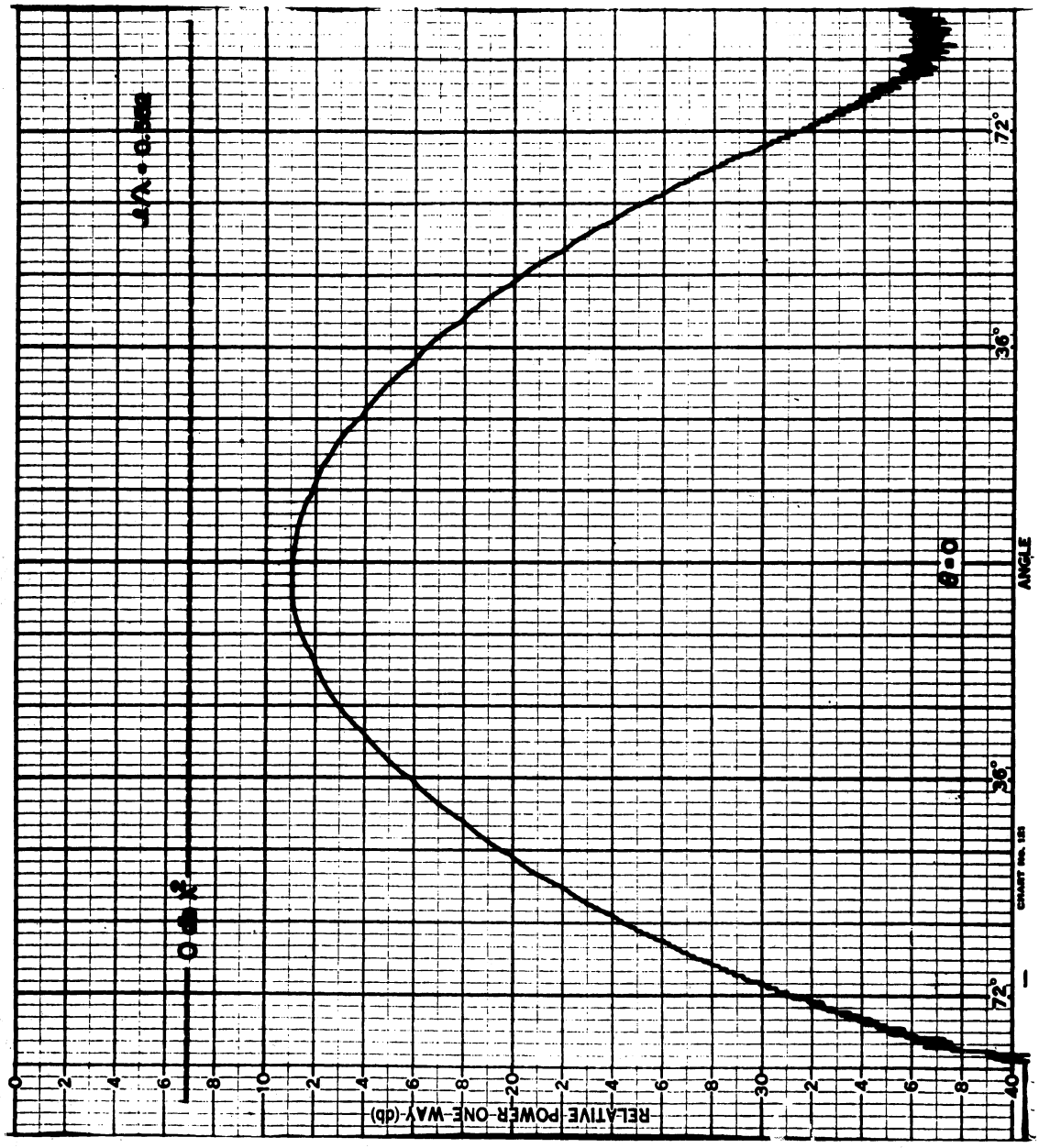
72°
36°
θ=0
36°
72°
ANGLE
RELATIVE POWER-ONE-WAY-(db)
0
2
4
6
8
10
2
4
6
8
20
2
4
6
8
30
2
4
6
8
40

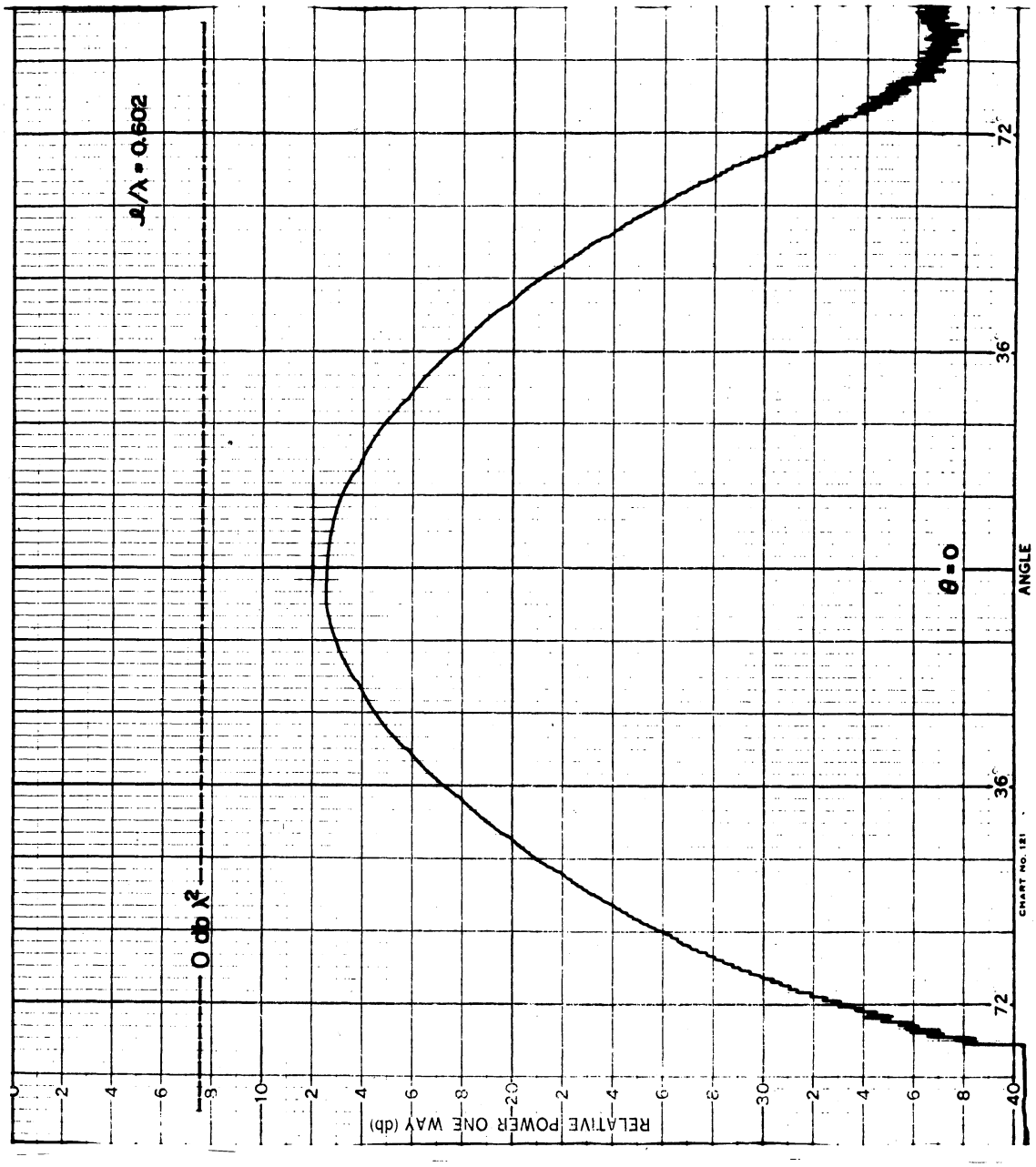
ℓ/λ = 0.502
0 db
RELATIVE POWER ONE WAY (db)
θ=0
ANGLE
72
36
36
72
CHART NO. 121

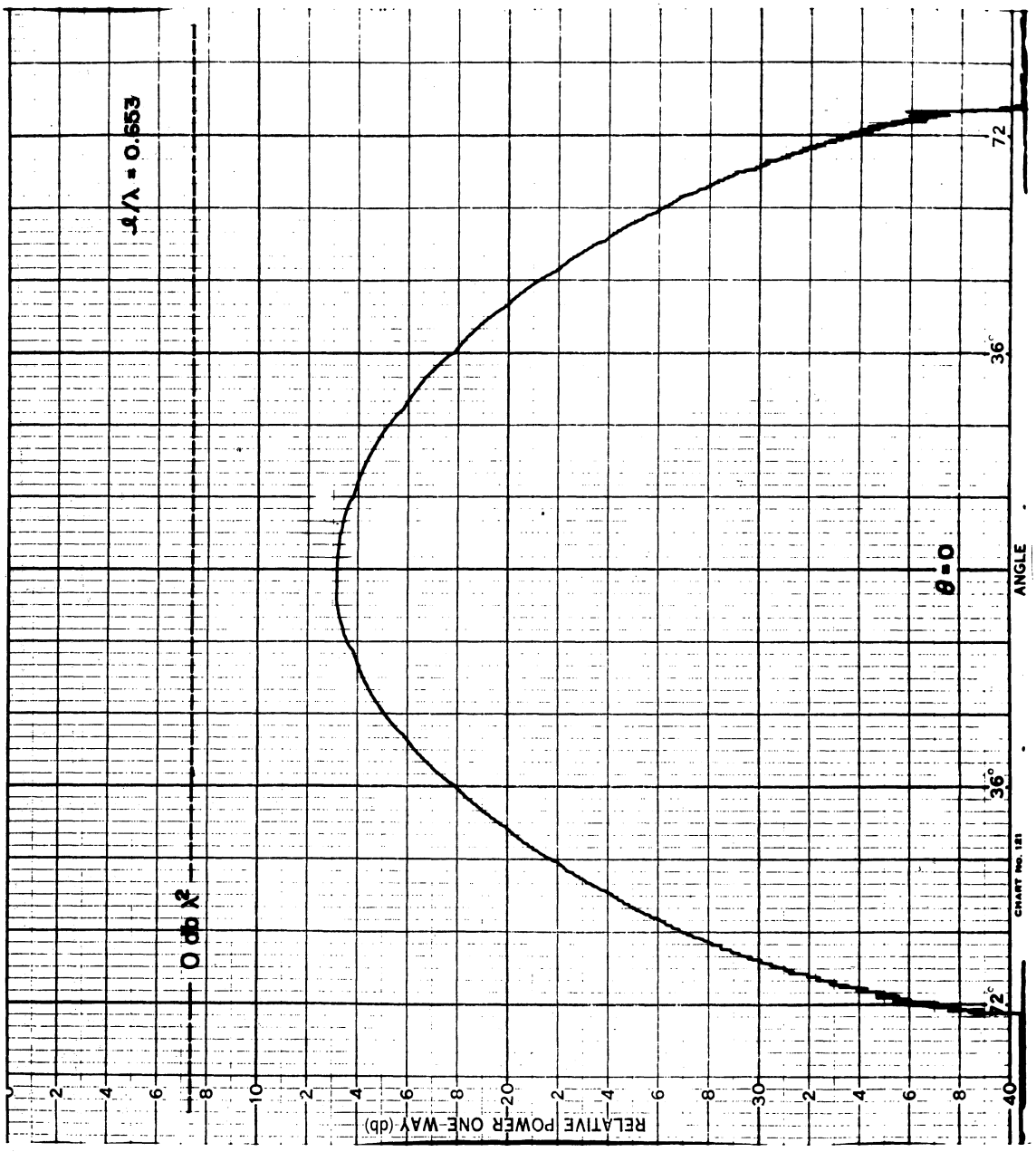
d/λ = 0.653
0 db
RELATIVE POWER ONE-WAY (db)
θ = 0
ANGLE
72
36°
36°
72
CHART NO. 121

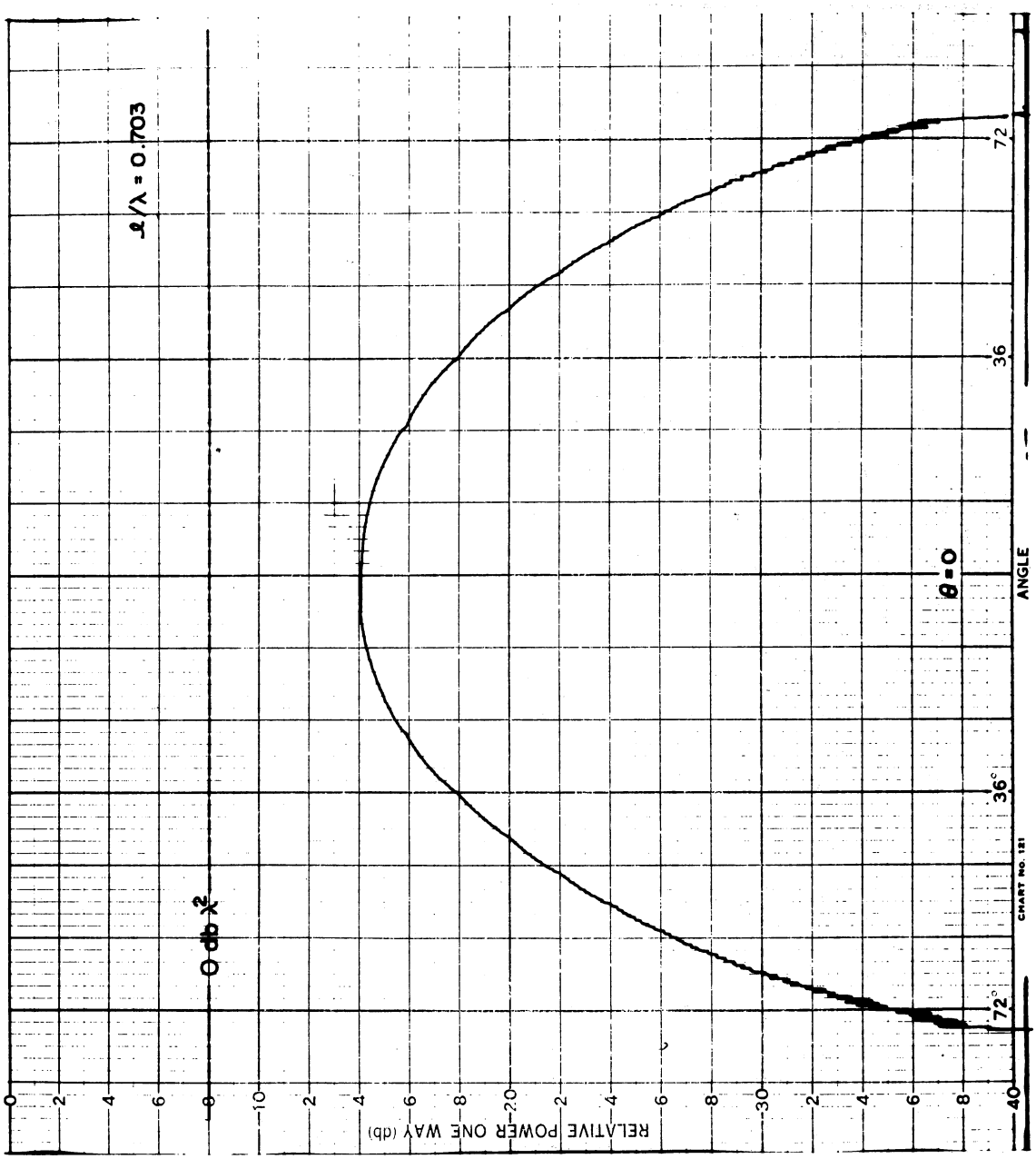
ℓ/λ = 0.703
0 db
θ=0
ANGLE
72°
36°
72
36
CHART No. 121
RELATIVE POWER ONE WAY (db)
0
2
4
6
8
10
2
4
6
8
20
2
4
6
8
30
2
4
6
8
40

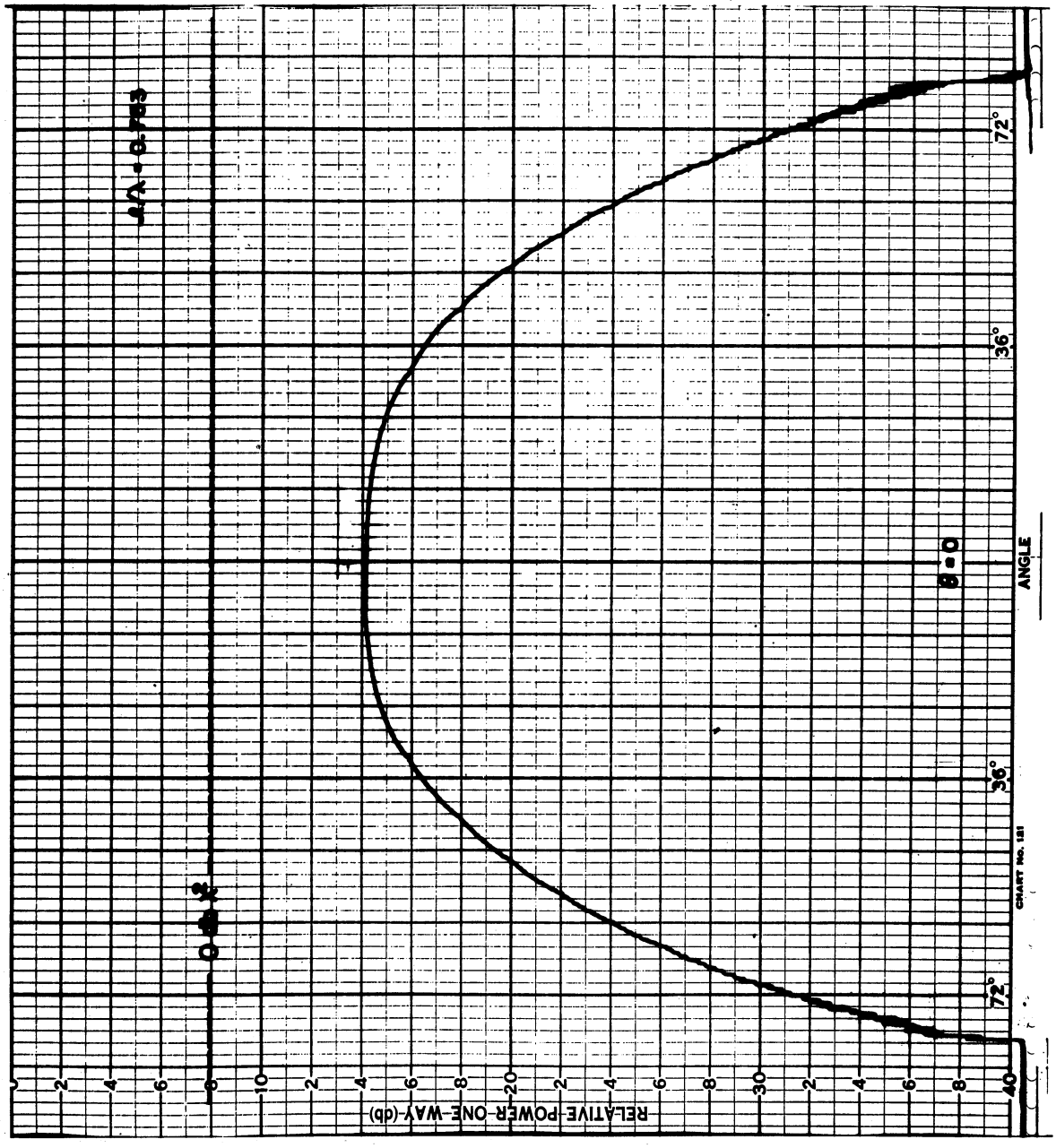
RELATIVE POWER ONE-WAY (db)
ANGLE
72°
36°
0
36°
72°
CHART NO. 121

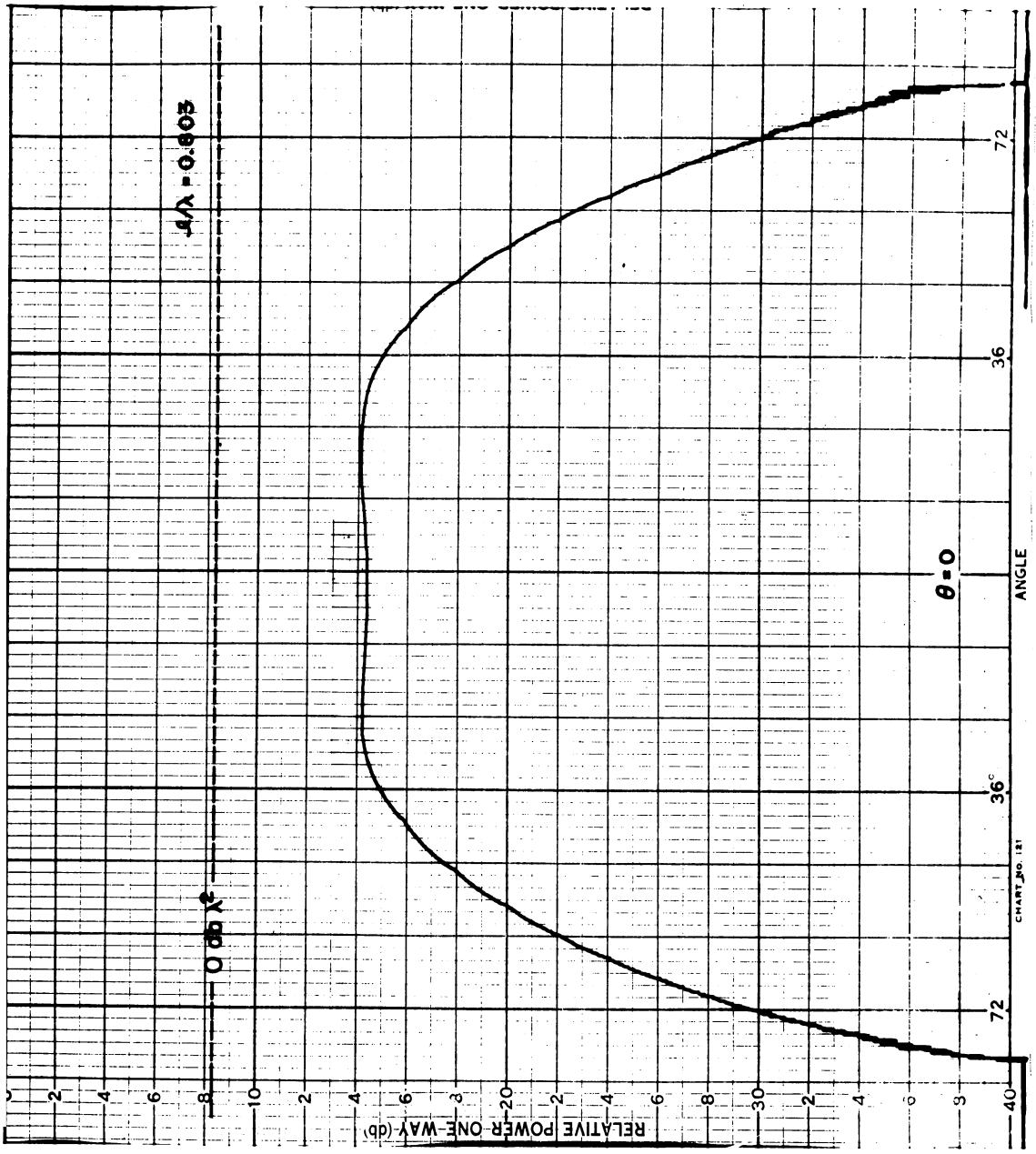
a/λ = 0.803
0 db
RELATIVE POWER-ONE-WAY (db)
θ=0
ANGLE
72
36
36°
72

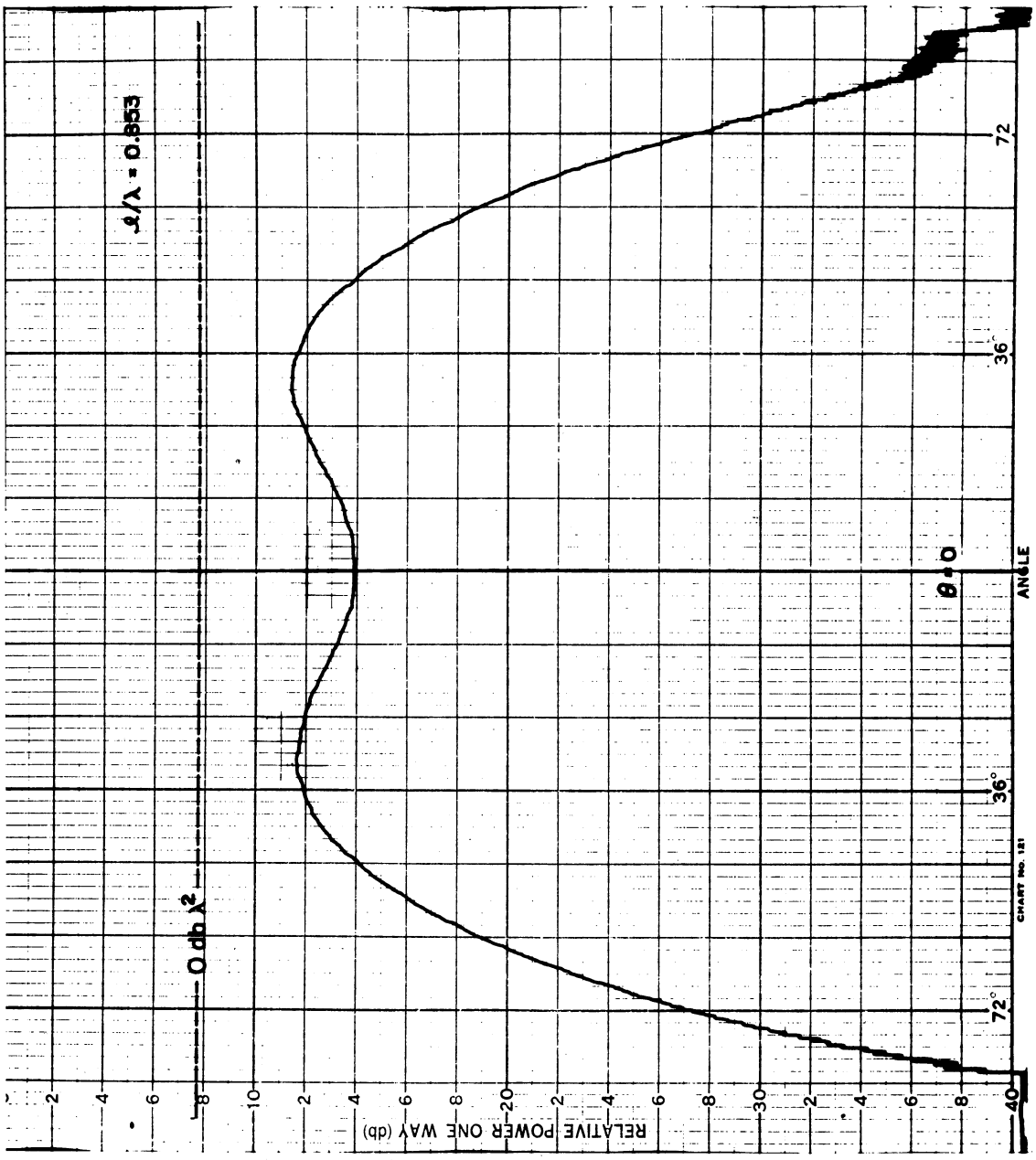
d/λ = 0.853
0 db
RELATIVE POWER ONE WAY (db)
θ = 0
ANGLE
72°
36°
36°
72
36
CHART No. 121

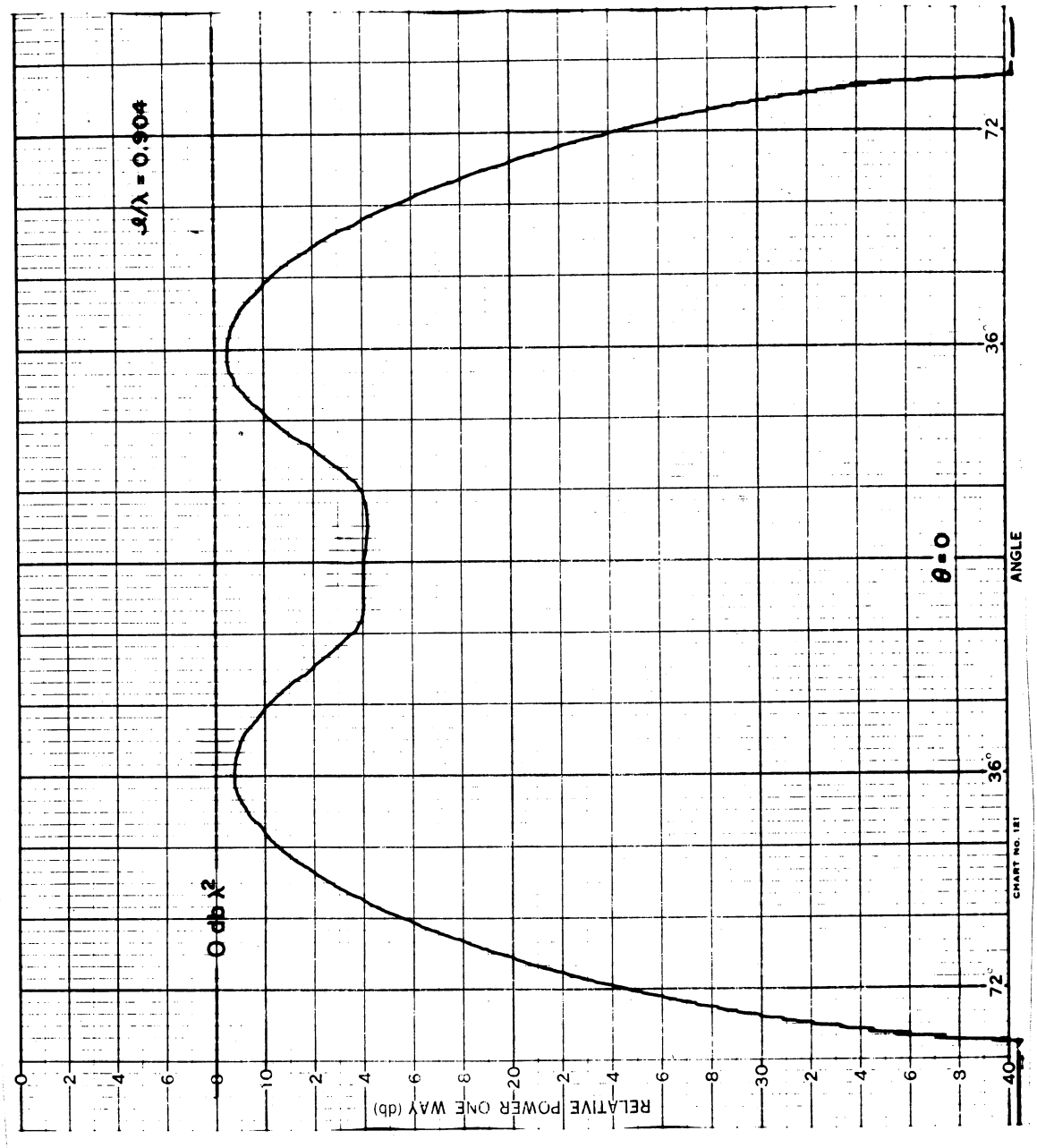
d/λ = 0.904
0 db χ²
θ=0
72°
36°
36°
72°
ANGLE
CHART NO. 121
RELATIVE POWER ONE WAY (db)
0
2
4
6
8
10
2
4
6
8
20
30
2
4
6
8
40

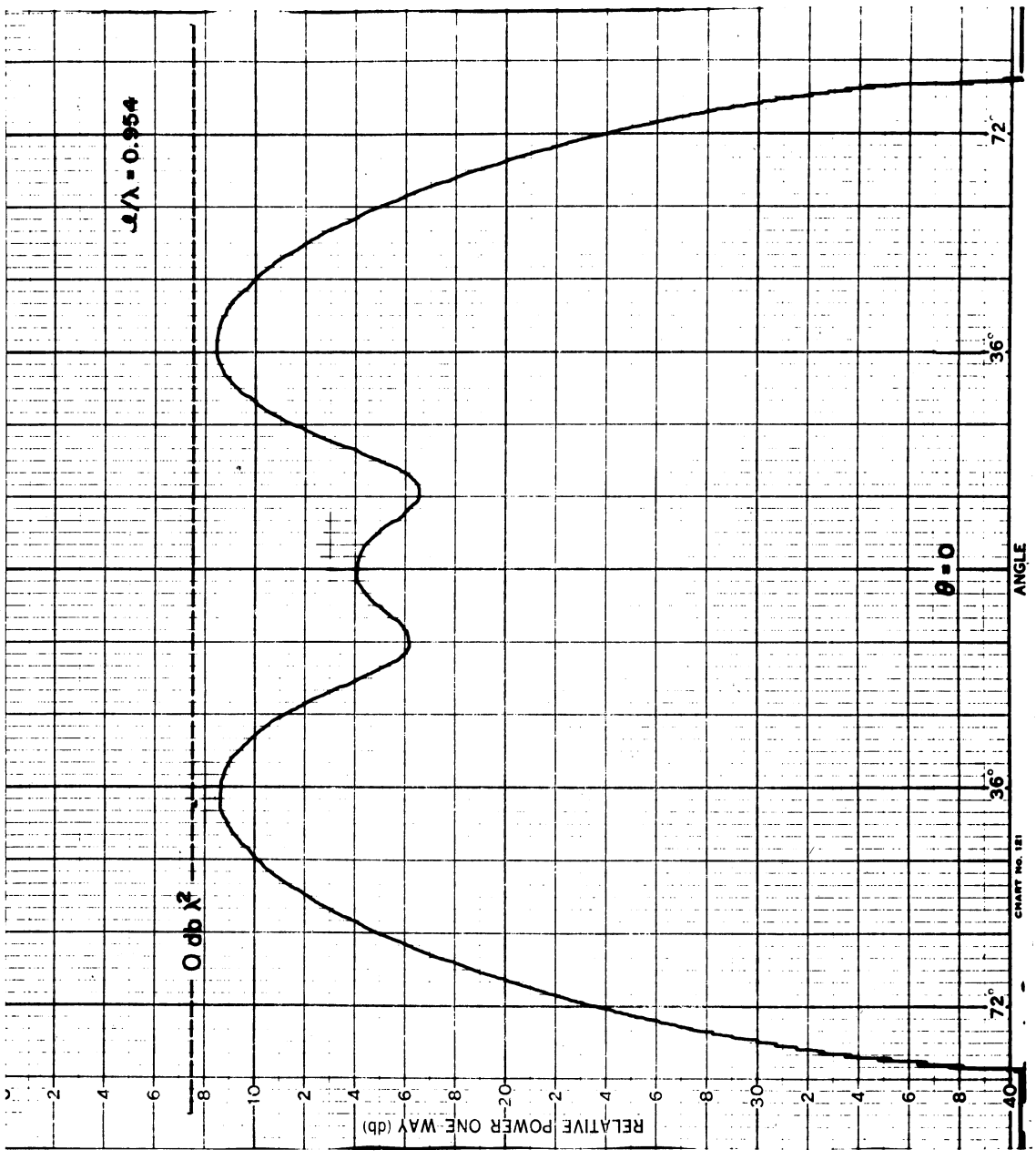
L/λ = 0.954
0 db
RELATIVE POWER ONE WAY (db)
ANGLE
Ø = 0
72°
36°
36°
72°
CHART NO. 121

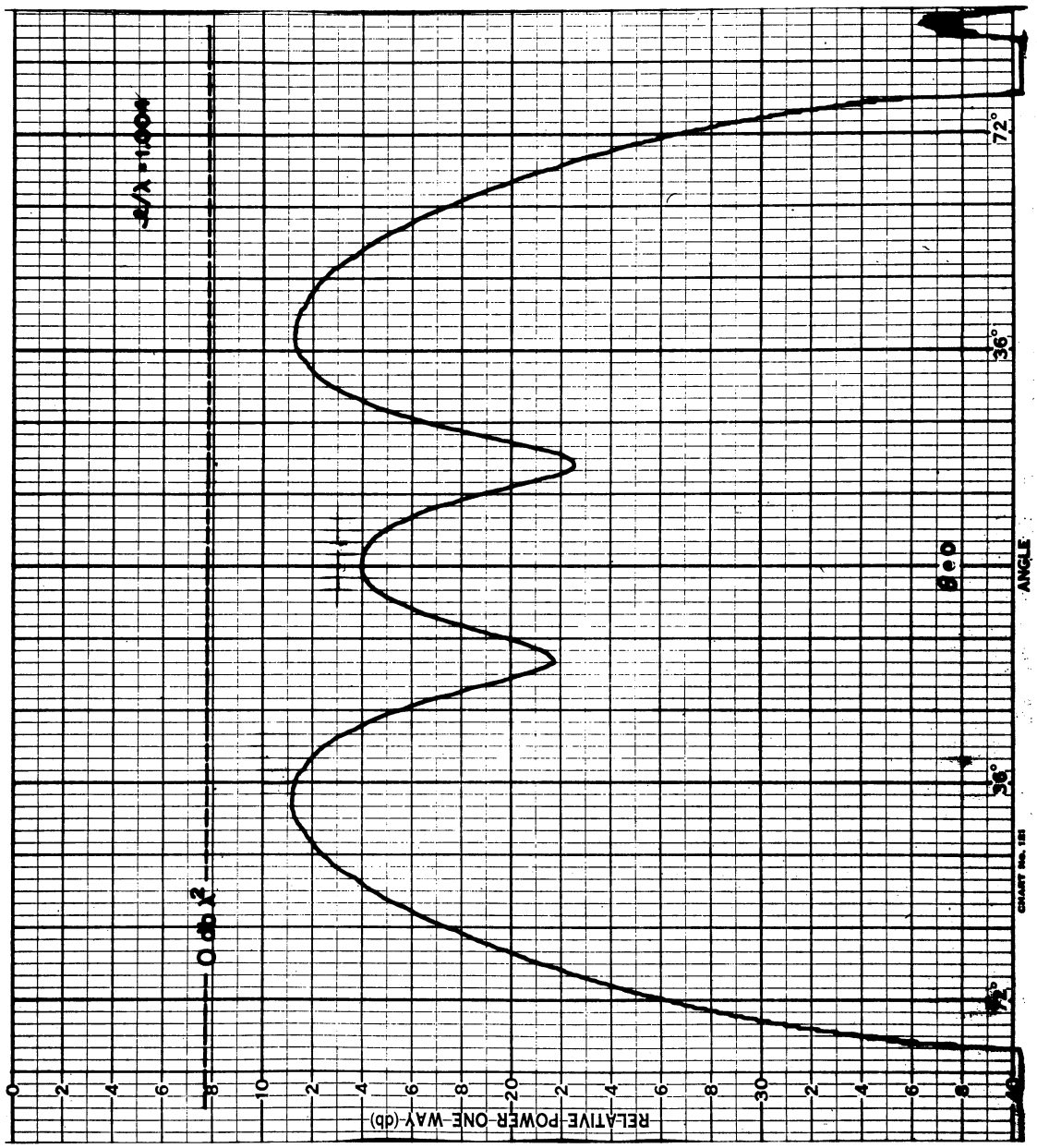
RELATIVE POWER ONE WAY (db)
ANGLE
72°
36°
0°
36°
72°
0 db
8 db

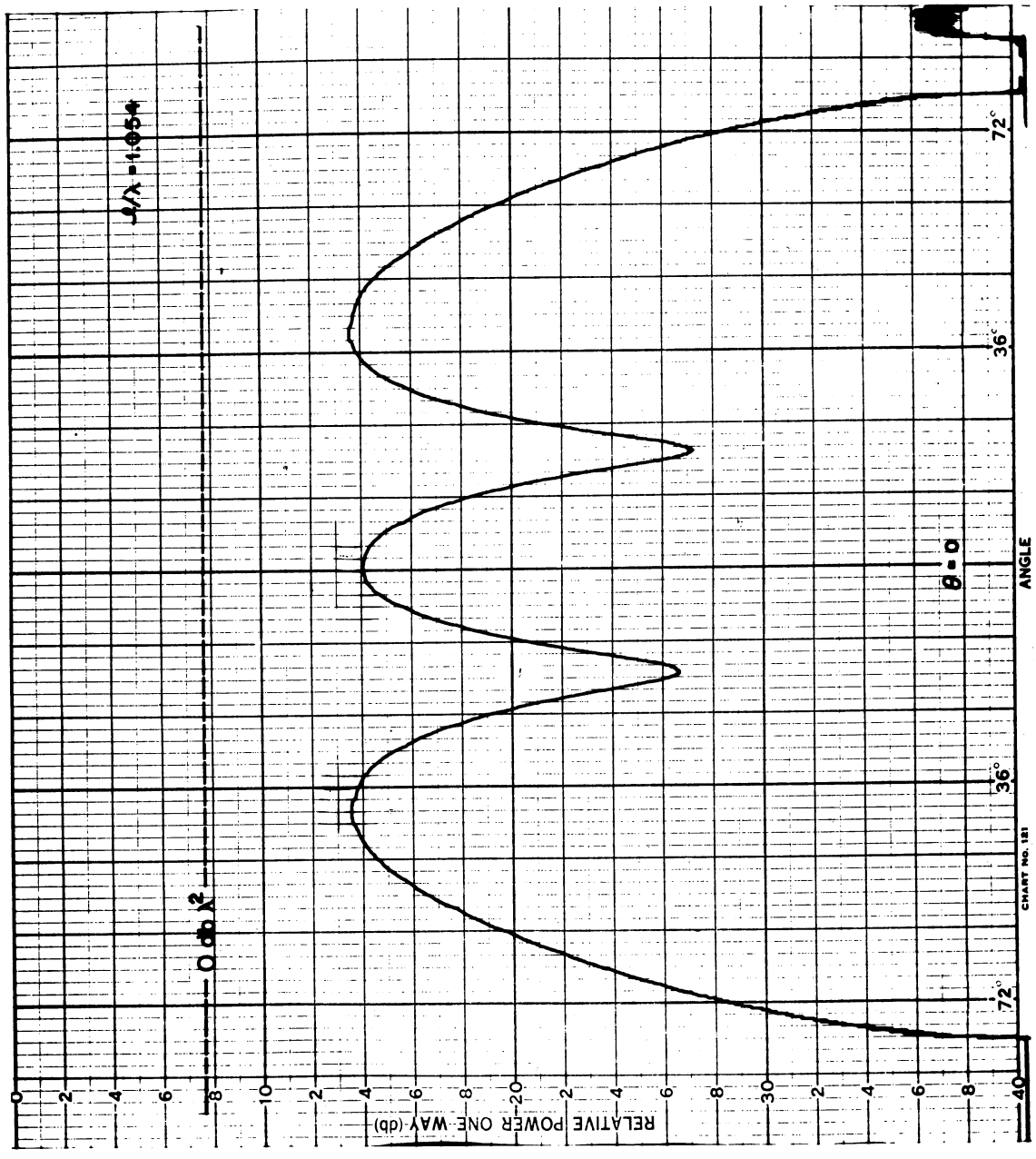
d/λ=1.054
2 db
θ=0
72°
36°
36°
72°
ANGLE
RELATIVE POWER ONE WAY (db)
0
2
4
6
8
10
2
4
6
8
20
2
4
6
8
30
2
4
6
8
40
CHART NO. 121

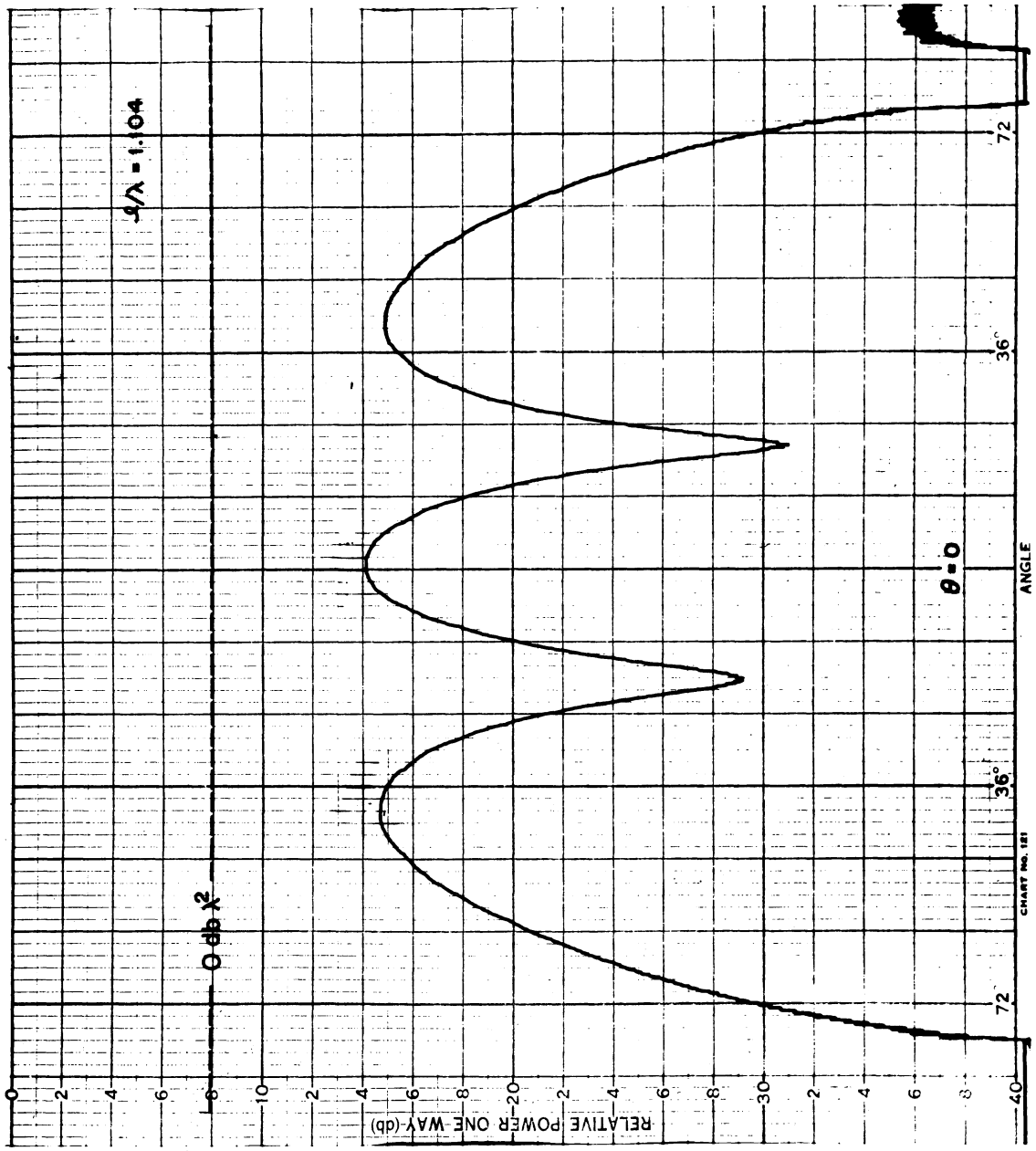
d/λ = 1.104
0 db
θ = 0
72°
36°
36°
72°
ANGLE
CHART NO. 181
RELATIVE POWER ONE WAY-(db)
0
2
4
6
8
10
20
30
40

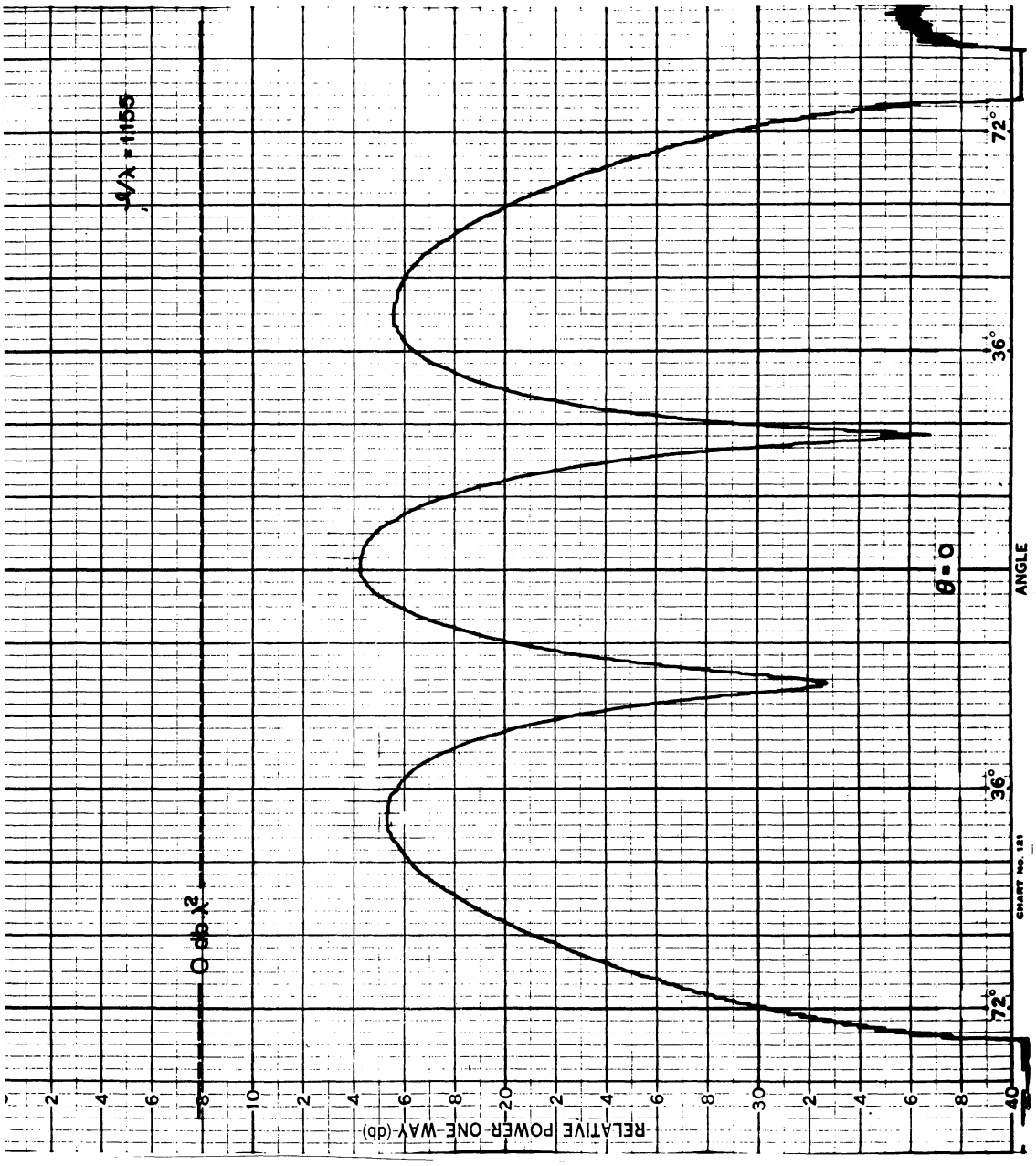
d/λ = 1.155
0 db
θ = 0
72°
36°
36°
72°
ANGLE
RELATIVE POWER ONE-WAY-(db)
CHART No. 121

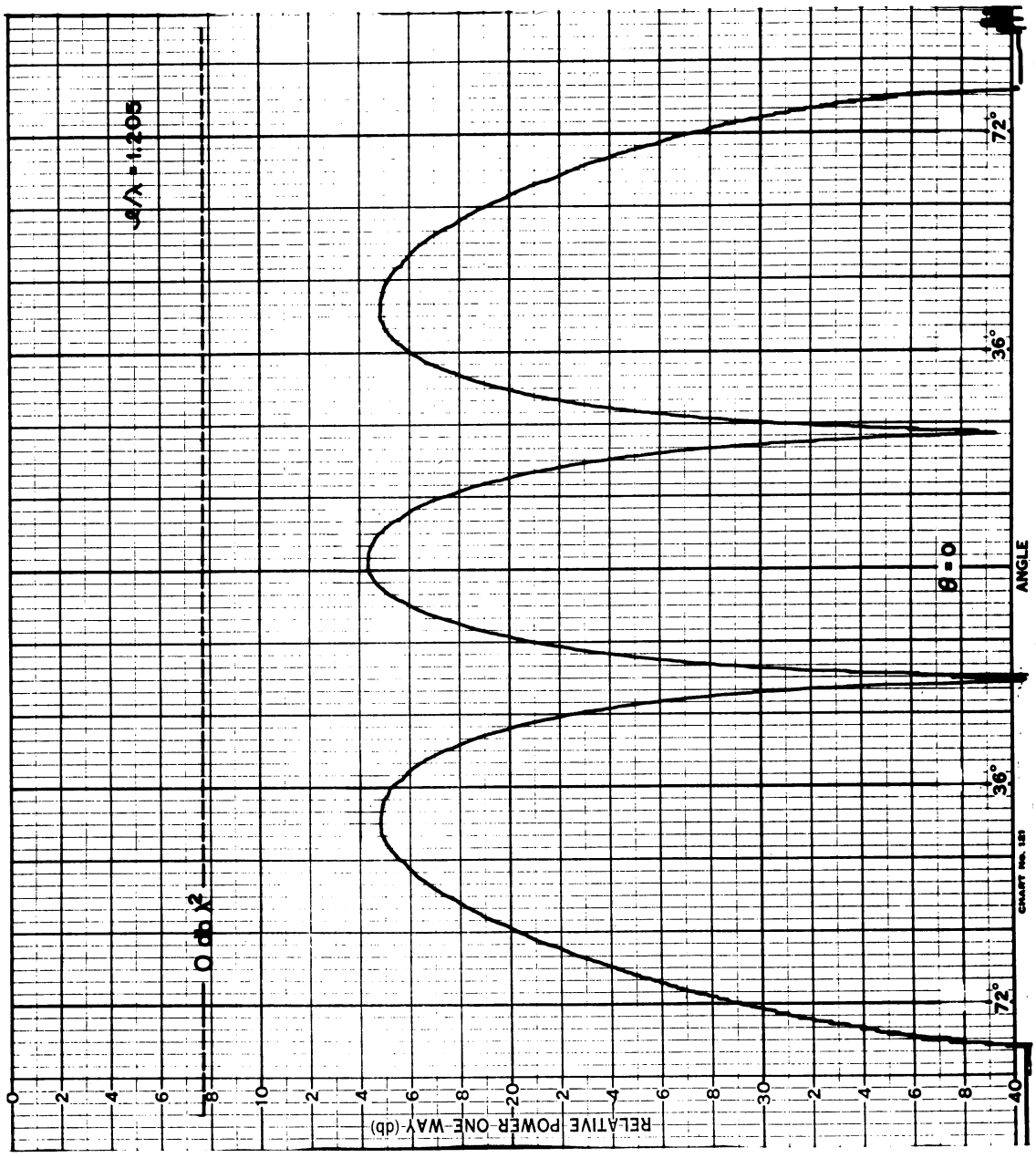
s/λ = 1.205
0 db
θ = 0
72°
36°
36°
72°
ANGLE
RELATIVE POWER ONE WAY (db)
0
2
4
6
8
10
2
4
6
8
20
2
4
6
8
30
2
4
6
8
40

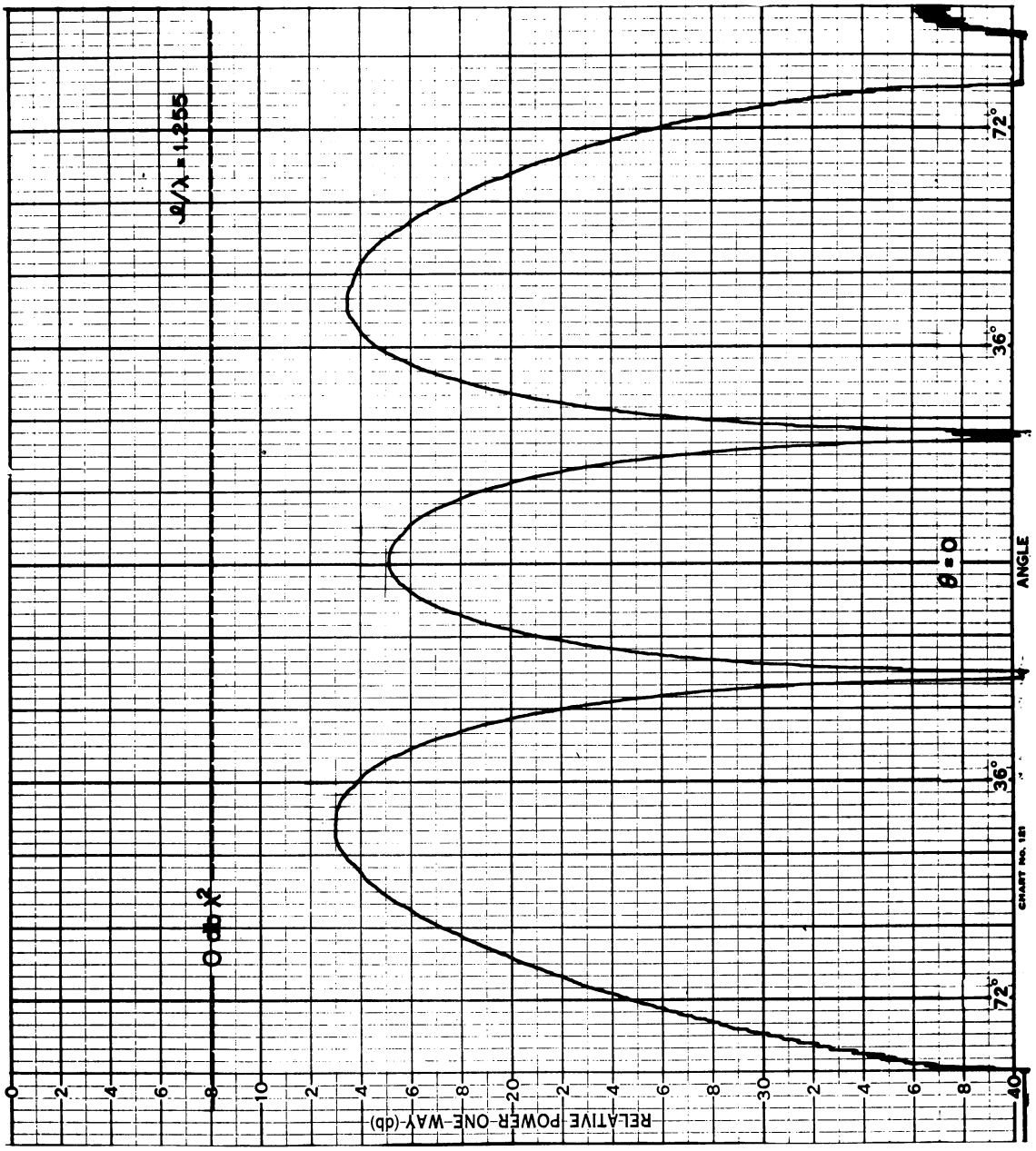
ℓ/λ = 1.255
0 db
θ = 0
ANGLE
72°
36°
36°
72°
RELATIVE POWER-ONE-WAY-(db)
0
2
4
6
8
10
2
4
6
8
20
2
4
6
8
30
2
4
6
8
40

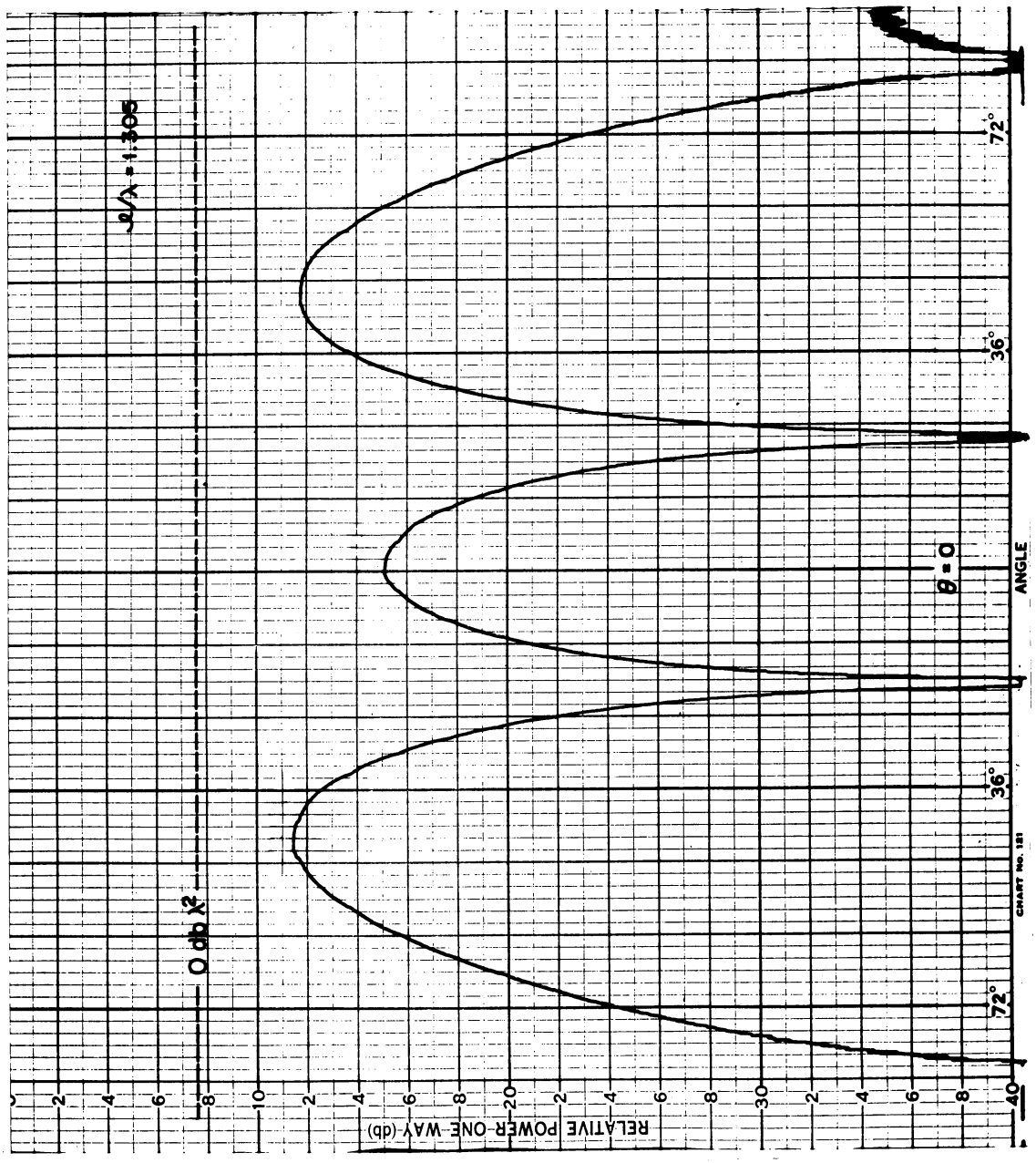
ℓ/λ = 1.305
0 db
θ = 0
72°
36°
36°
72°
ANGLE
RELATIVE POWER-ONE-WAY-(db)
0
2
4
6
8
10
2
4
6
8
20
2
4
6
8
30
2
4
6
8
40

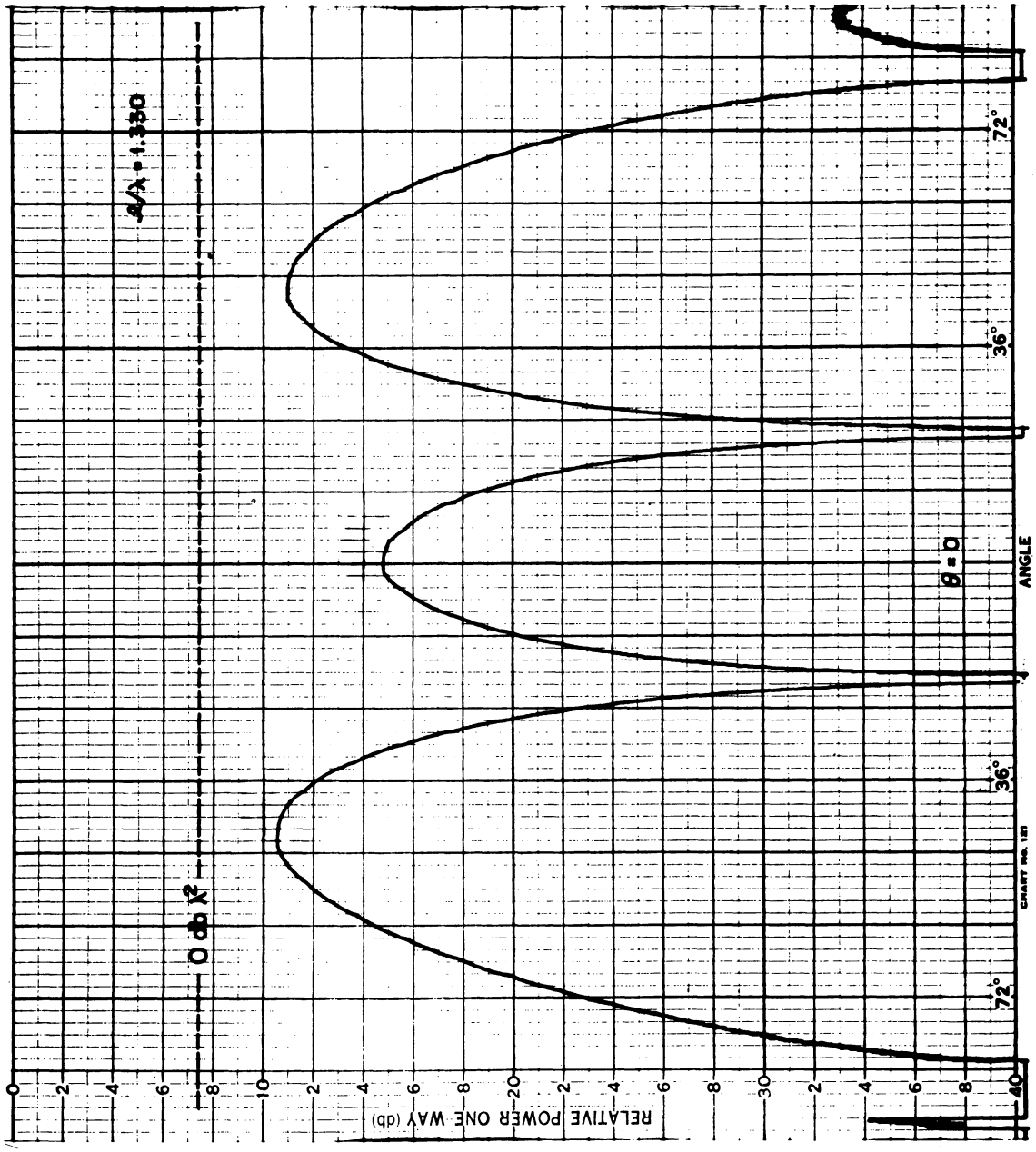
A/λ = 1.330
0 db
θ = 0
72°
36°
36°
72°
ANGLE
RELATIVE POWER ONE WAY (db)
0
2
4
6
8
10
2
4
6
8
20
2
4
6
8
30
2
4
6
8
40

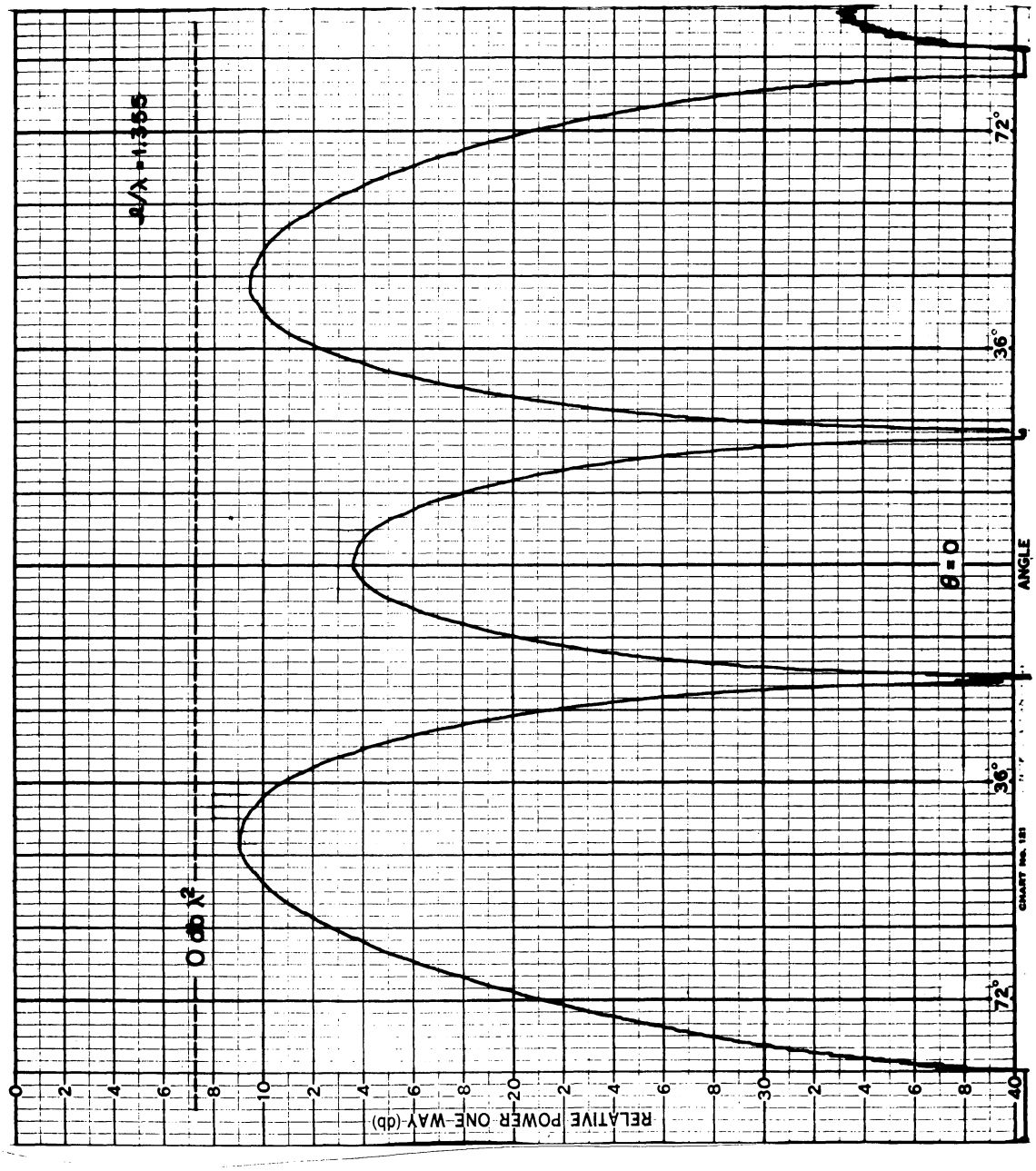
d/λ = 1.355
0 db
θ = 0
72°
36°
36°
72°
ANGLE
RELATIVE POWER ONE-WAY (db)
0
2
4
6
8
10
2
4
6
8
20
2
4
6
8
30
2
4
6
8
40

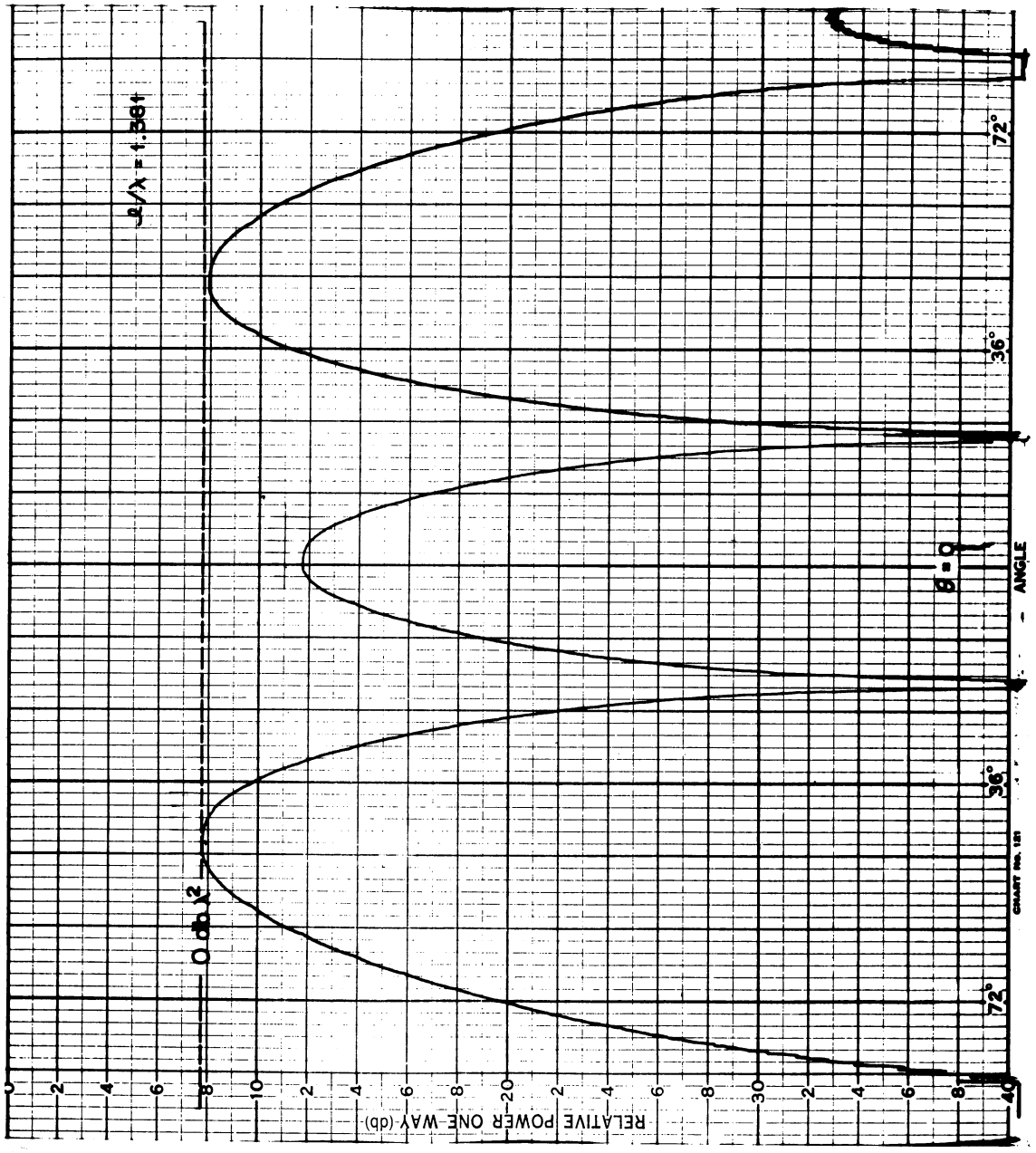
2/λ = 1.361
0 db
72°
36°
θ = 0
36°
72°
ANGLE
RELATIVE POWER ONE WAY (db)
0
2
4
6
8
10
2
4
6
8
20
2
4
6
8
30
2
4
6
8
40

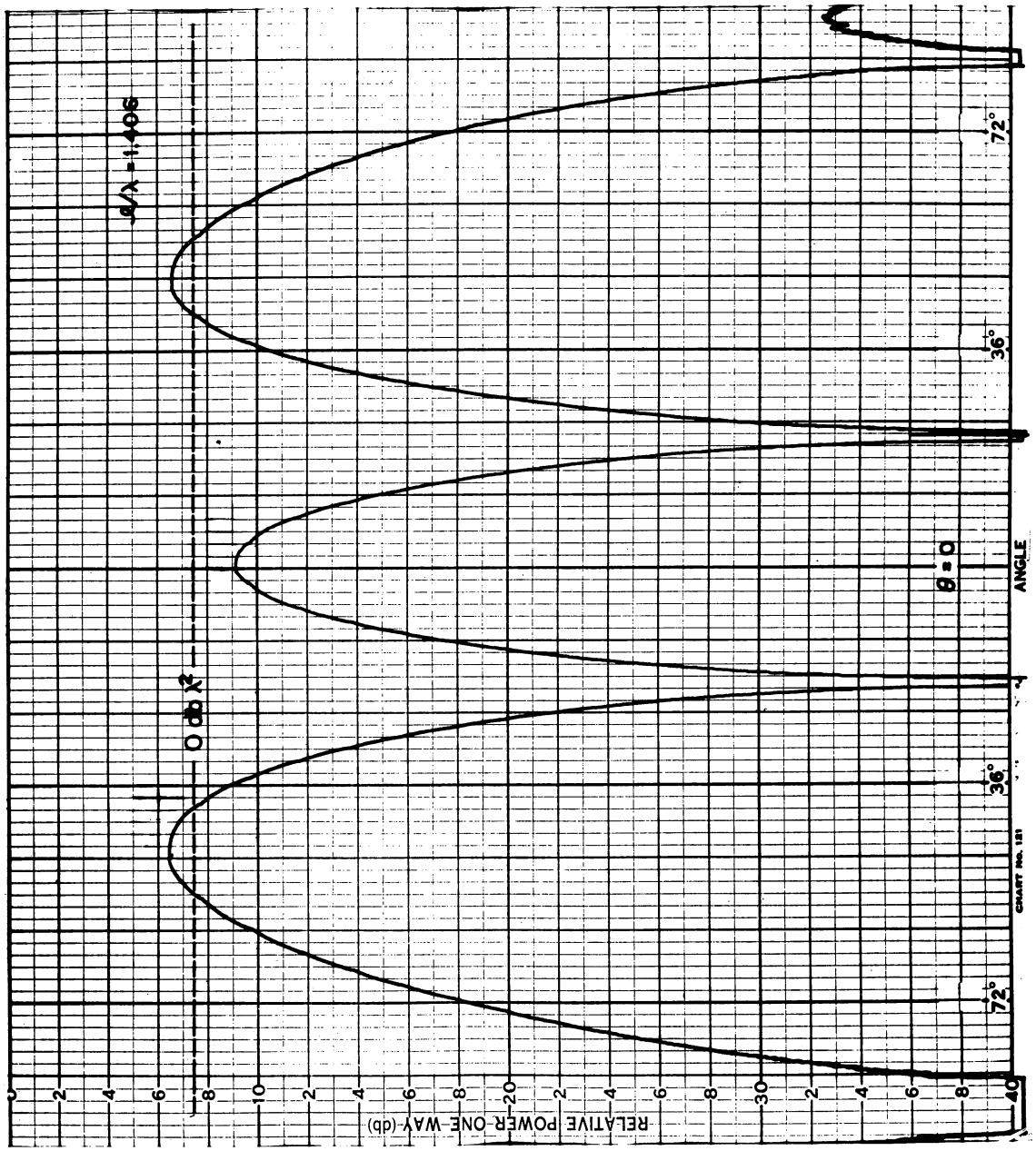
d/λ = 1.406
0 dB re
θ = 0
72°
36°
36°
72°
ANGLE
RELATIVE POWER ONE-WAY (db)
0
2
4
6
8
10
2
4
6
8
20
2
4
6
8
30
2
4
6
8
40

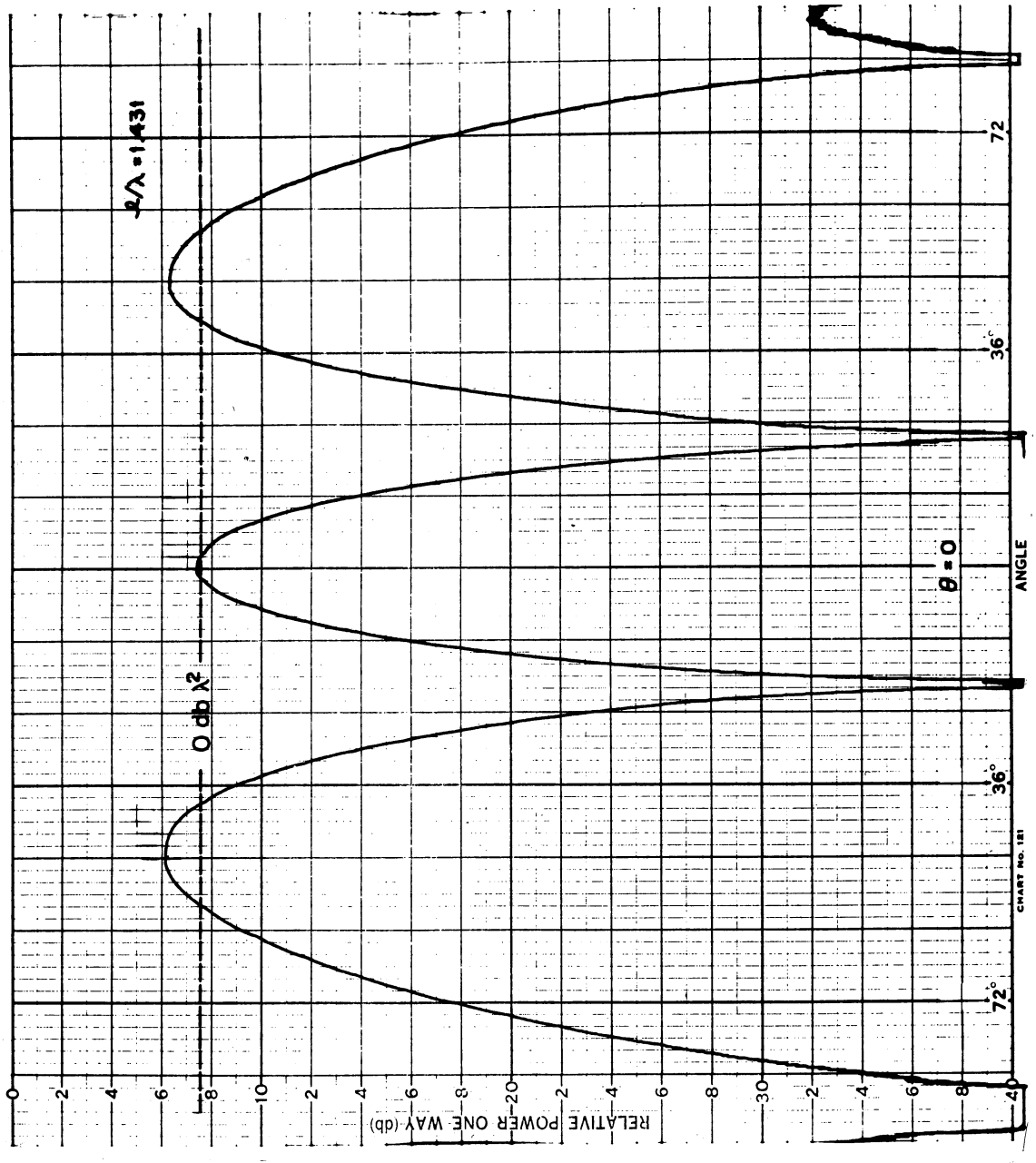
ℓ/λ = 1.431
0 db λ²
θ = 0
72°
36°
36°
72°
ANGLE
RELATIVE POWER ONE WAY (db)
CHART No. 121

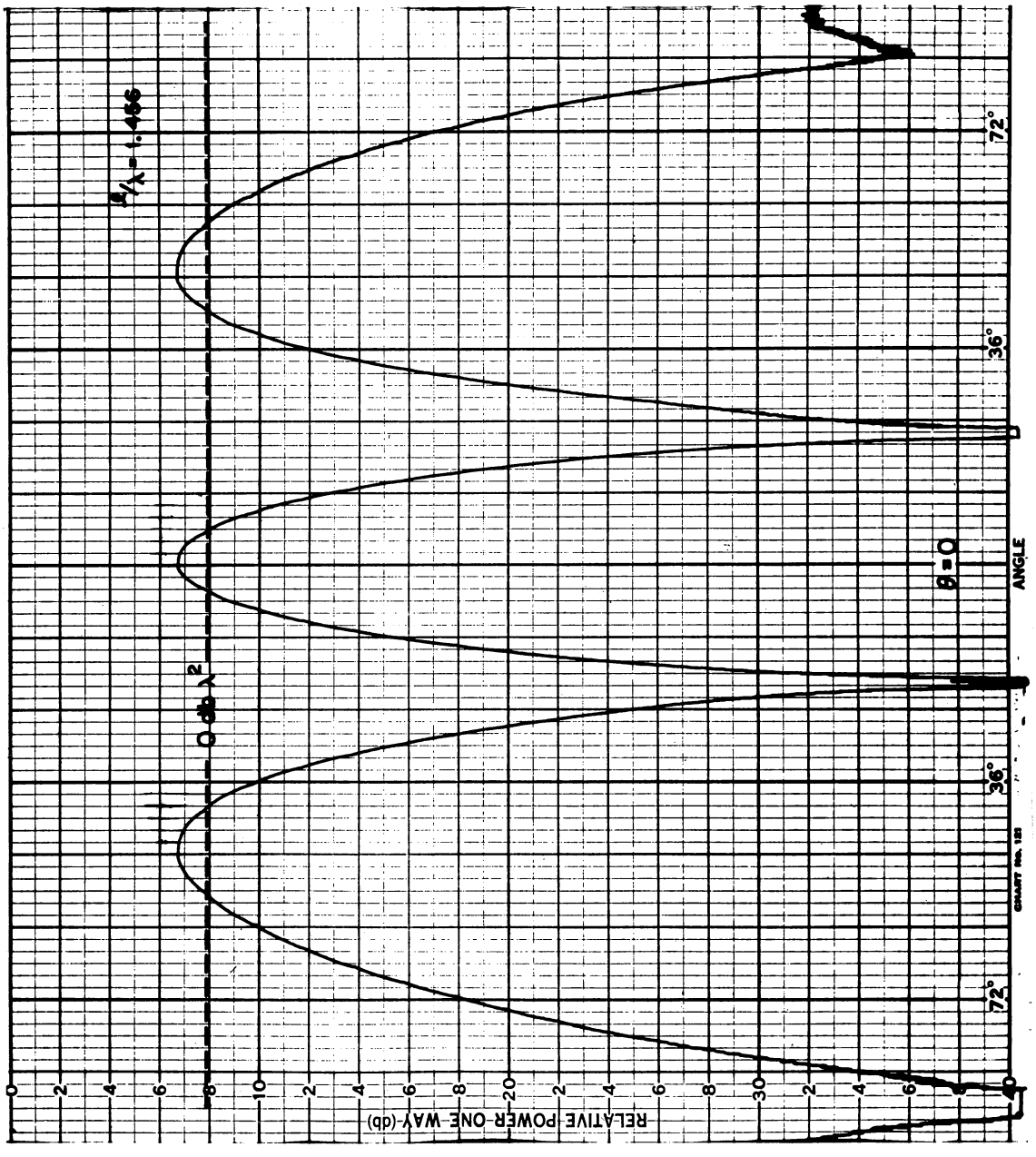
d/λ = 1.466
0 db
θ = 0
72°
36°
36°
72°
ANGLE
RELATIVE POWER-ONE WAY-(db)
0
2
4
6
8
10
20
30
40

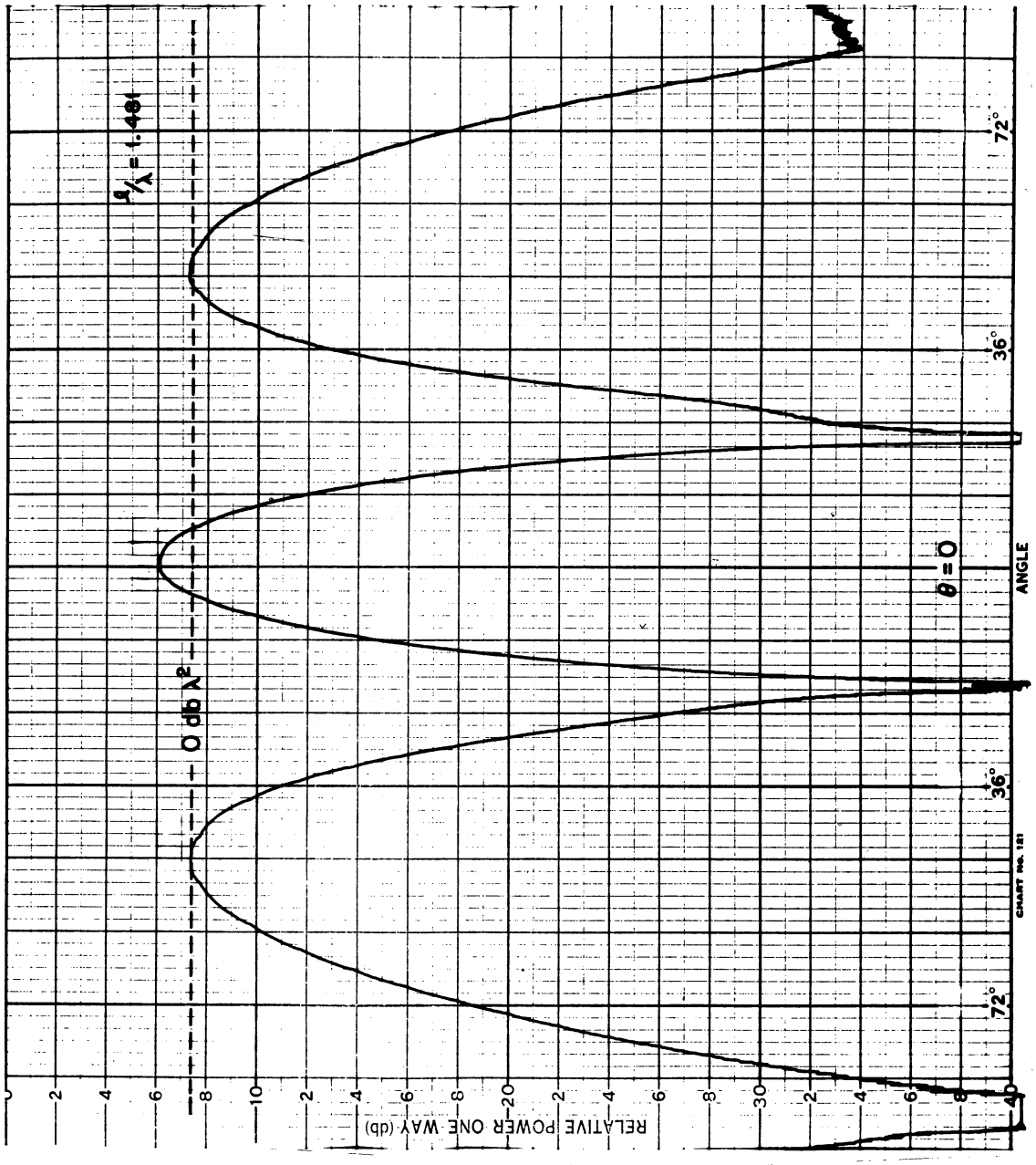
$\ell/\lambda = 1.461$
0 db
$\theta = 0$
72°
36°
36°
72°
ANGLE
RELATIVE POWER ONE WAY (db)
0
2
4
6
8
10
2
4
6
8
20
2
4
6
8
30
2
4
6
8
40

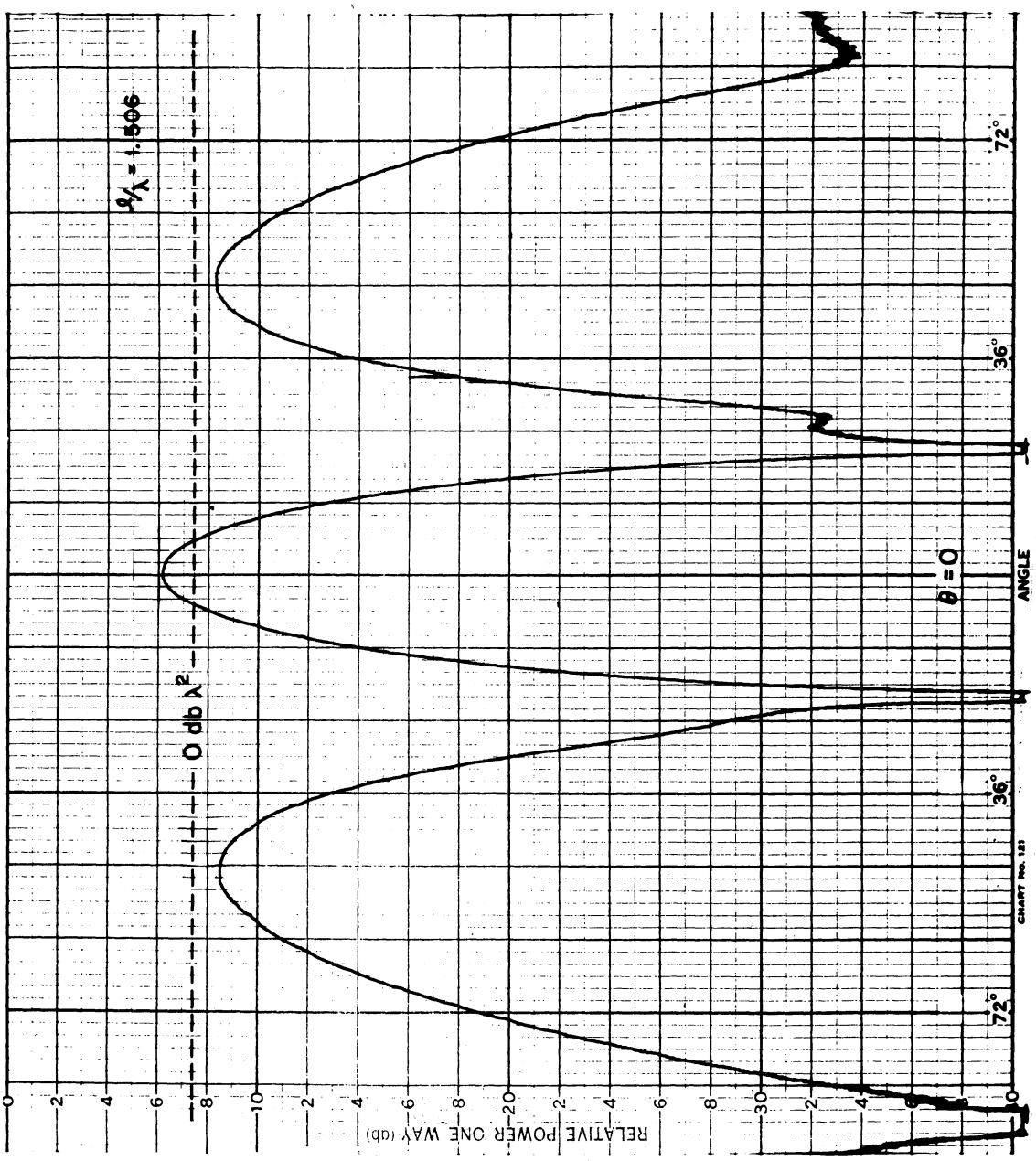
$\ell/\lambda = 1.506$
0 db λ^2
$\theta = 0$
72°
36°
36°
72°
ANGLE
RELATIVE POWER ONE WAY (db)
0
2
4
6
8
10
2
4
6
8
20
2
4
6
8
30
2
4
6
8
10

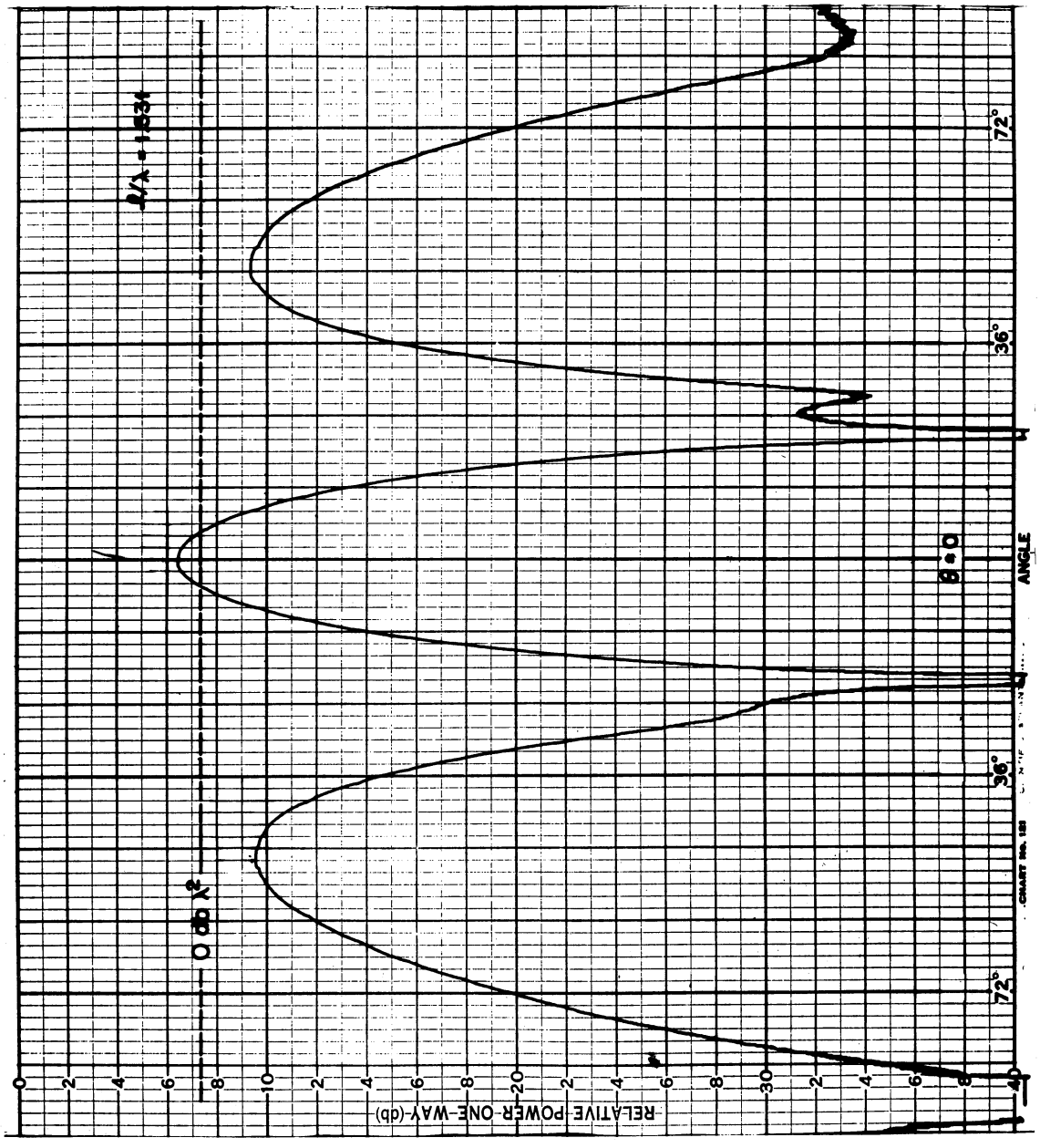
RELATIVE POWER ONE-WAY (db)
ANGLE
72°
36°
0
36°
72°

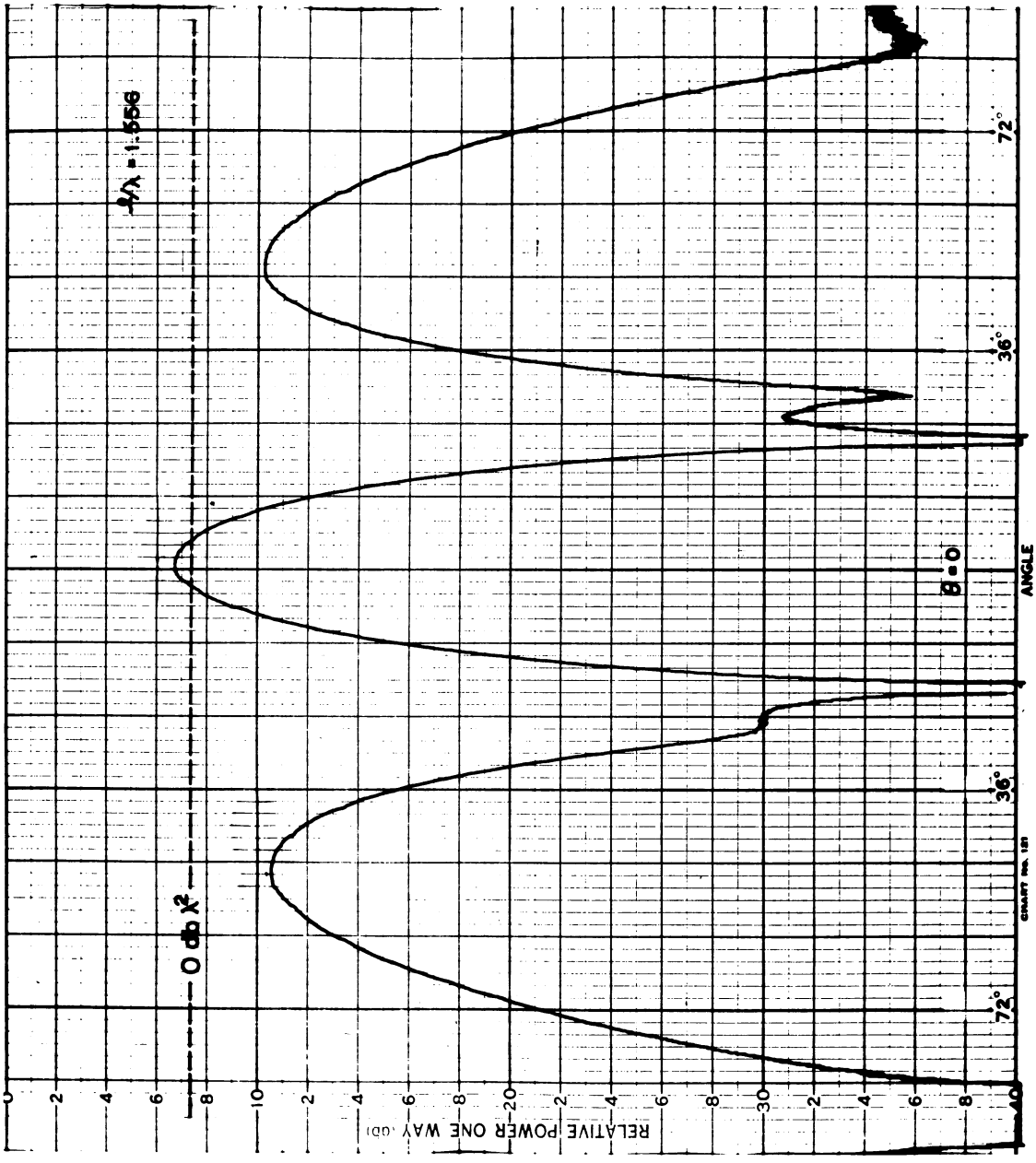
λ/λ = 1.556
0 db χ²
RELATIVE POWER ONE WAY (db)
0
2
4
6
8
10
2
4
6
8
20
2
4
6
8
30
2
4
6
8
40
72°
36°
θ = 0
36°
72°
ANGLE

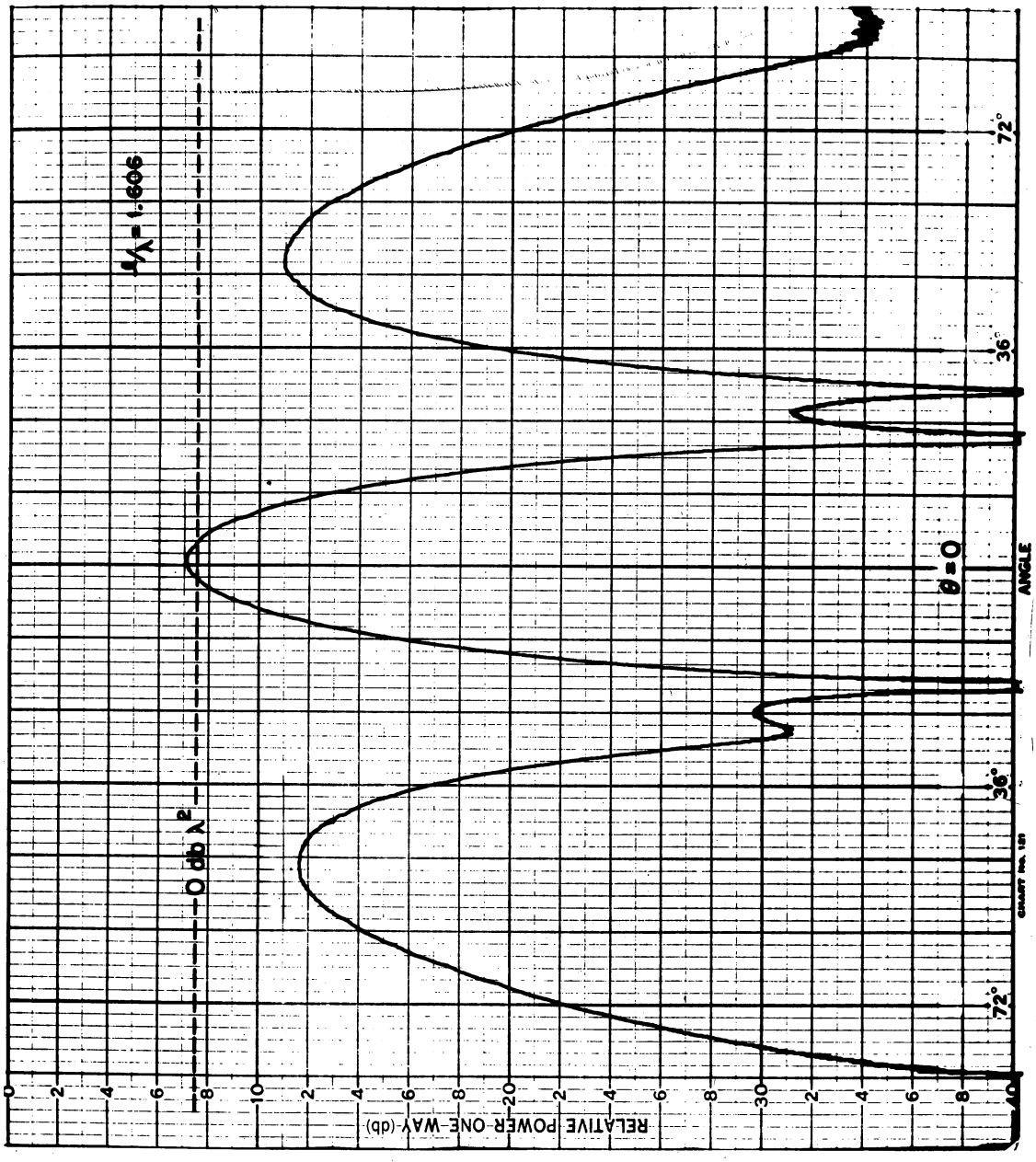
$\ell/\lambda = 1.606$
0 db
$\theta = 0$
72°
36°
36°
72°
ANGLE
RELATIVE POWER ONE-WAY (db)
0 2 4 6 8 10 2 4 6 8 20 2 4 6 8 30 2 4 6 8 40

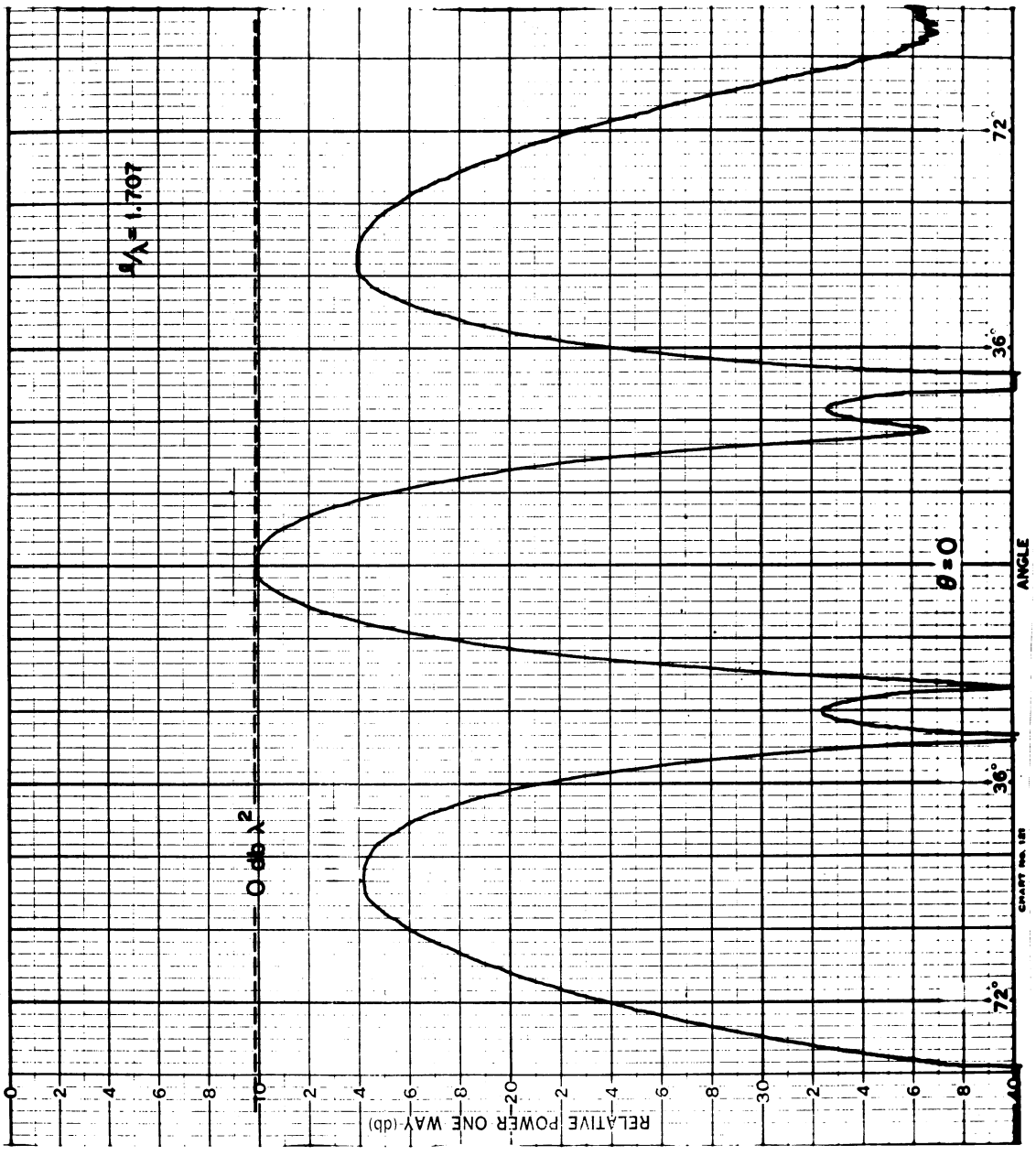
f/λ = 1.707
0 db
θ = 0
72°
36°
36°
72°
ANGLE
RELATIVE POWER ONE WAY (db)
0
2
4
6
8
10
2
4
6
8
20
2
4
6
8
30
2
4
6
8
40

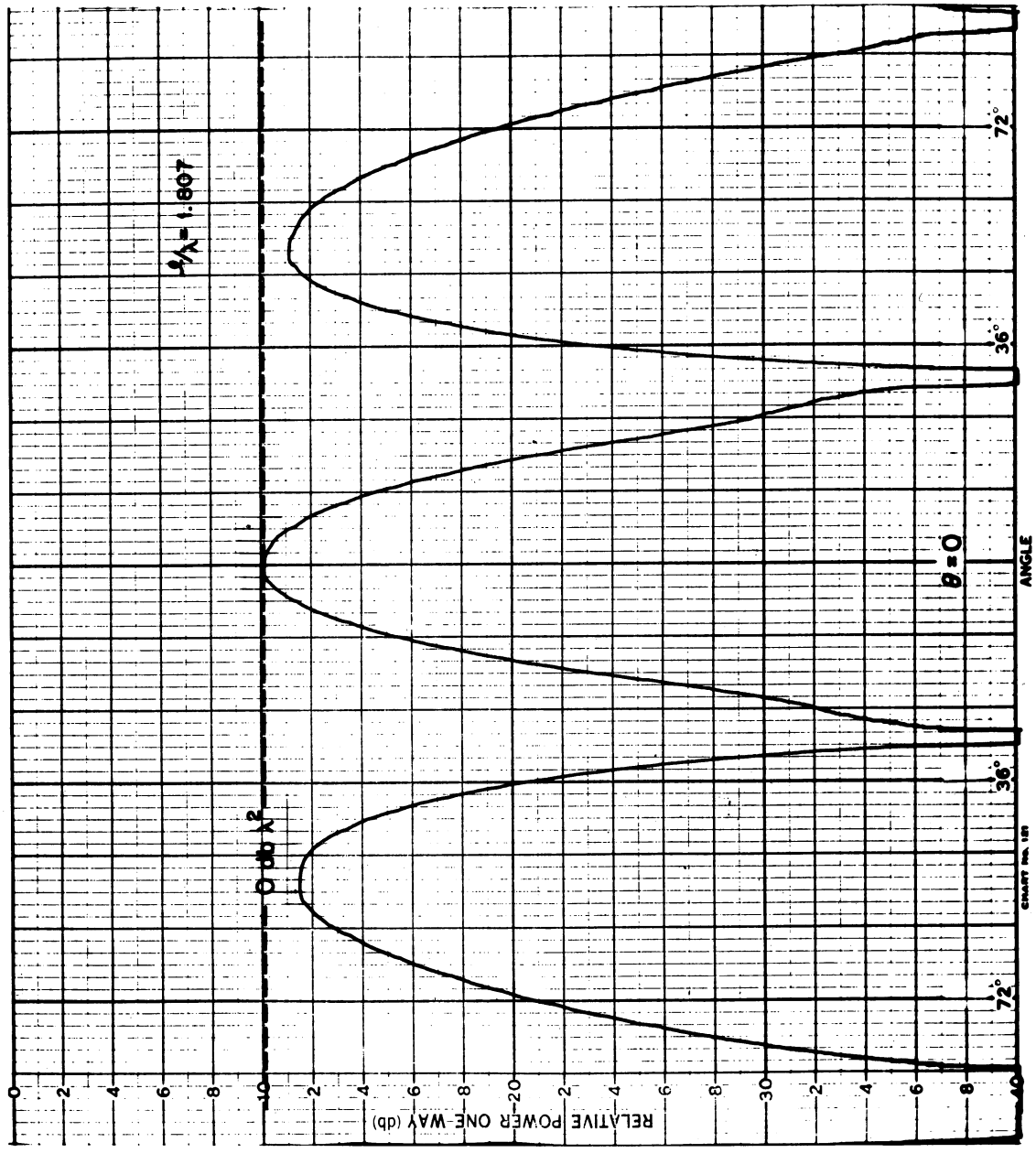
$\ell/\lambda = 1.807$
0 db
$\theta = 0$
72°
36°
36°
72°
ANGLE
RELATIVE POWER ONE-WAY (db)
0
2
4
6
8
10
2
4
6
8
20
2
4
6
8
30
2
4
6
8
40

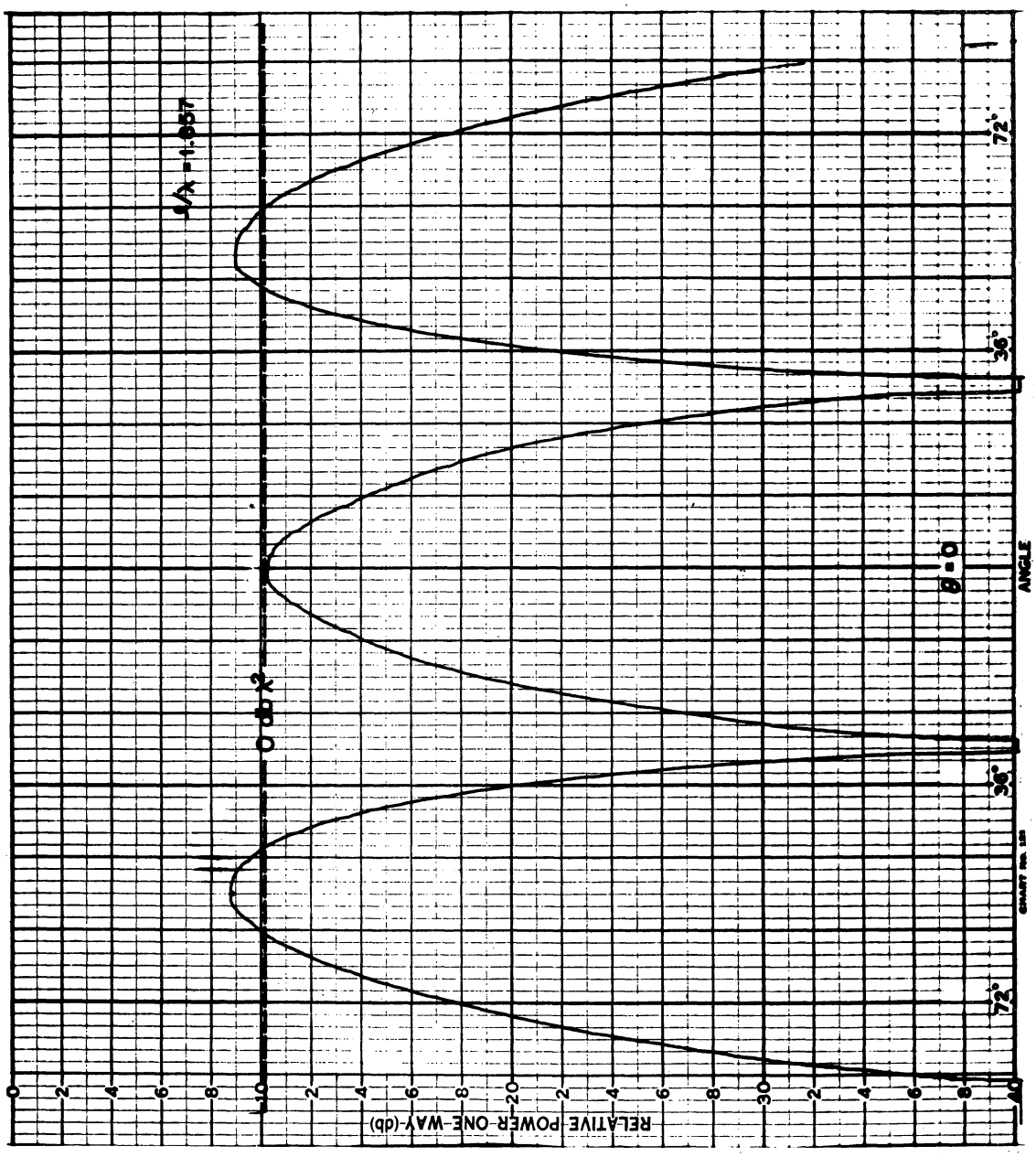
d/λ = 1.057
0 db
θ = 0
72°
36°
36°
72°
ANGLE
RELATIVE POWER-ONE-WAY (db)
0
2
4
6
8
10
2
4
6
8
20
2
4
6
8
30
2
4
6
8
40

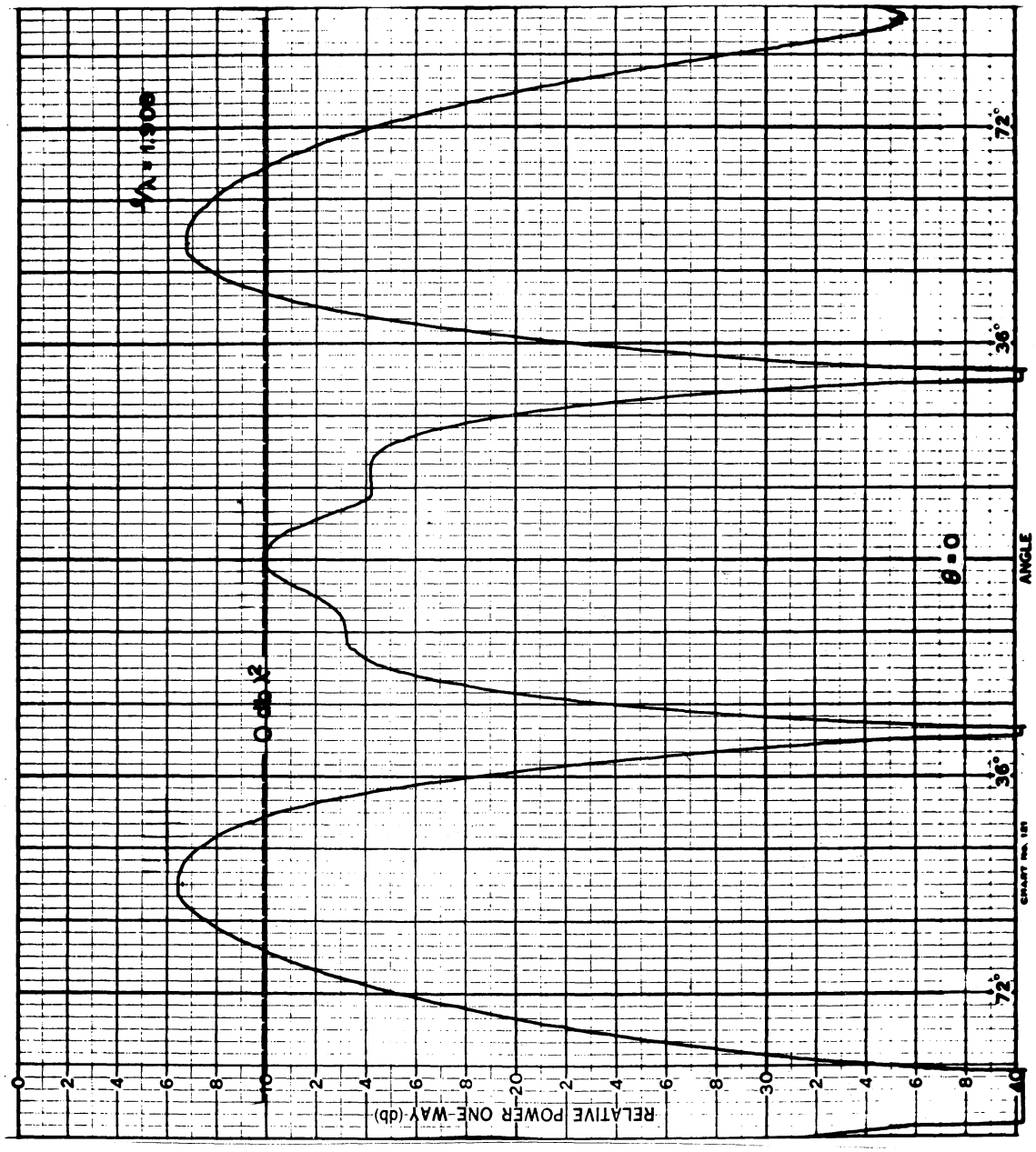
RELATIVE POWER ONE-WAY (db)
0
2
4
6
8
10
2
4
6
8
20
2
4
6
8
30
2
4
6
8
40
72°
36°
θ=0
36°
72°
ANGLE
0 db

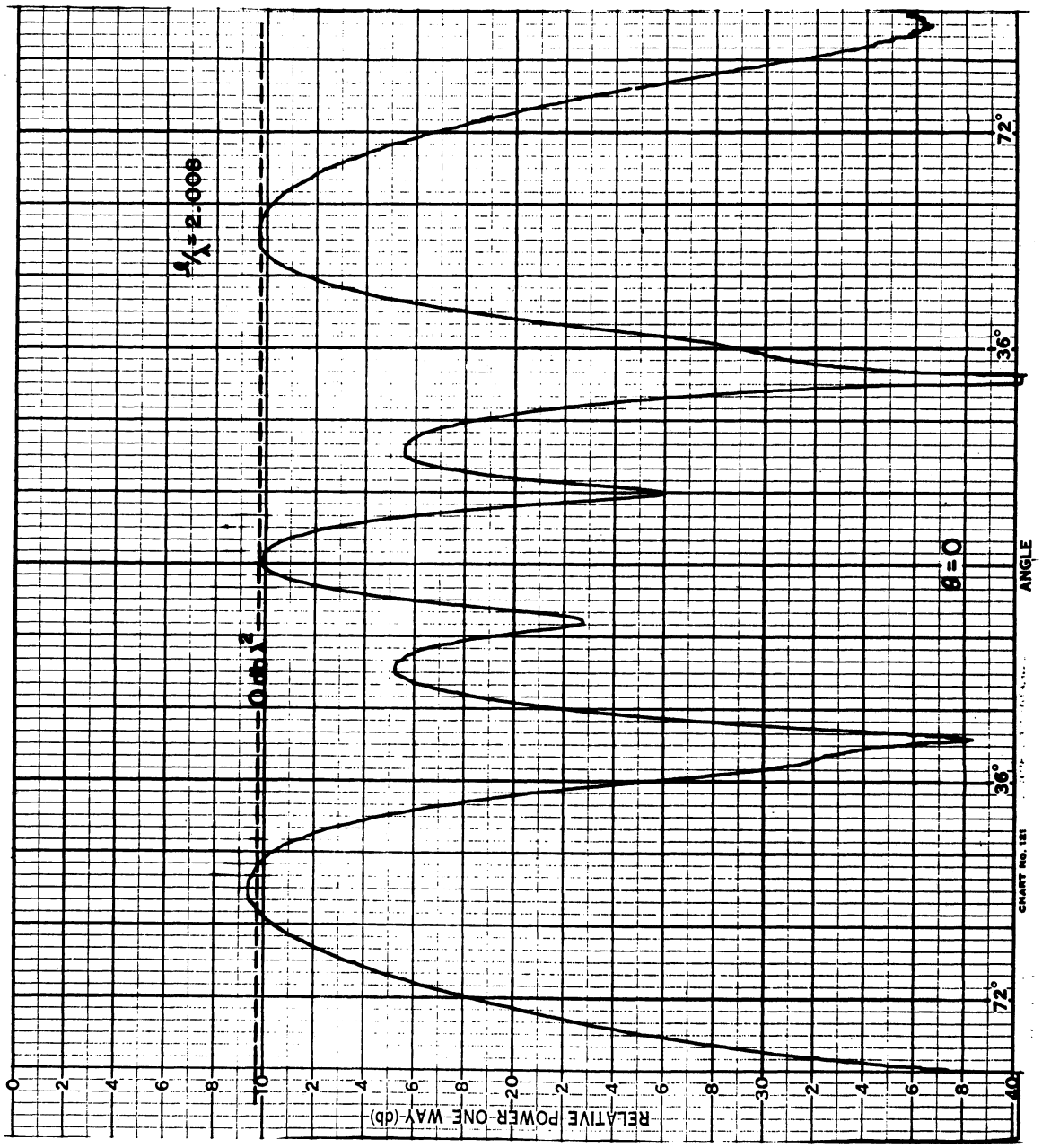
d/λ=2.008
0 db
θ=0
72°
36°
36°
72°
ANGLE
RELATIVE POWER-ONE-WAY-(db)
0
2
4
6
8
10
2
4
6
8
20
2
4
6
8
30
2
4
6
8
40
CHART No. 181

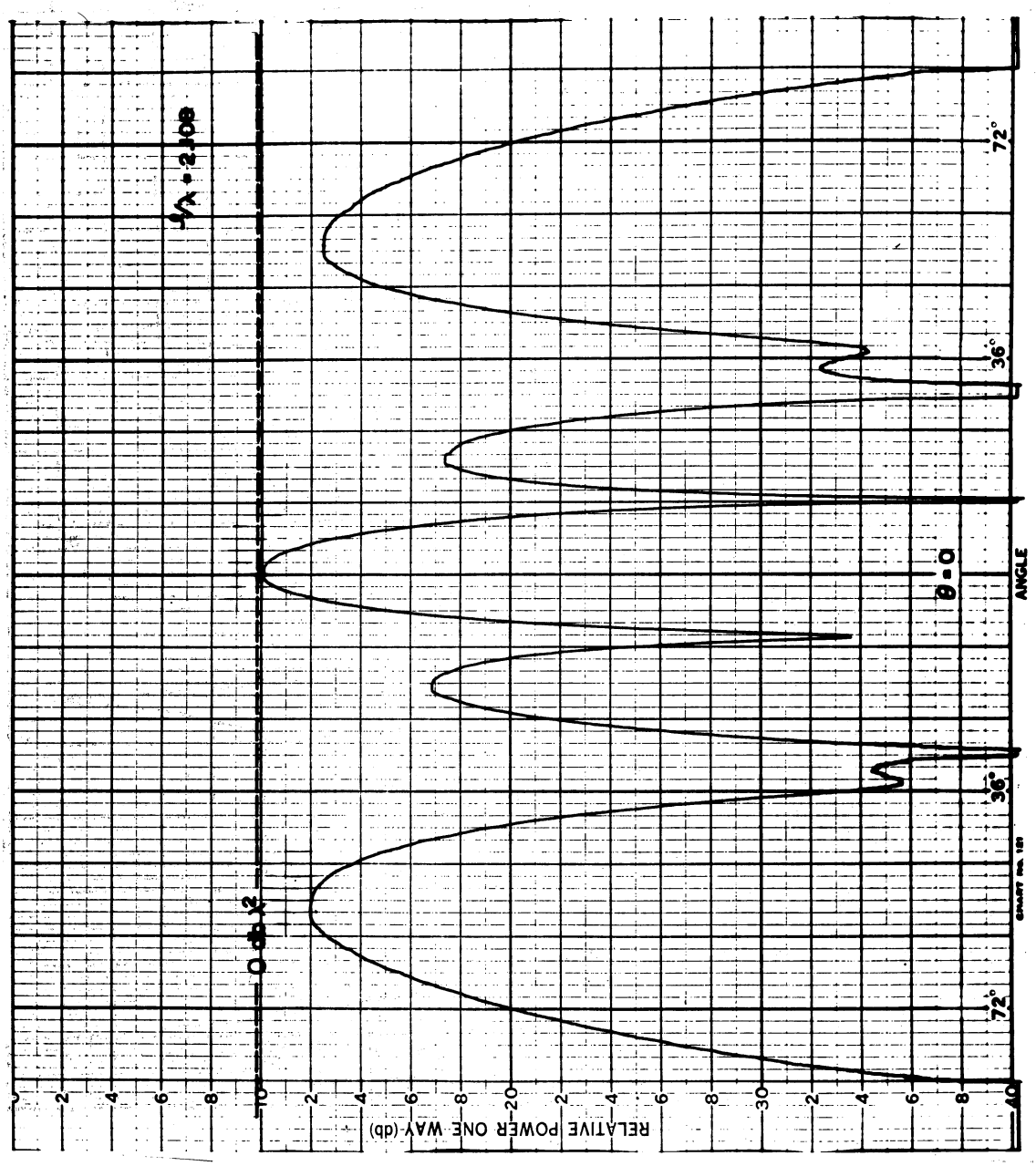
$l/\lambda = 2.108$
0 db
θ=0
72°
36°
36°
72°
ANGLE
RELATIVE POWER ONE WAY (db)
0
2
4
6
8
10
2
4
6
8
20
2
4
6
8
30
2
4
6
8
40

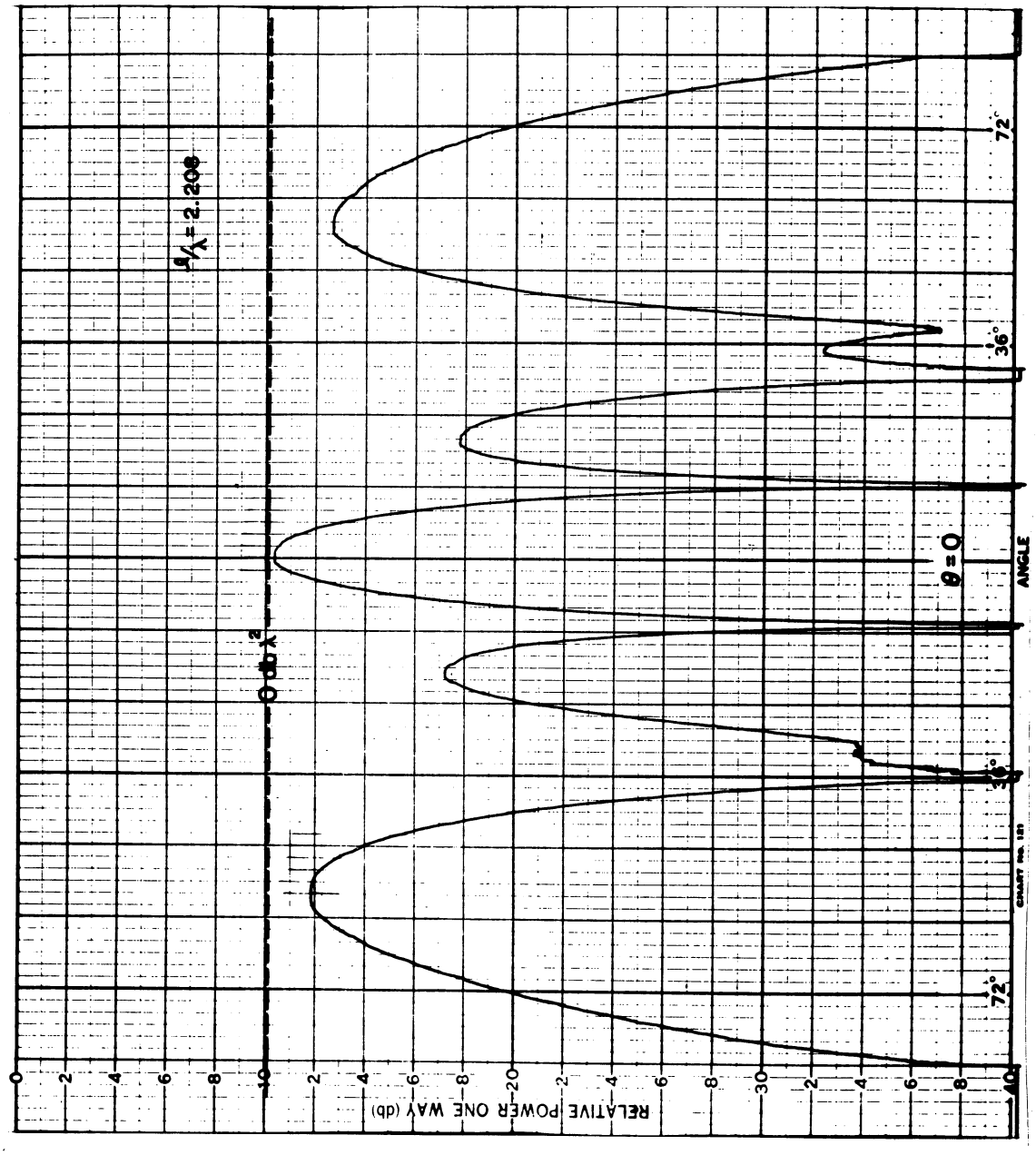
$d/\lambda = 2.208$
0 db
RELATIVE POWER ONE WAY (db)
0
2
4
6
8
10
20
30
40
72°
36°
30°
72°
θ = 0
ANGLE

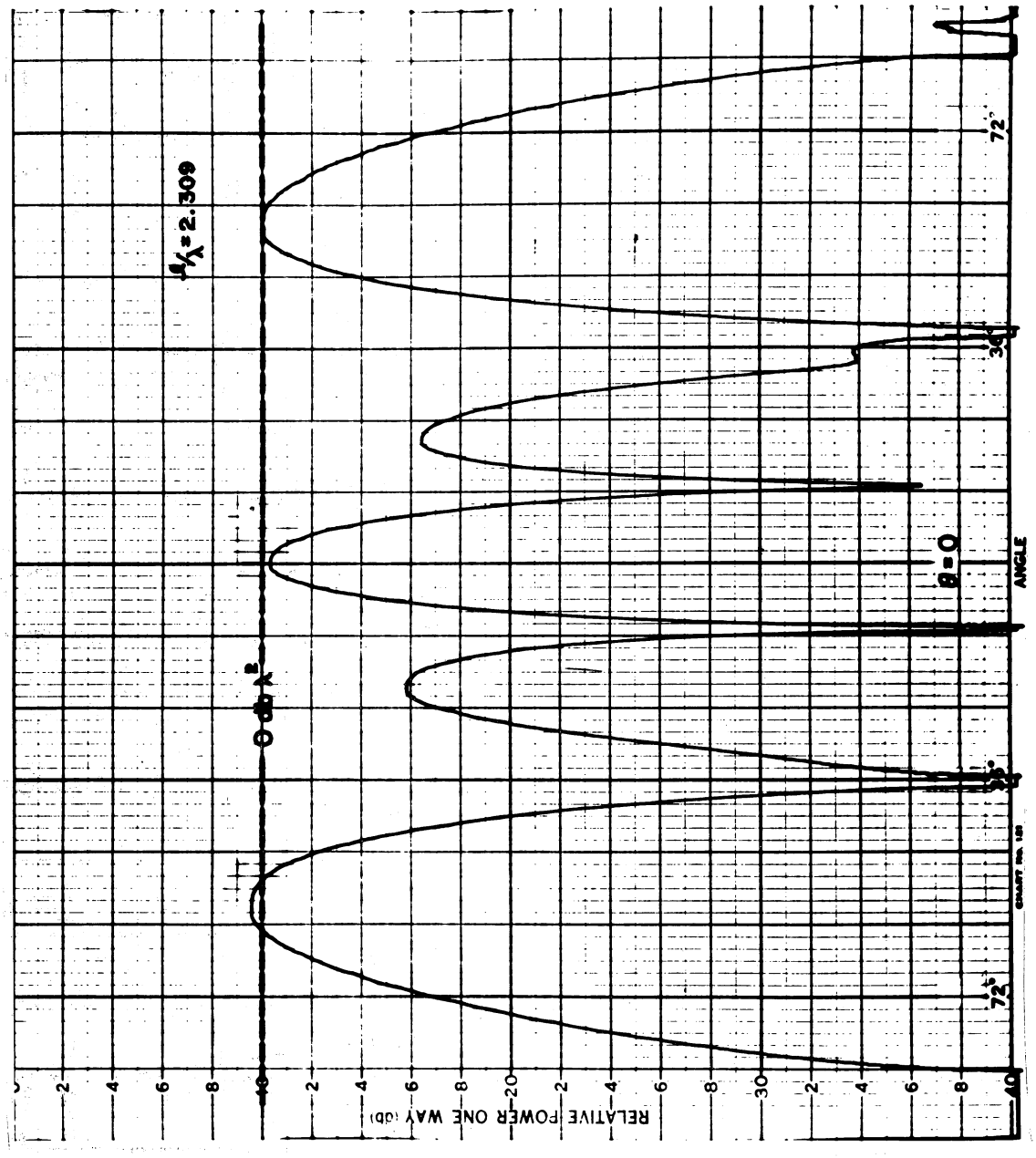
d/λ = 2.309
θ = 0
ANGLE
RELATIVE POWER ONE WAY (dB)

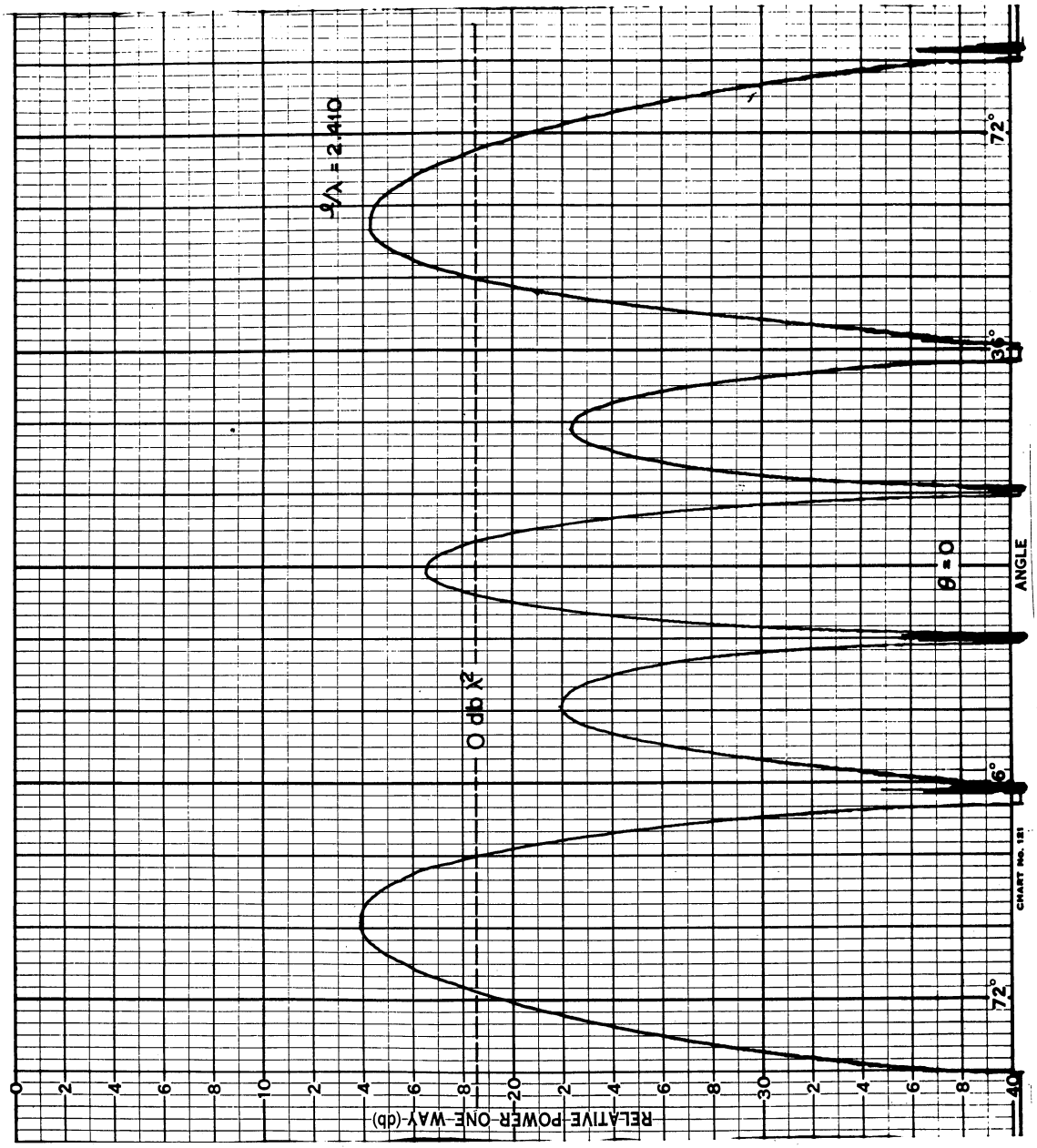
$g/\lambda = 2.410$
72°
36°
θ = 0
ANGLE
0 db
6°
72°
CHART No. 121
RELATIVE POWER ONE-WAY-(db)
0
2
4
6
8
10
2
4
6
8
20
2
4
6
8
30
2
4
6
8
40

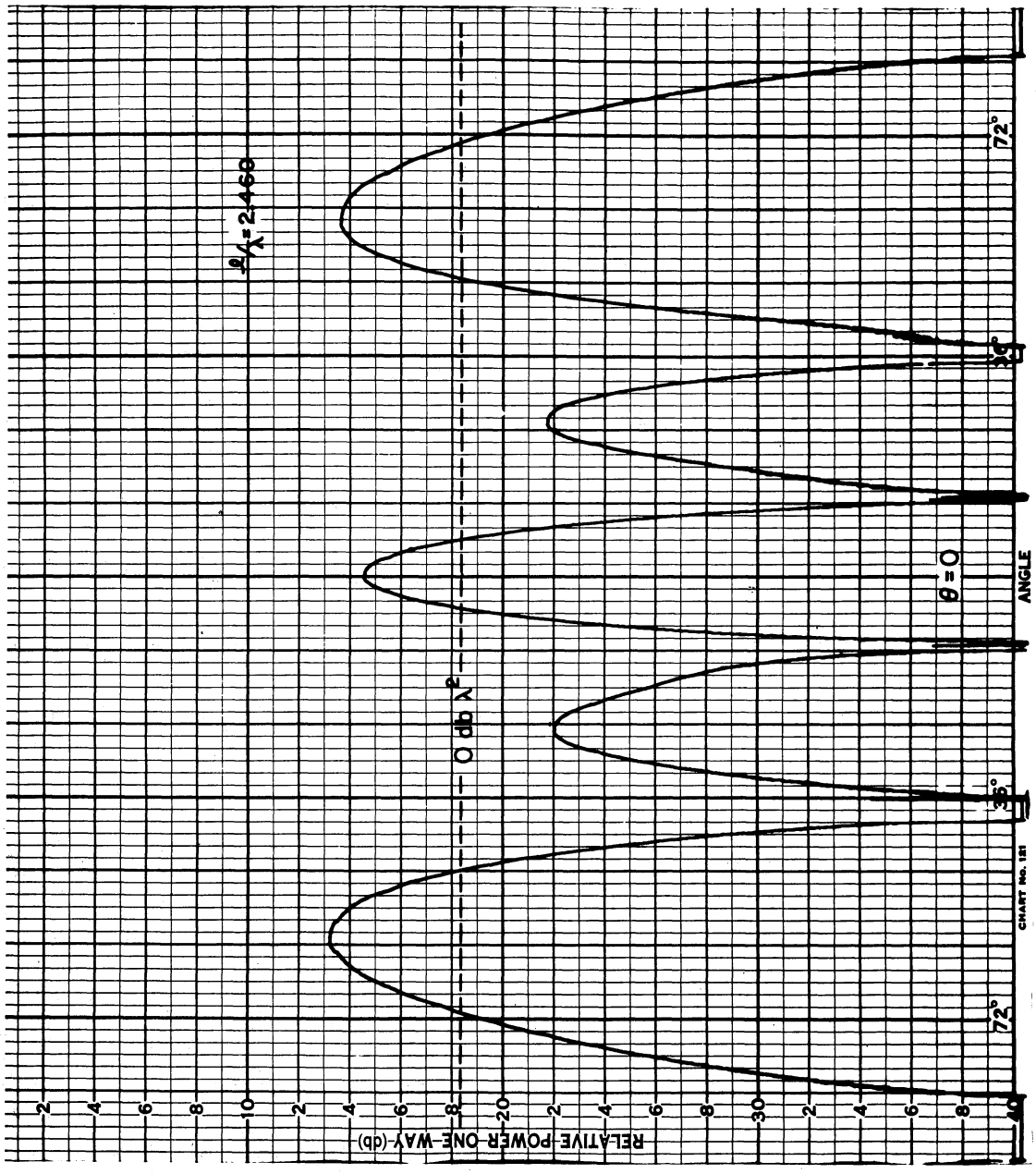
2l/λ=2.460
0 db
θ=0
ANGLE
72°
36°
90°
72°
RELATIVE POWER ONE-WAY (db)
-2
-4
-6
-8
-10
-2
-4
-6
-8
-20
-2
-4
-6
-8
-30
-2
-4
-6
-8
-40

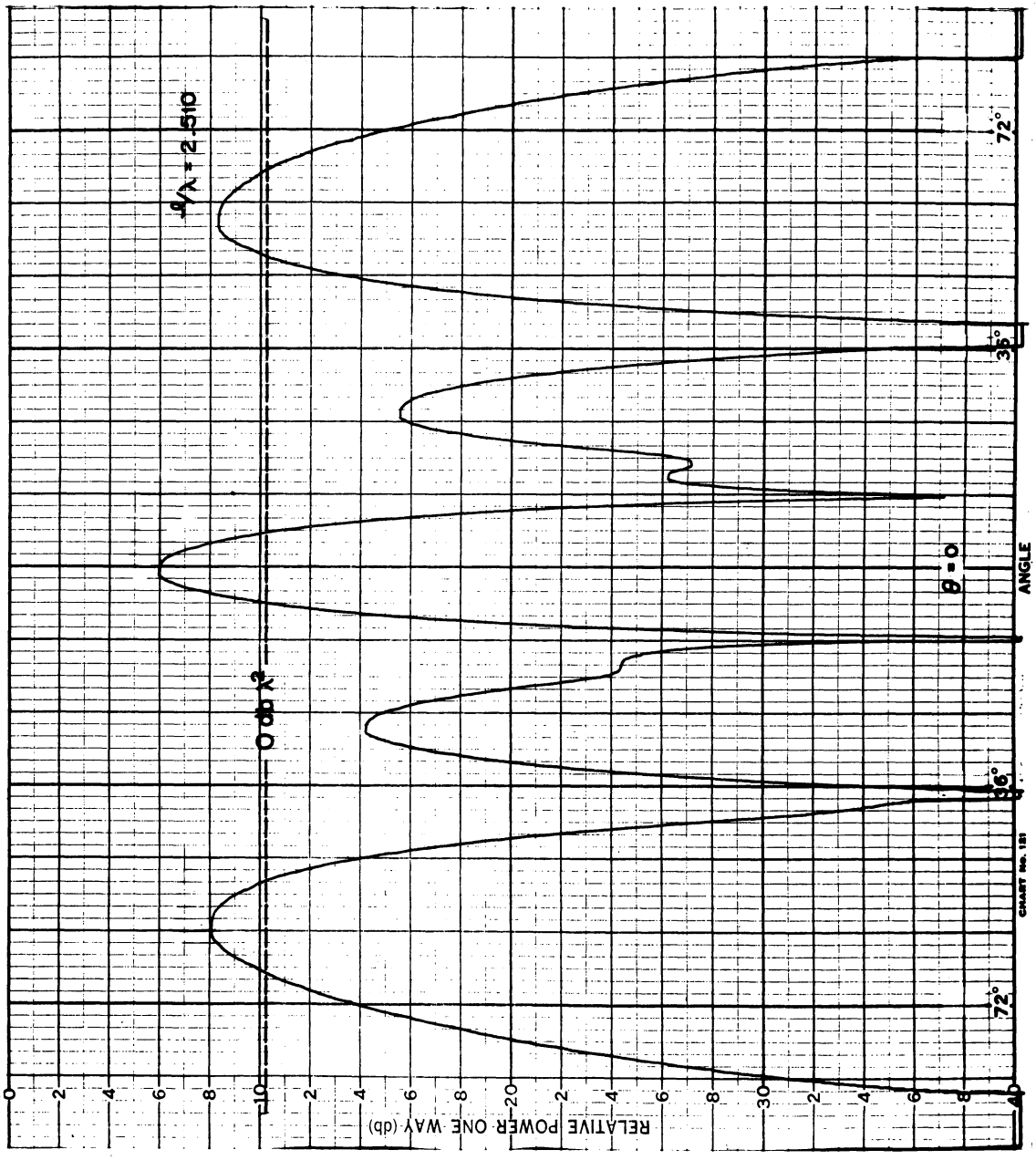
d/λ = 2.510
0 db
θ = 0
ANGLE
72°
36°
36°
72°
RELATIVE POWER ONE WAY (db)
0
2
4
6
8
10
2
4
6
8
20
2
4
6
8
30
2
4
6
8
40

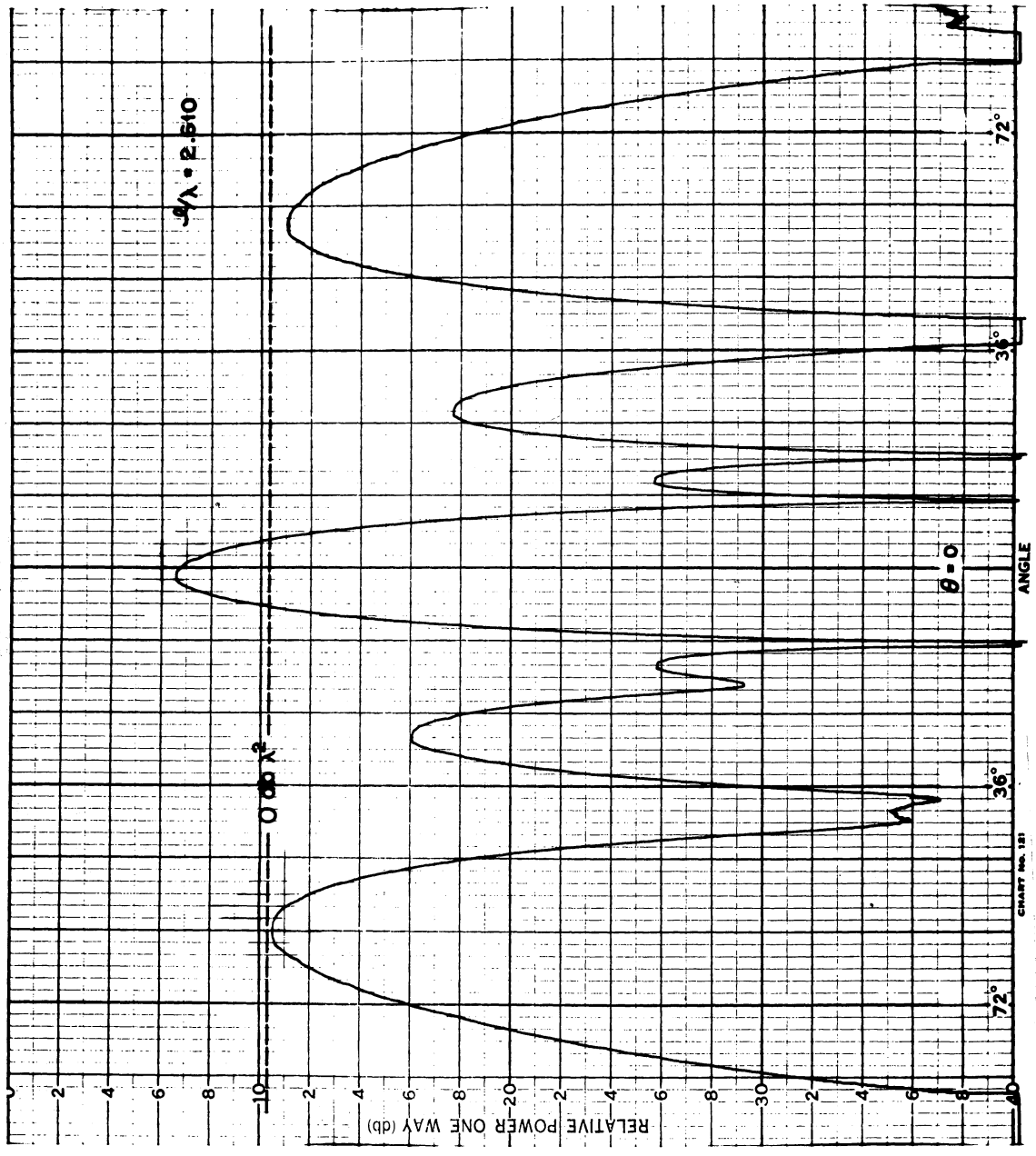
RELATIVE POWER ONE WAY (db)
θ - 0
ANGLE
72°
36°
36°
72°
CHART No. 181

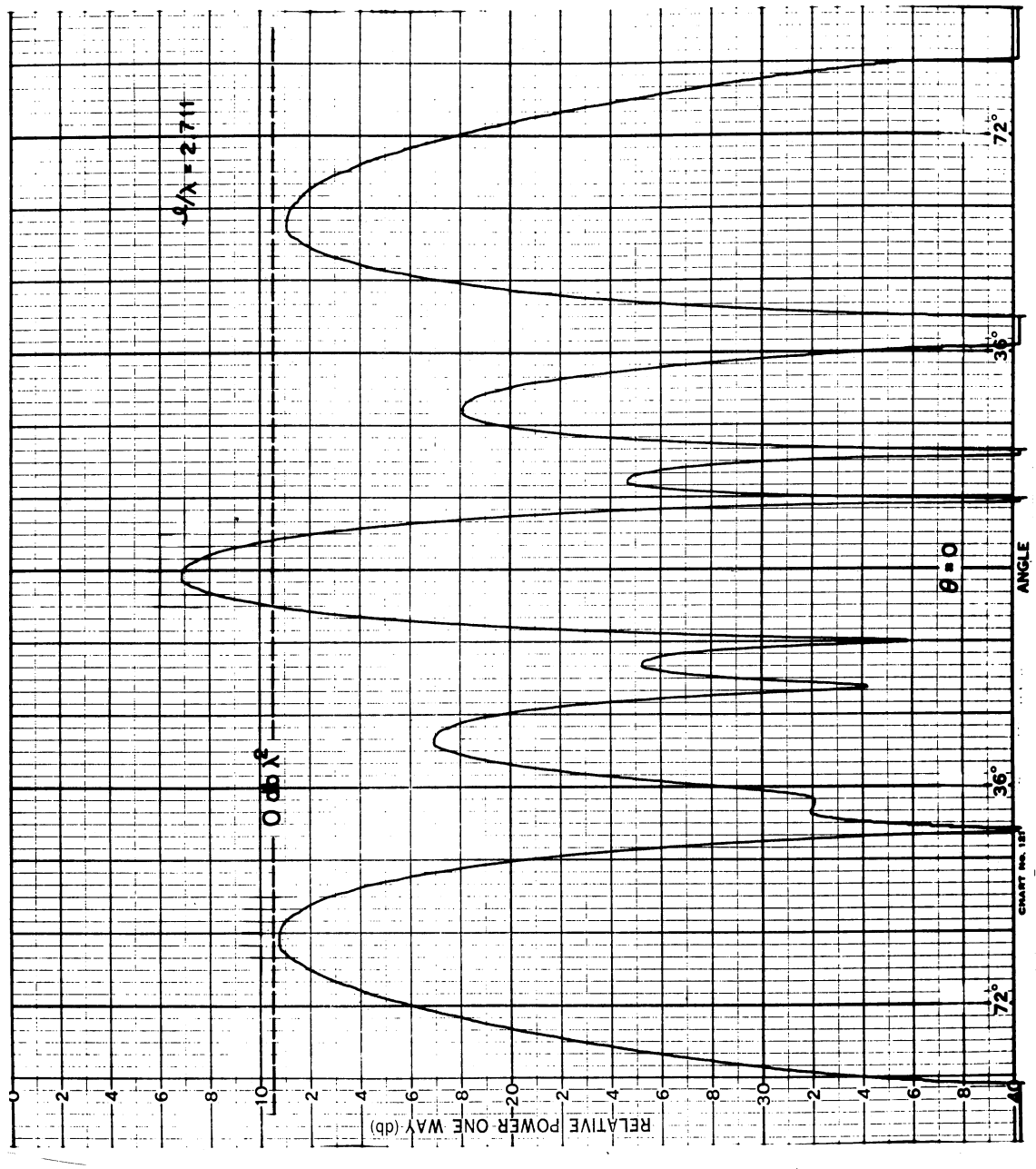
d/λ = 2.711
0 dB
θ = 0
ANGLE
72°
36°
36°
72°
RELATIVE POWER ONE WAY (db)
0
2
4
6
8
10
2
4
6
8
20
2
4
6
8
30
2
4
6
8
40

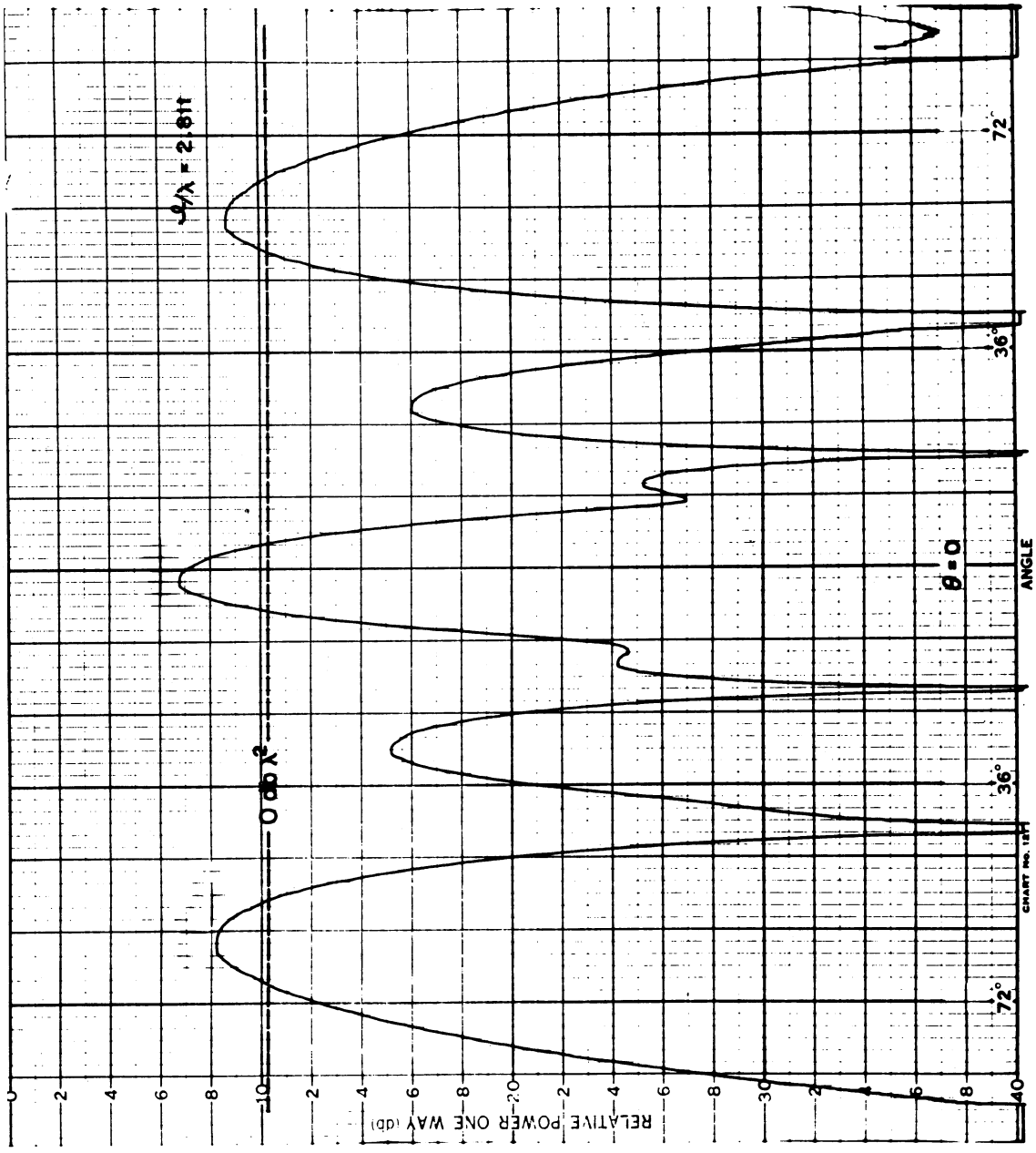
d/λ = 2.811
θ = 0
72°
36°
36°
72°
ANGLE
RELATIVE POWER ONE WAY (db)

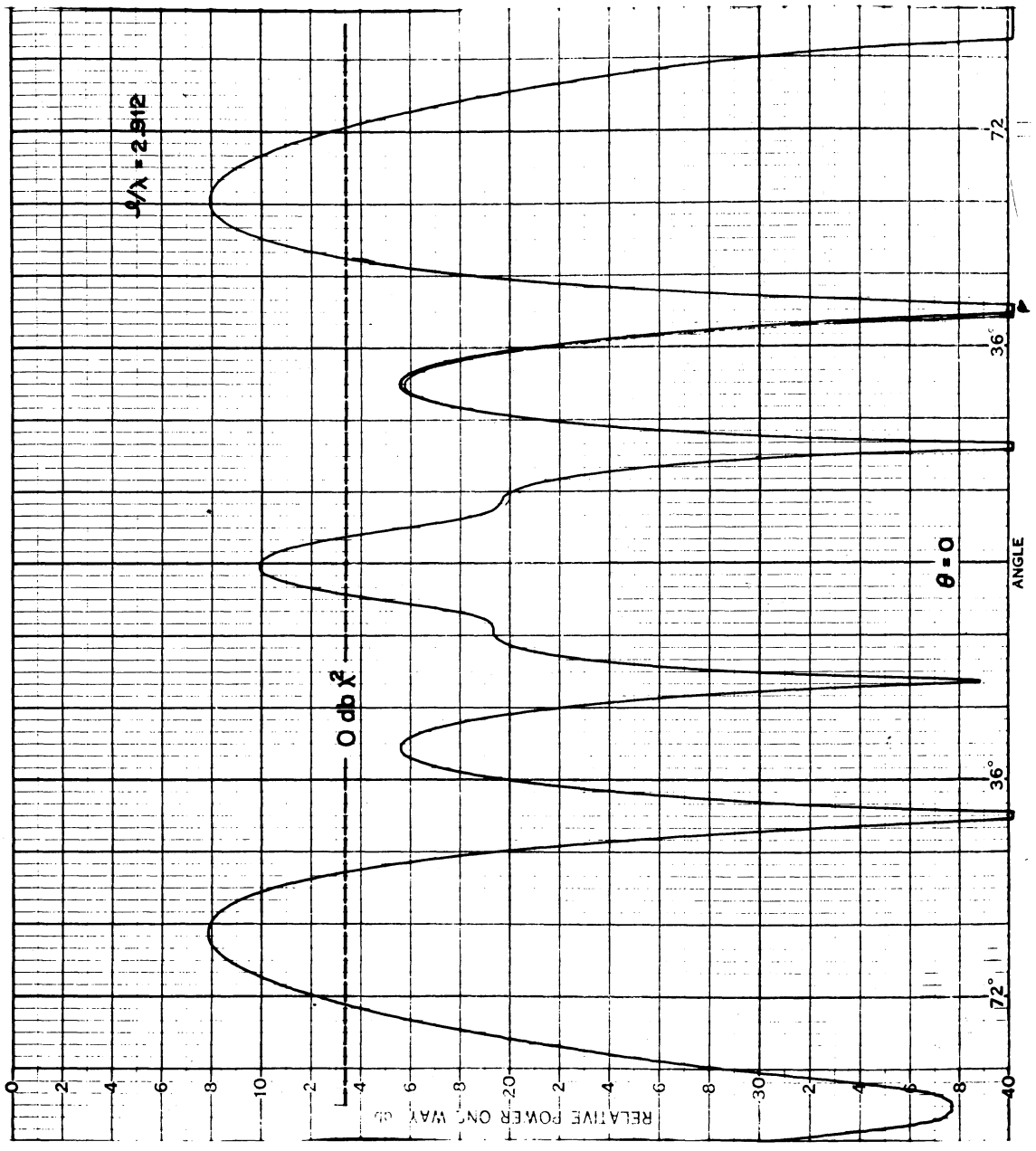
$\ell/\lambda = 2.312$
0 db
$\theta = 0$
72°
36°
36°
72°
ANGLE
RELATIVE POWER ONE WAY, db
0
2
4
6
8
10
20
30
40

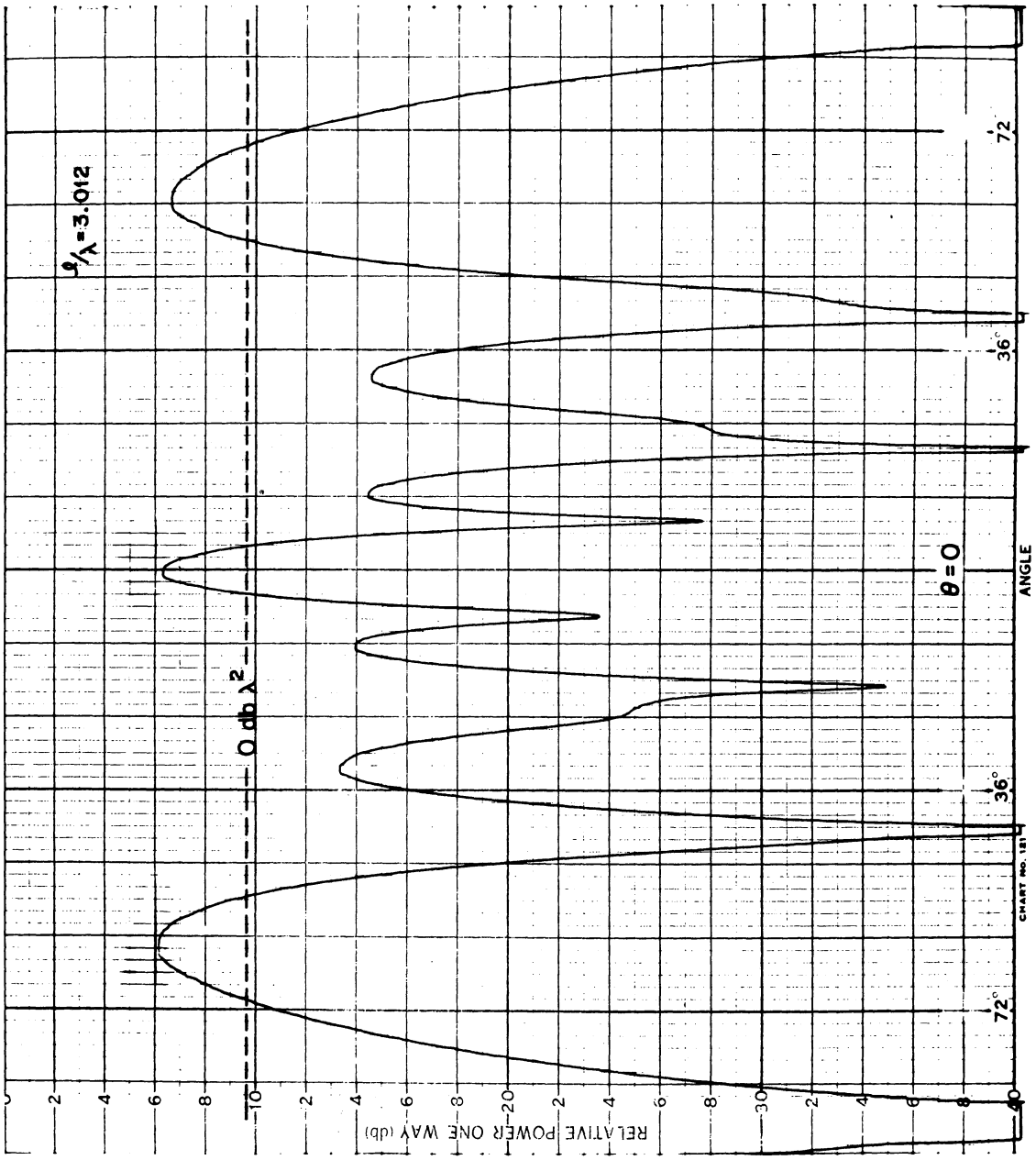
$\ell/\lambda = 3.012$
0 db λ^2
$\theta = 0$
72°
36°
36°
72°
ANGLE
RELATIVE POWER ONE WAY (db)
0 2 4 6 8 10 2 4 6 8 20 2 4 6 8 30 2 4 6 8 40
CHART No. 181

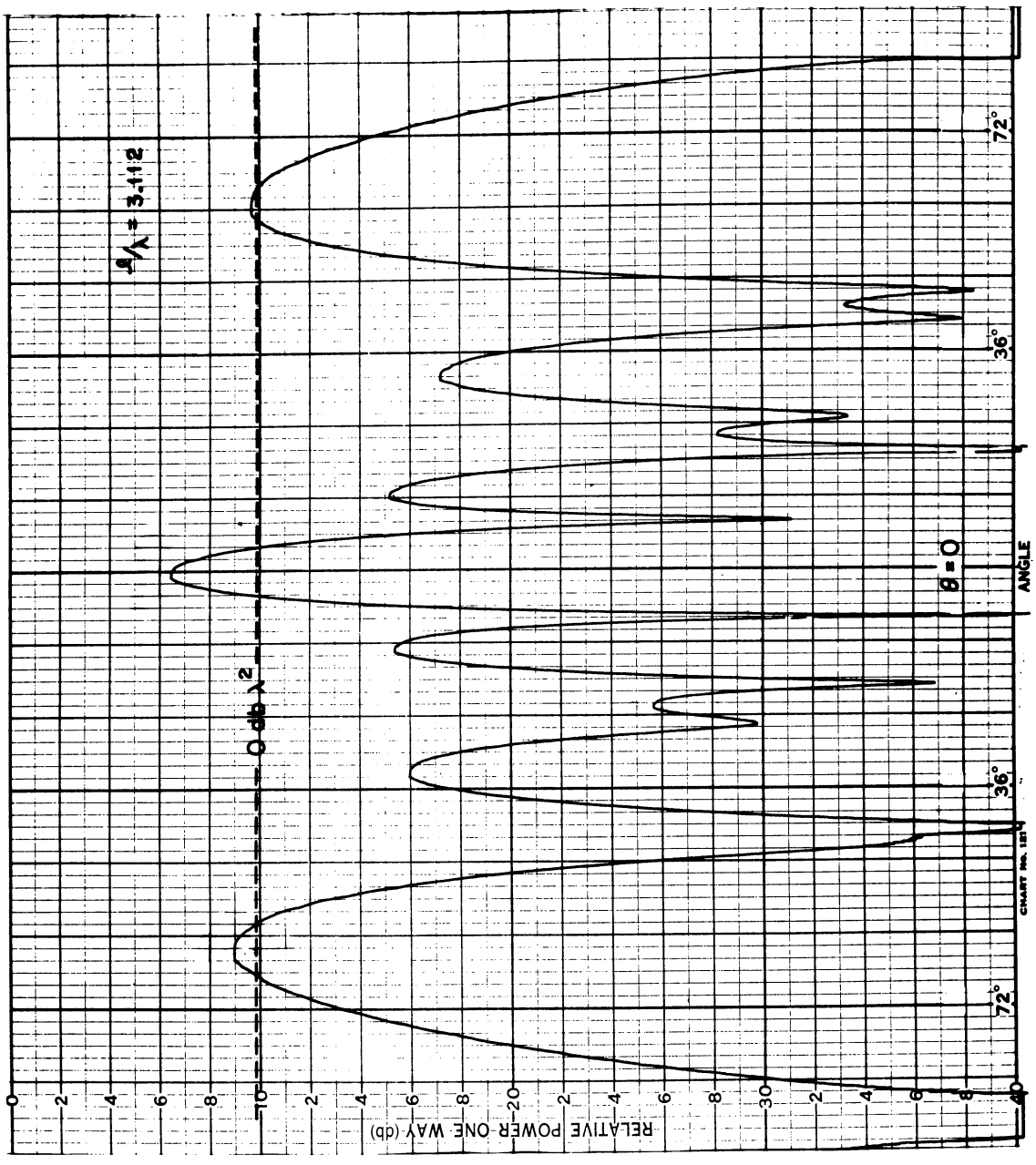
d/λ = 3.112
0 db λ²
θ = 0
ANGLE
72°
36°
36°
72°
RELATIVE POWER-ONE WAY (db)
0
2
4
6
8
10
2
4
6
8
20
2
4
6
8
30
2
4
6
8
40

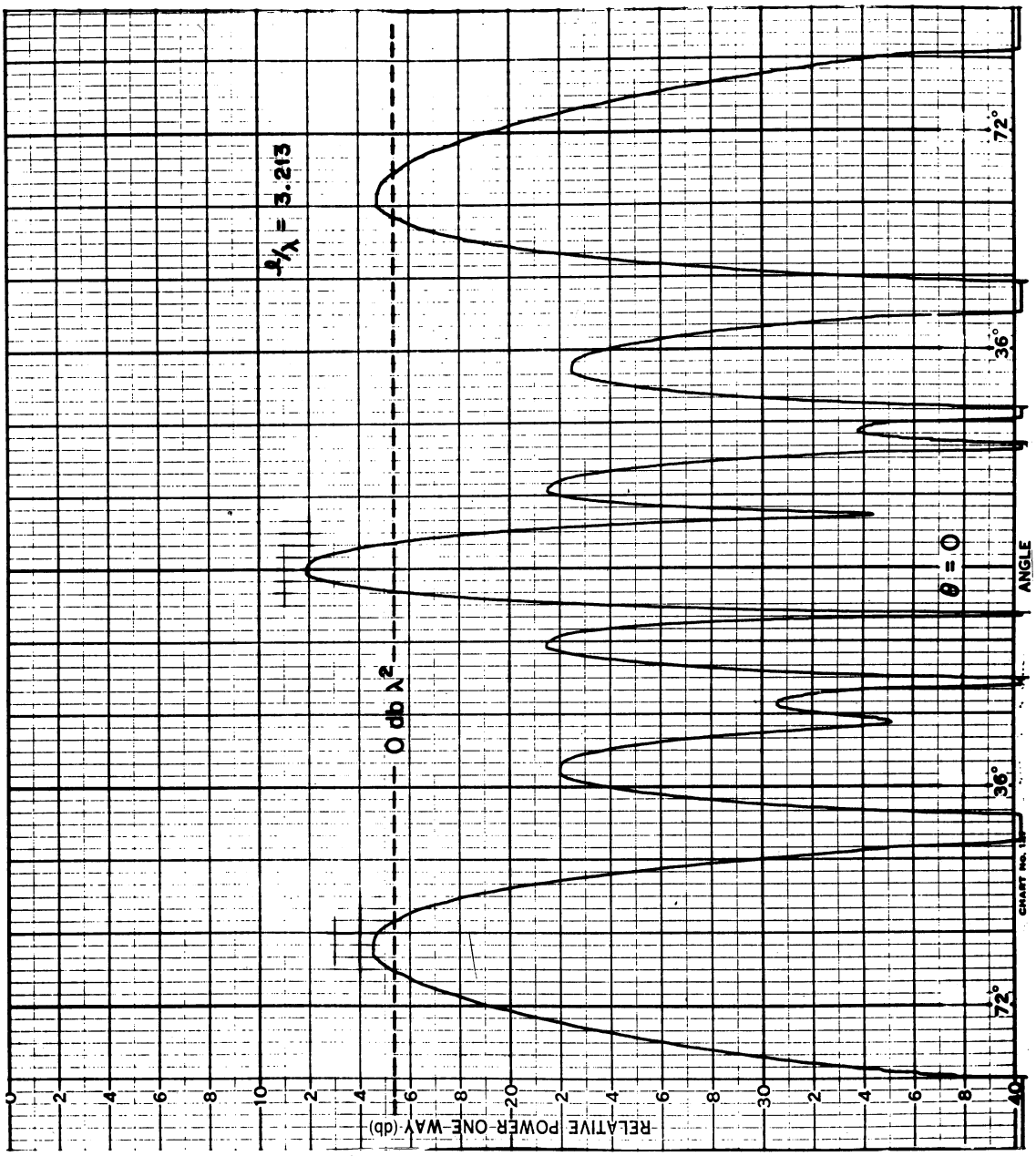
$d/\lambda = 3.213$
0 db
$\theta = 0$
ANGLE
72°
36°
36°
72°
RELATIVE POWER ONE-WAY (db)
0 2 4 6 8 10 2 4 6 8 20 2 4 6 8 30 2 4 6 8 40

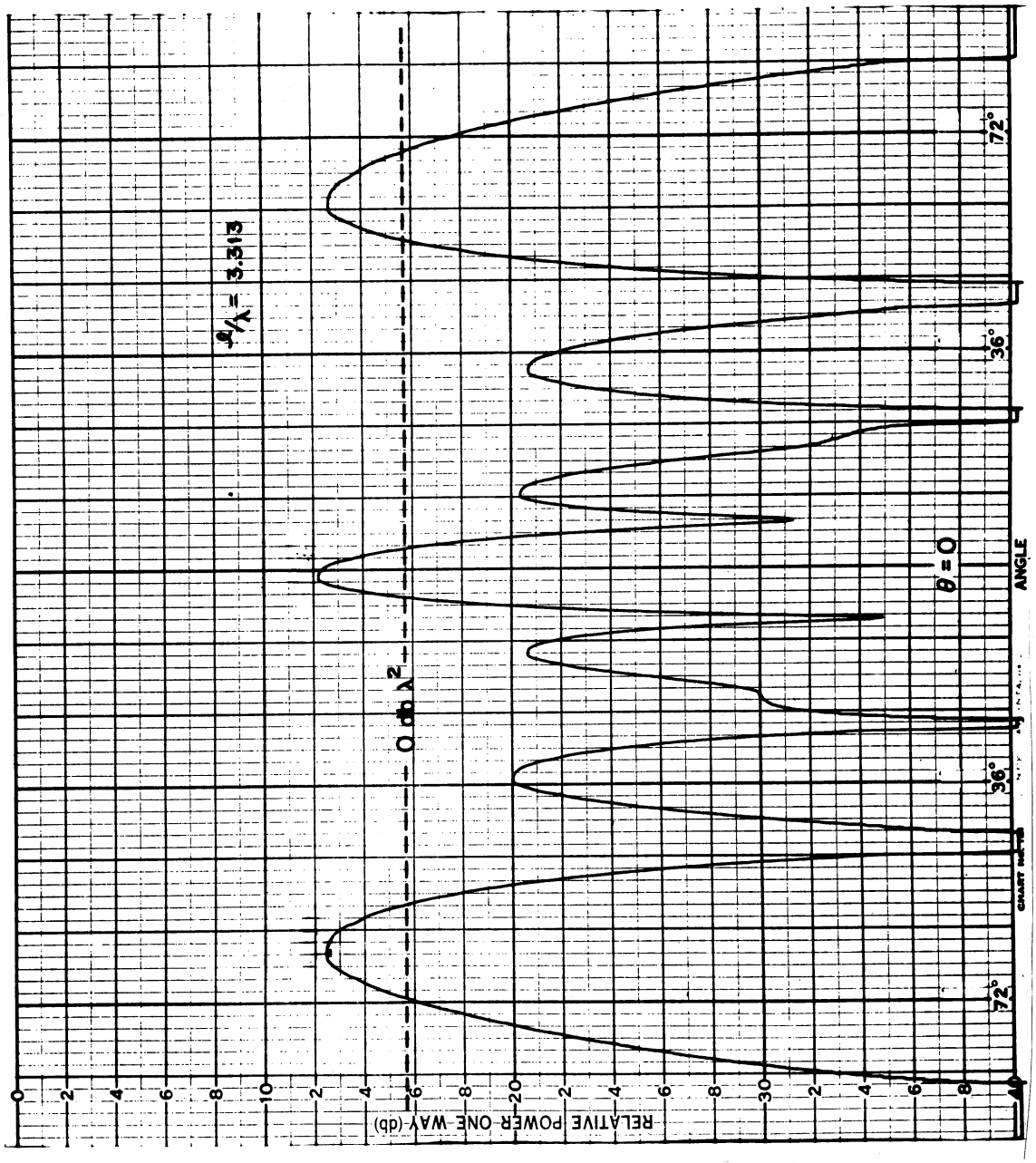
$\ell/\lambda = 3.313$
0 db
$\theta = 0$
72°
36°
36°
72°
ANGLE
RELATIVE POWER ONE WAY (db)
0 2 4 6 8 10 2 4 6 8 20 2 4 6 8 30 2 4 6 8 40

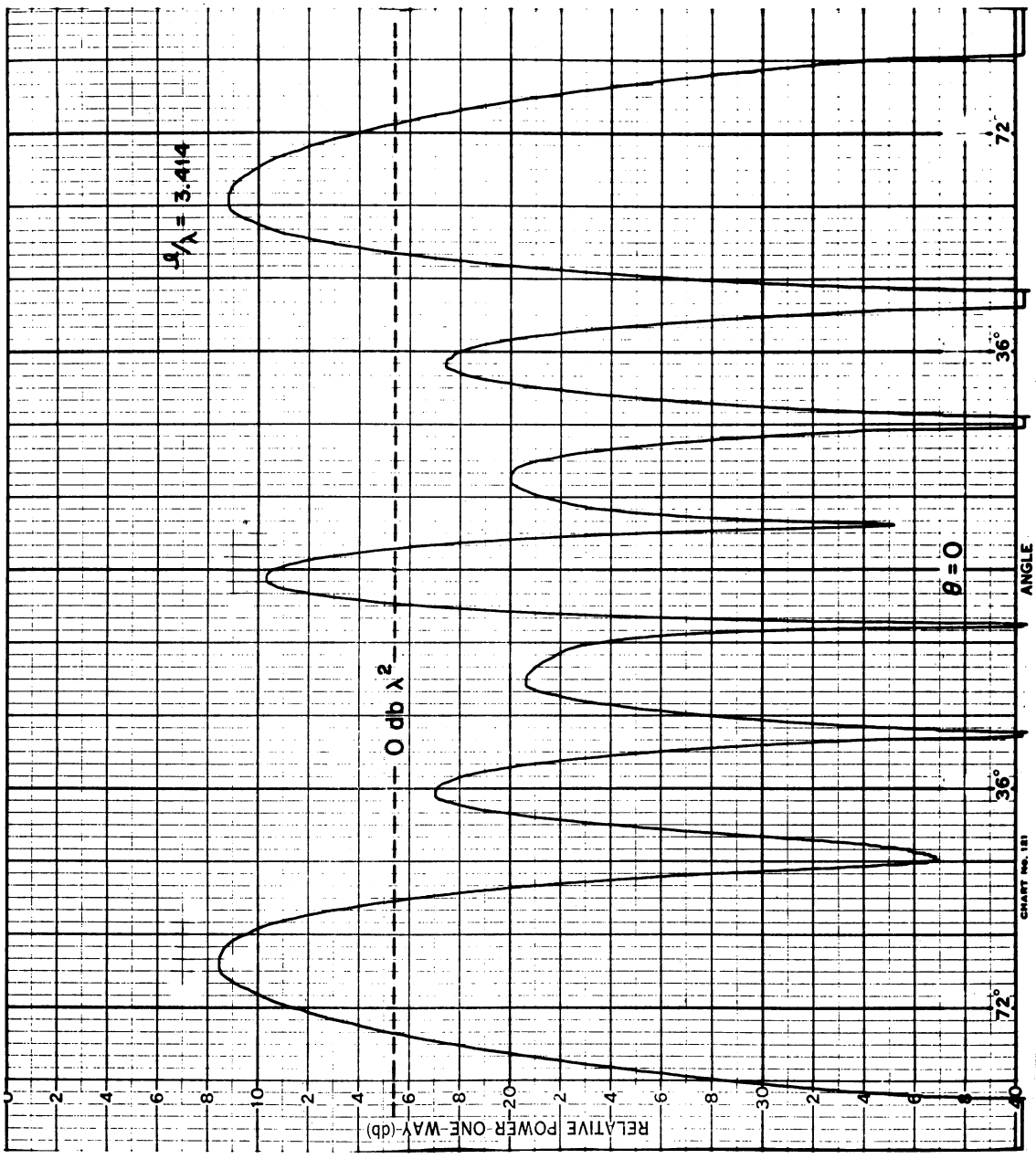
$\ell/\lambda = 3.414$
0 db λ^2
$\theta = 0$
72°
36°
36°
72°
ANGLE
RELATIVE POWER ONE-WAY-(db)
0 2 4 6 8 10 2 4 6 8 20 2 4 6 8 30 2 4 6 8 40
CHART No. 181

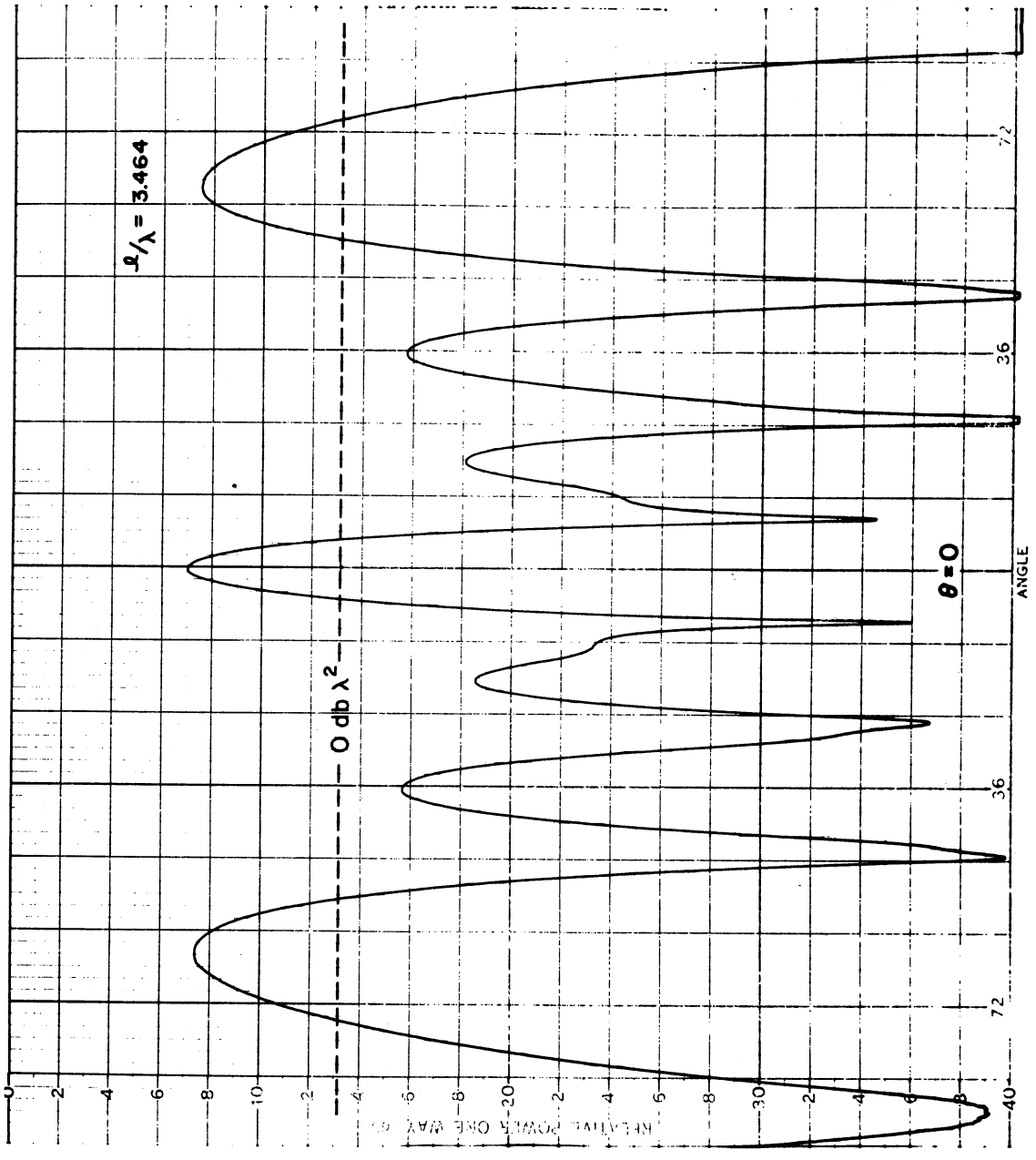
ℓ/λ = 3.464
0 db λ²
θ=0
ANGLE
72
36
36
72
RELATIVE POWER ONE WAY dB

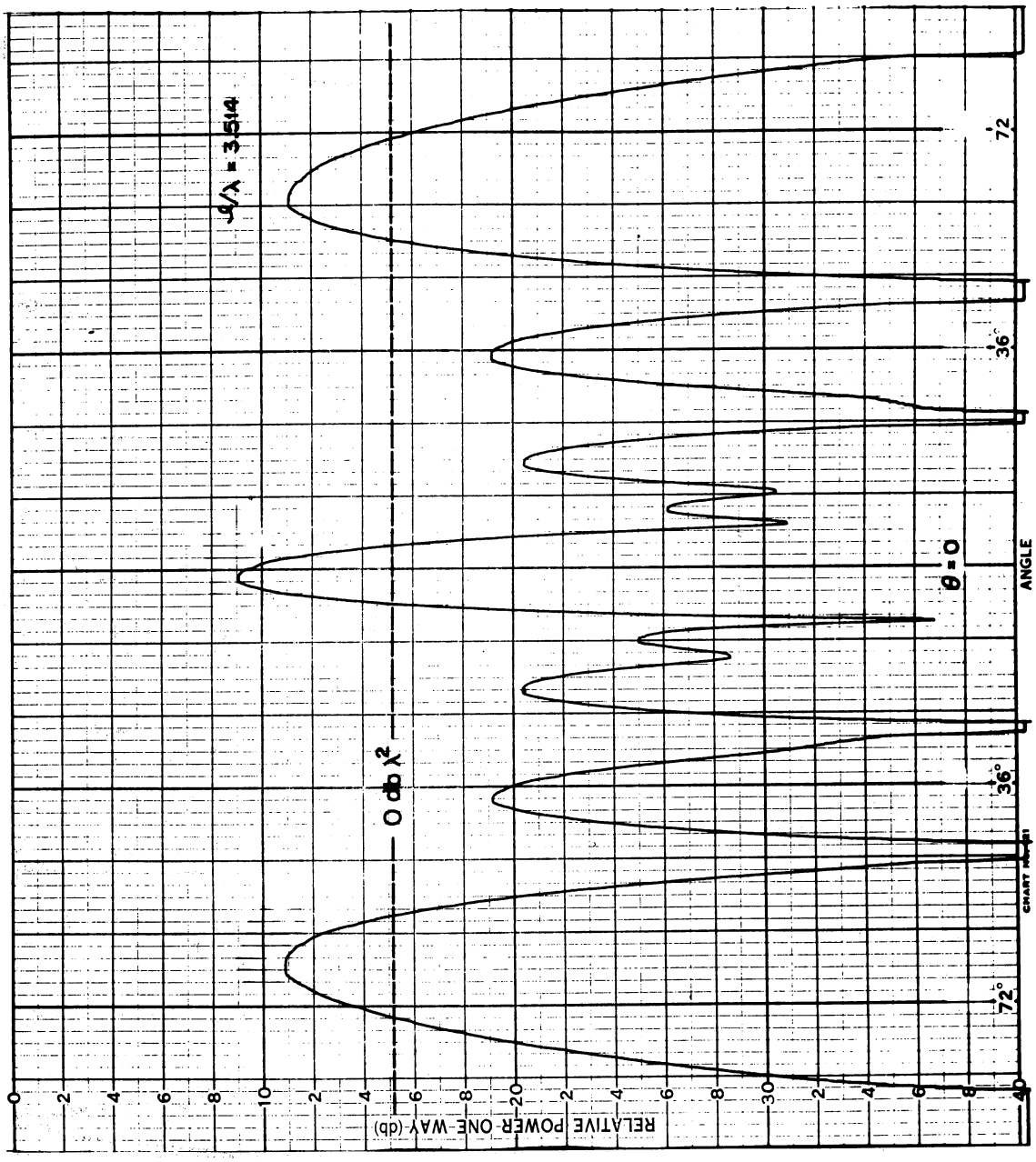
d/λ = 3.514
0 db λ²
θ = 0
72°
36°
36°
72°
ANGLE
RELATIVE POWER ONE-WAY (db)
0
2
4
6
8
10
2
4
6
8
20
2
4
6
8
30
2
4
6
8
40

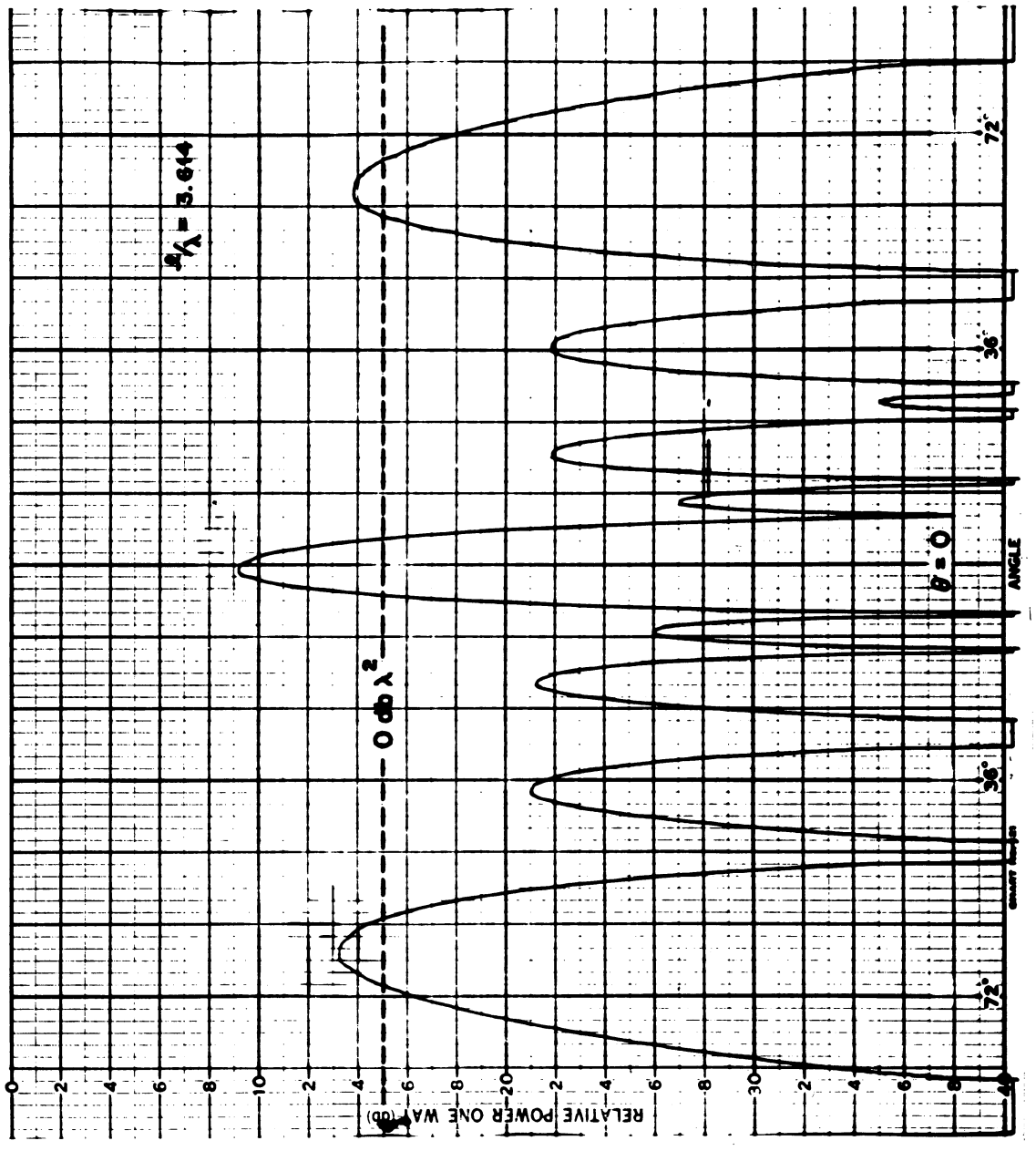
$R/\lambda = 3.614$
0 dB λ^2
$\theta = 0$
72°
36°
36°
72°
ANGLE
RELATIVE POWER ONE WAY (DB)
0
2
4
6
8
10
2
4
6
8
20
2
4
6
8
30
2
4
6
8
40

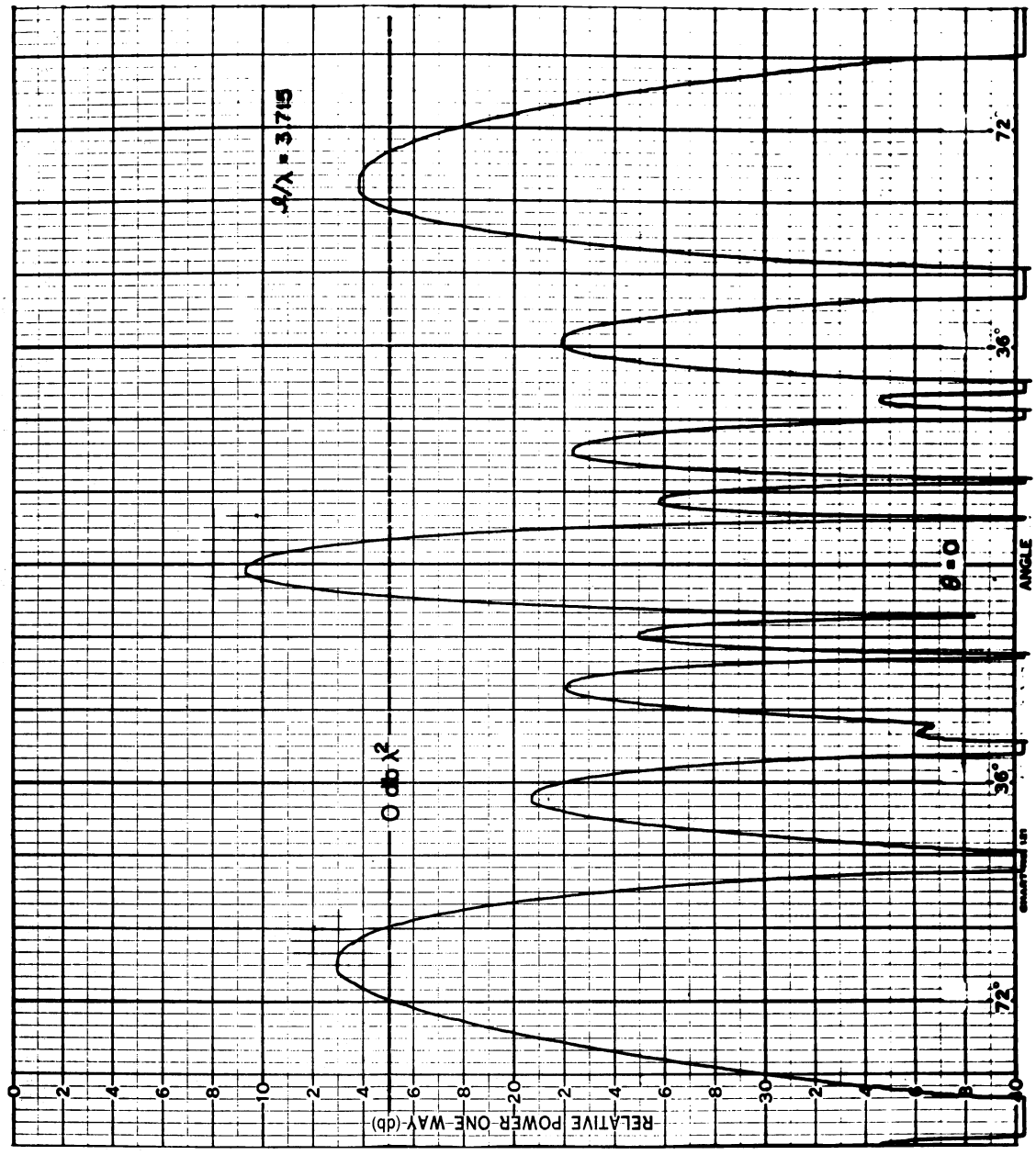
d/λ = 3.75
0 db χ²
θ = 0
72°
36°
36°
72°
ANGLE
RELATIVE POWER ONE-WAY (db)
0
2
4
6
8
10
2
4
6
8
20
2
4
6
8
30
2
4
6
8
40

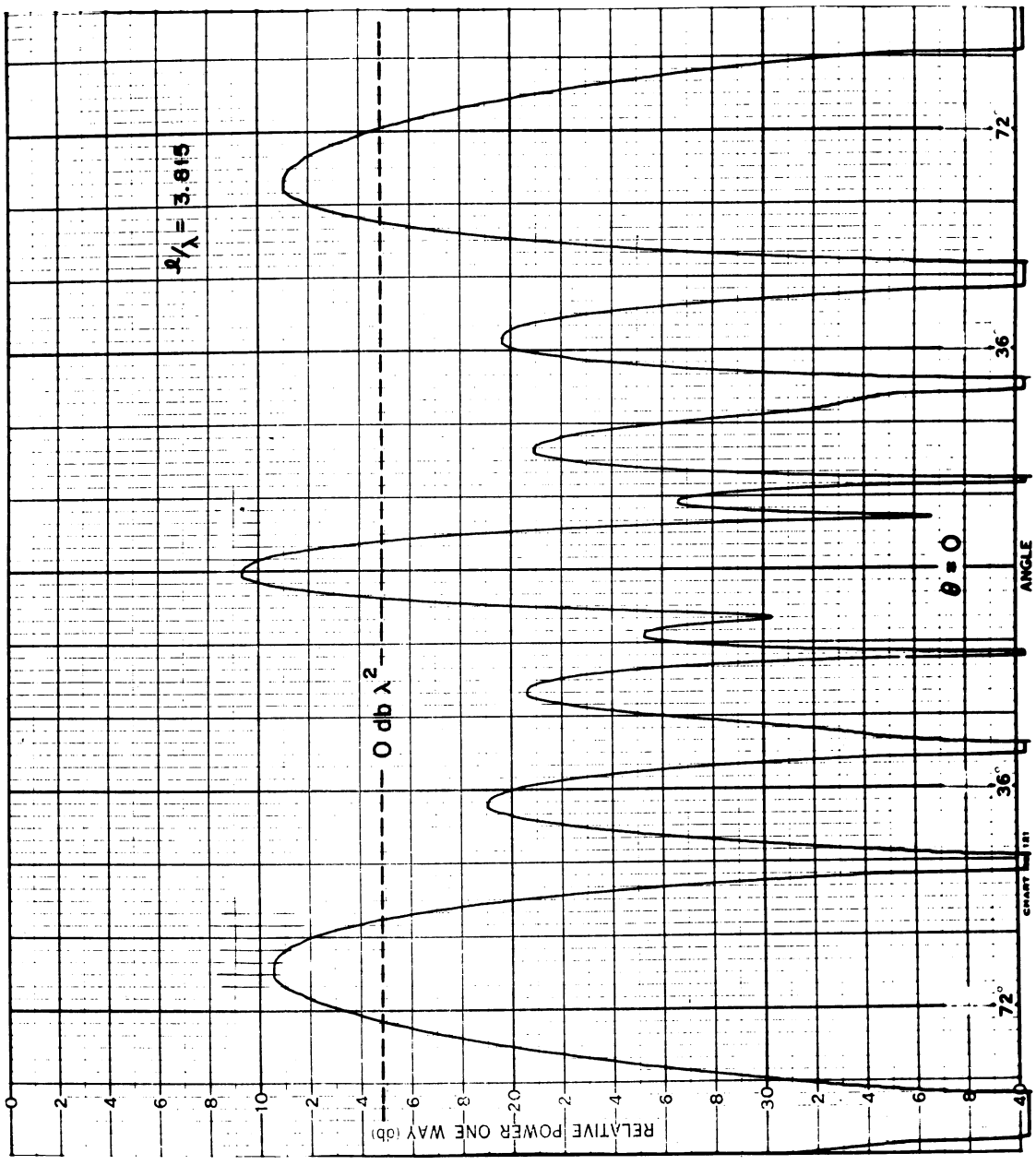
$\ell/\lambda = 3.815$
0 db λ^2
$\theta = 0$
72°
36°
36°
72°
ANGLE
RELATIVE POWER ONE WAY (db)
0 2 4 6 8 10 2 4 6 8 20 2 4 6 8 30 2 4 6 8 40

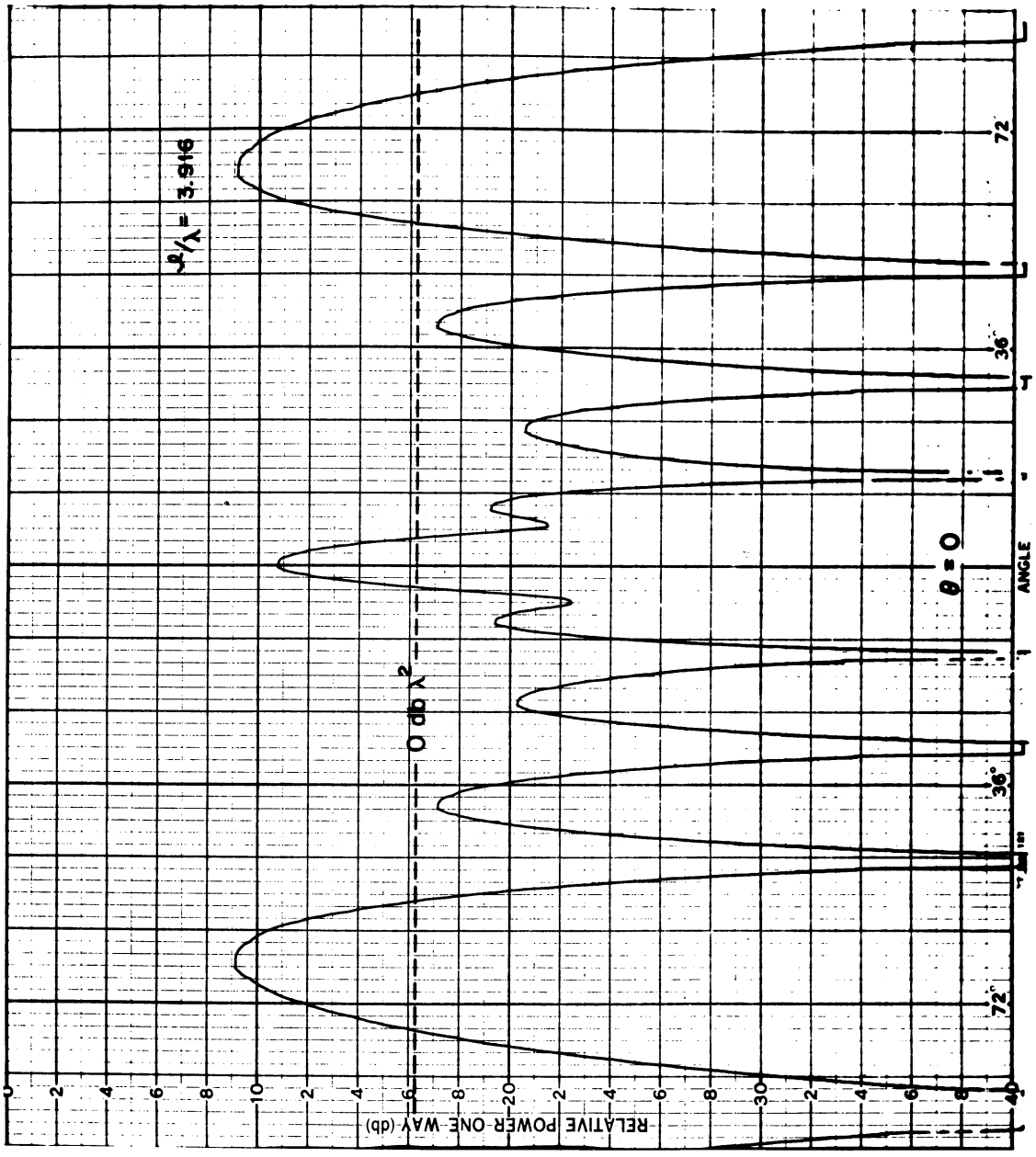
ℓ/λ = 3.916
0 db
θ = 0
ANGLE
72°
36°
36°
72°
RELATIVE POWER ONE WAY (db)
0
2
4
6
8
10
2
4
6
8
20
2
4
6
8
30
2
4
6
8
40

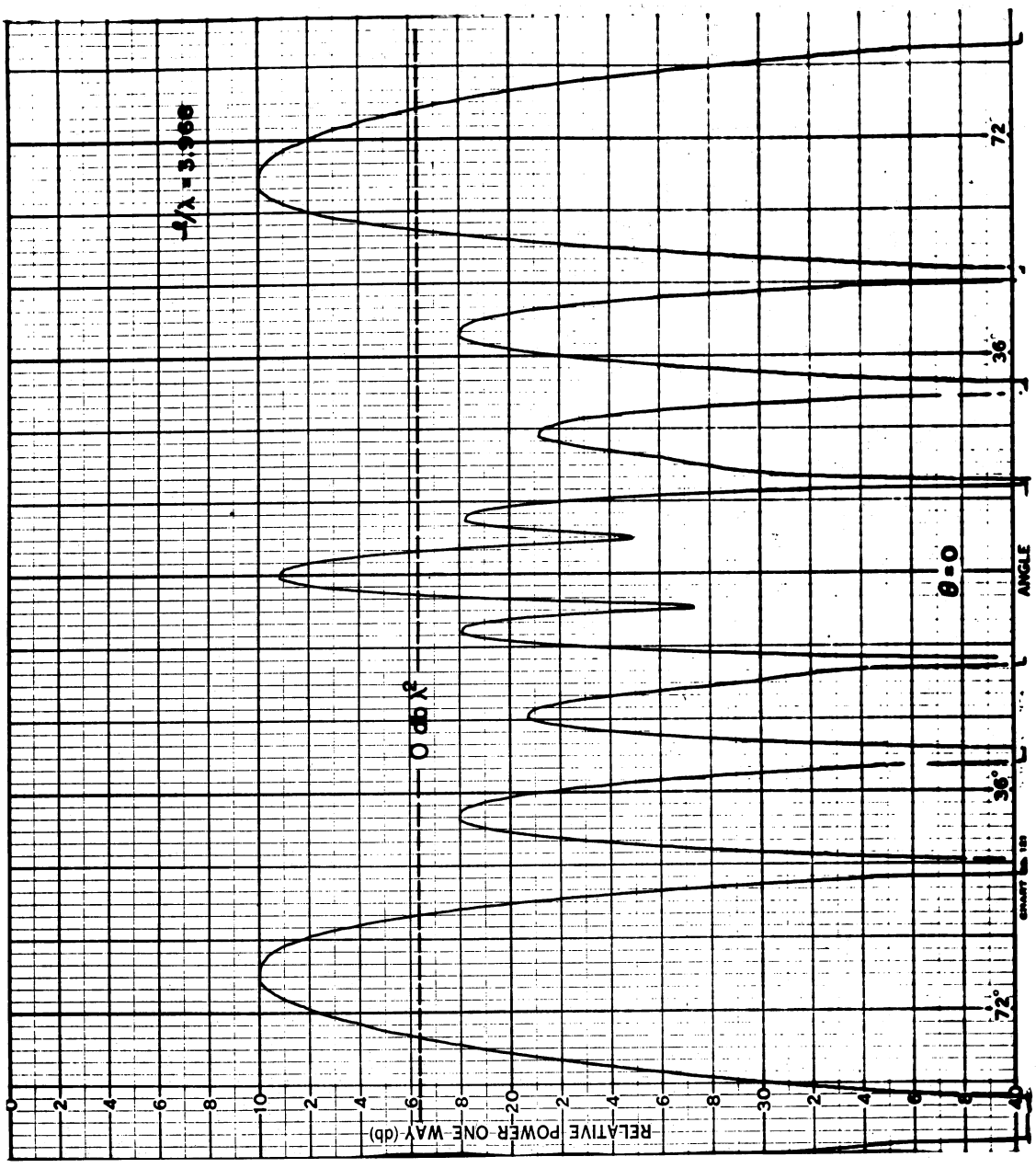
d/λ = 3.968
0 dB
θ=0
ANGLE
72°
36°
36°
72°
RELATIVE POWER ONE WAY (db)
0 2 4 6 8 10 2 4 6 8 20 2 4 6 8 30 2 4 6 8 40

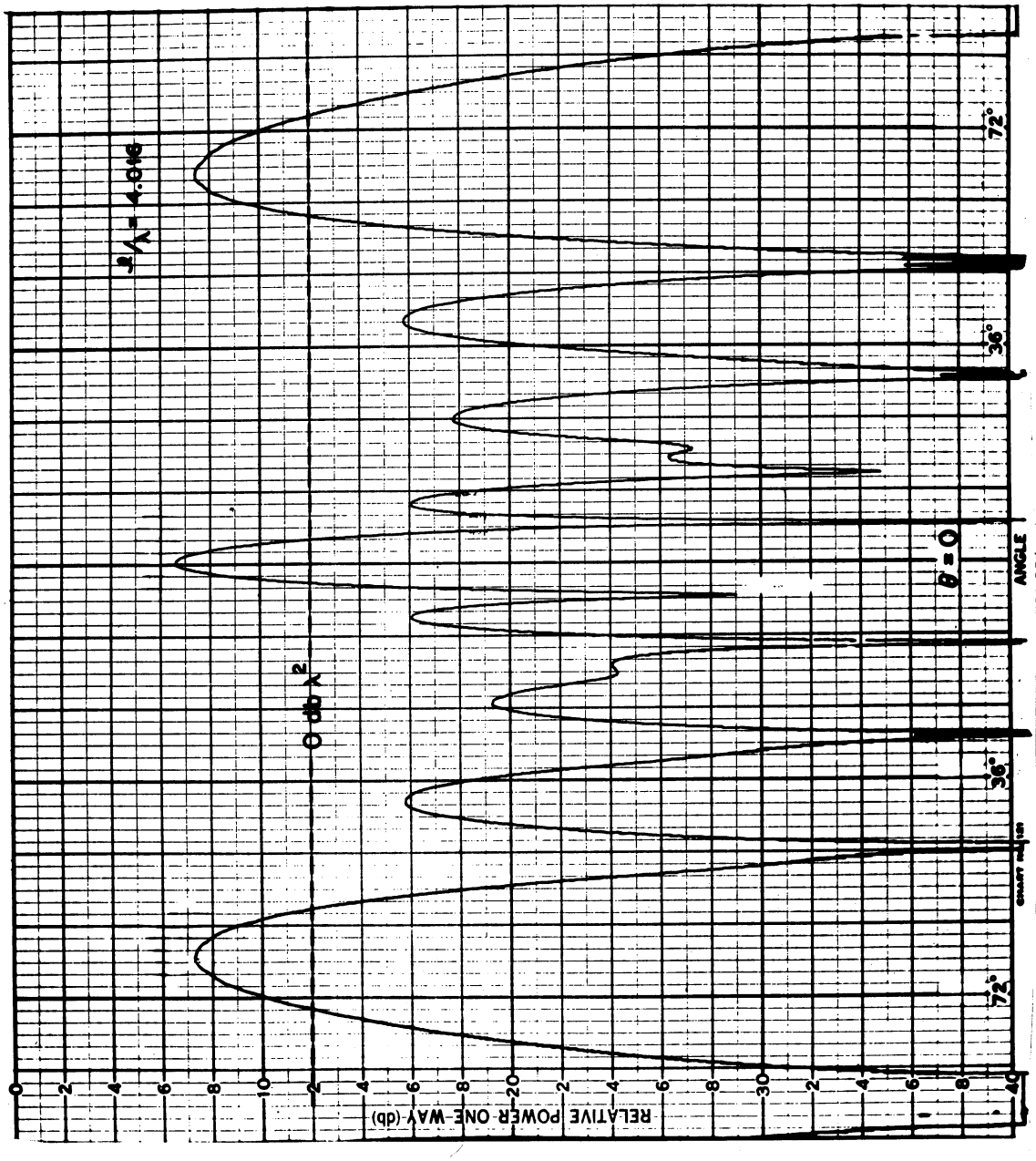
λ/λ = 4.046
0 db
72°
36°
θ = 0
ANGLE
36°
72°
RELATIVE POWER ONE-WAY (db)
0 2 4 6 8 10 2 4 6 8 20 2 4 6 8 30 2 4 6 8 40

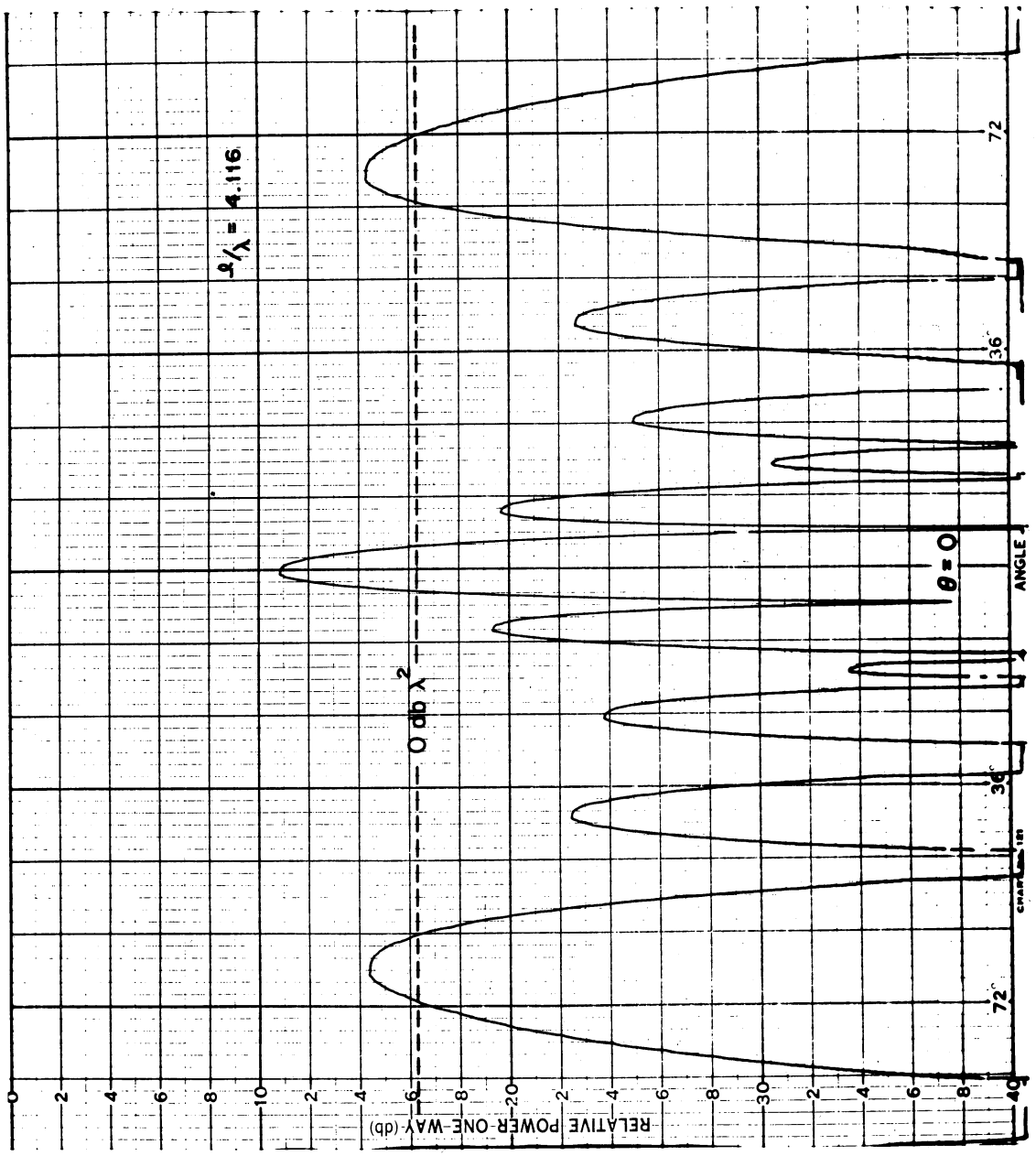
$\ell/\lambda = 4.116$
0 db λ^2
θ = 0
ANGLE
72°
36°
36°
72°
RELATIVE POWER-ONE-WAY (db)
0
2
4
6
8
10
2
4
6
8
20
2
4
6
8
30
2
4
6
8
40

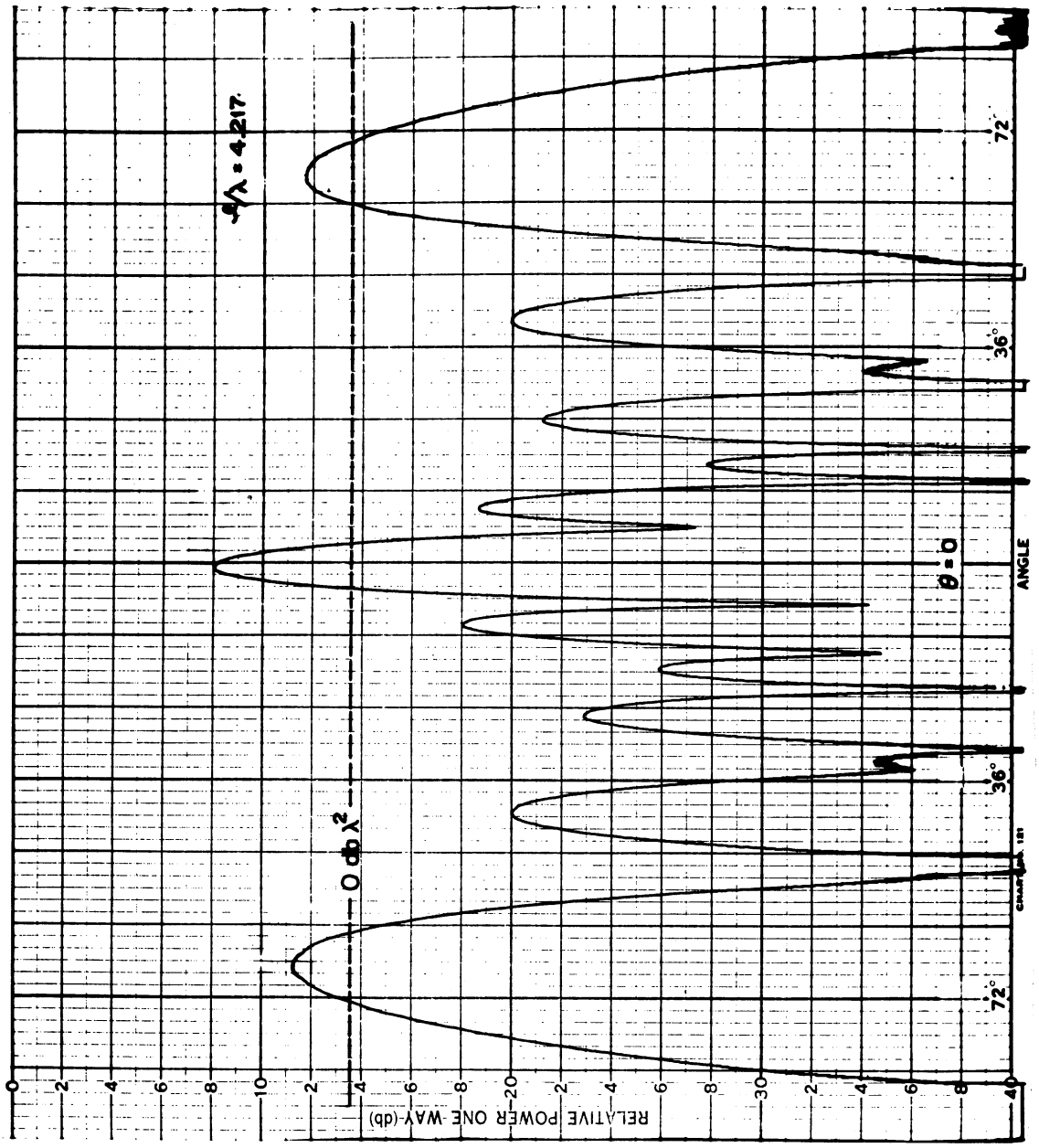
d/λ = 4.217
0 db
θ = 0
72°
36°
36°
72°
ANGLE
RELATIVE POWER ONE-WAY (db)
0
2
4
6
8
10
2
4
6
8
20
2
4
6
8
30
2
4
6
8
40

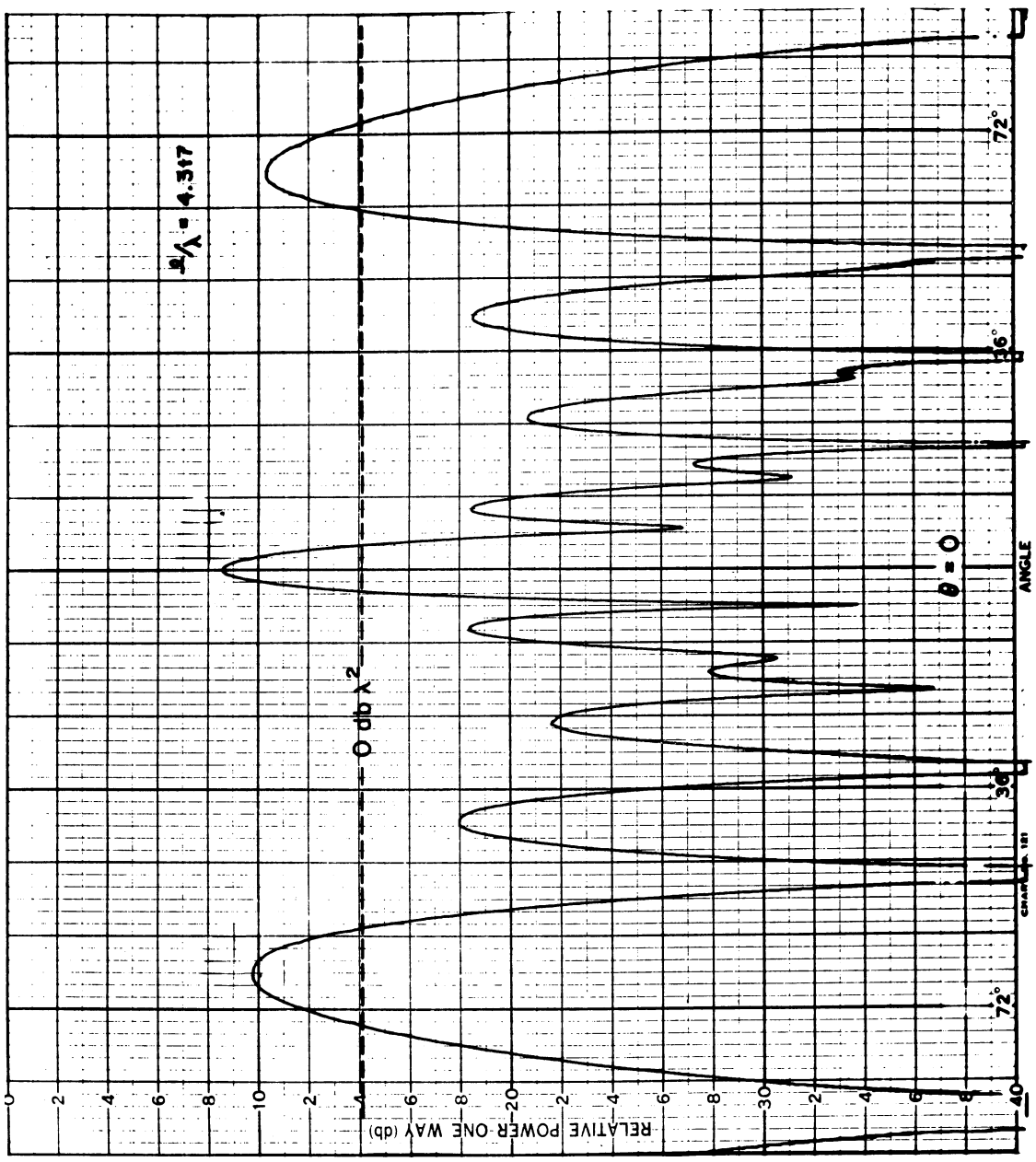
RELATIVE POWER-ONE WAY (db)
0 db
$\frac{1}{2}\lambda = 4.317$
θ = 0
ANGLE
72°
36°
36°
72°

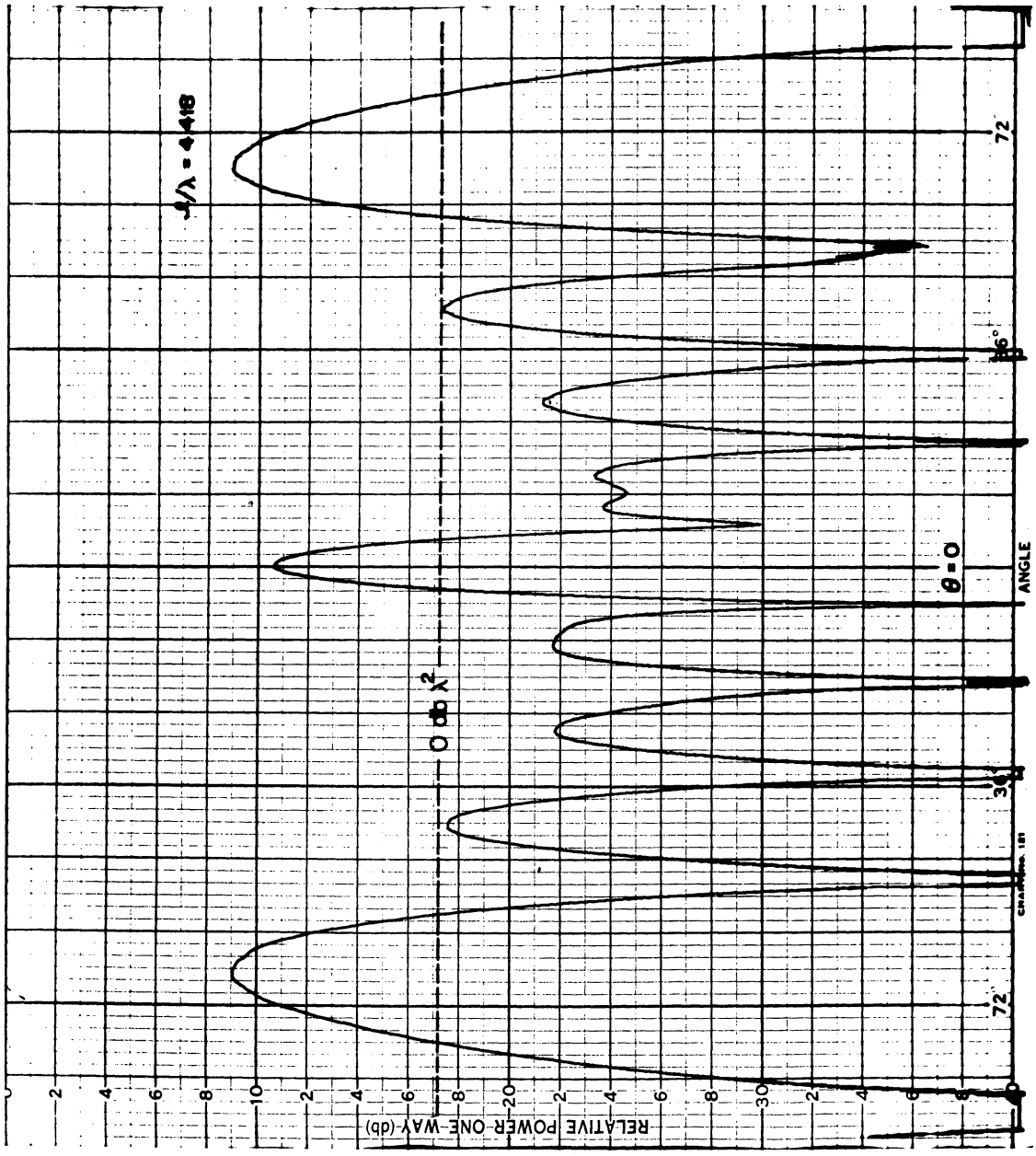
d/λ = 4.48
0 dB
θ = 0
ANGLE
RELATIVE POWER-ONE-WAY-(db)
72
36
30
72

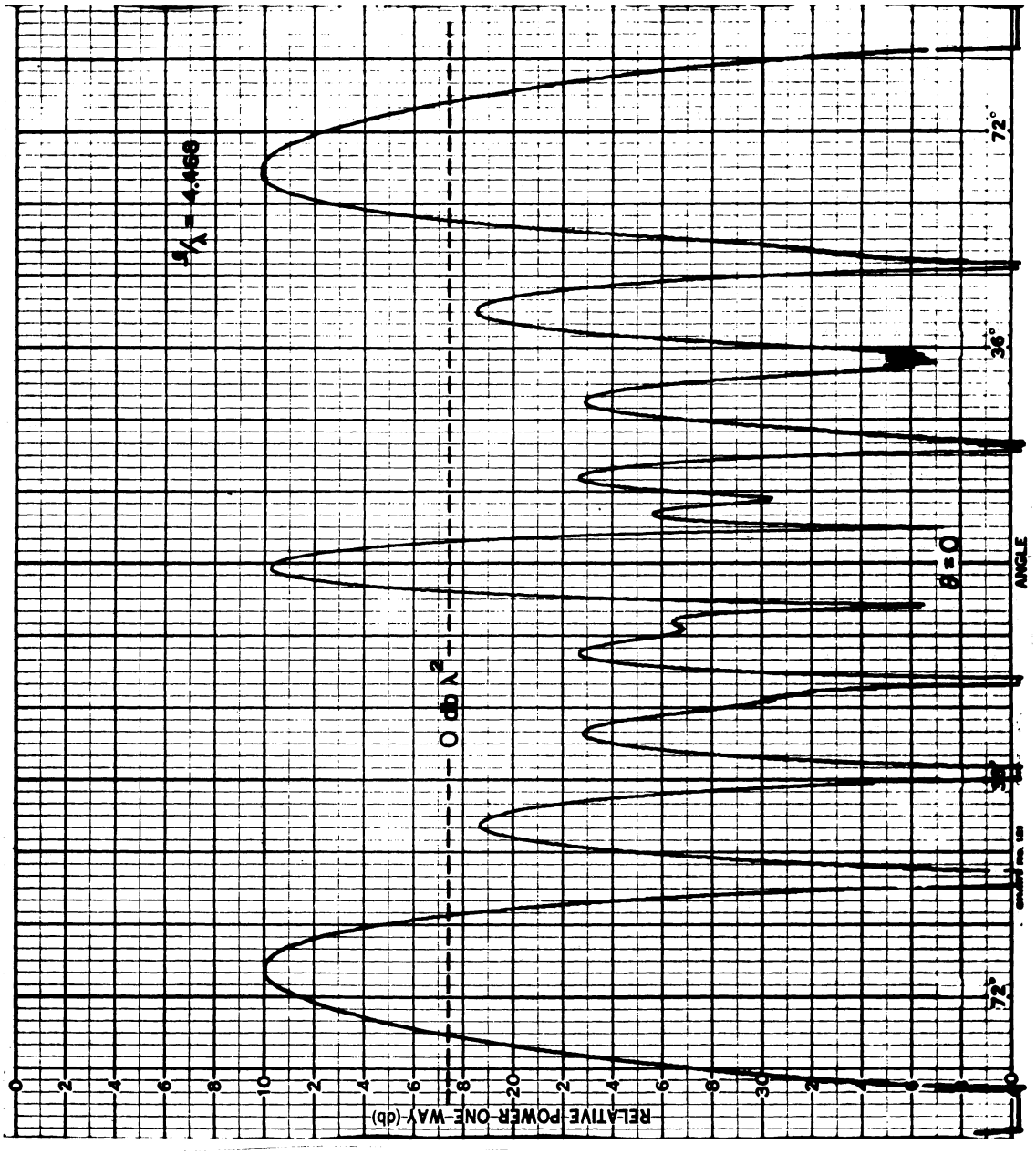
$\frac{d}{\lambda} = 4.468$
0 dB
$\theta = 0$
72°
36°
72°
ANGLE
RELATIVE POWER ONE WAY (db)
0
2
4
6
8
10
2
4
6
8
20
2
4
6
8
30
2
1
0

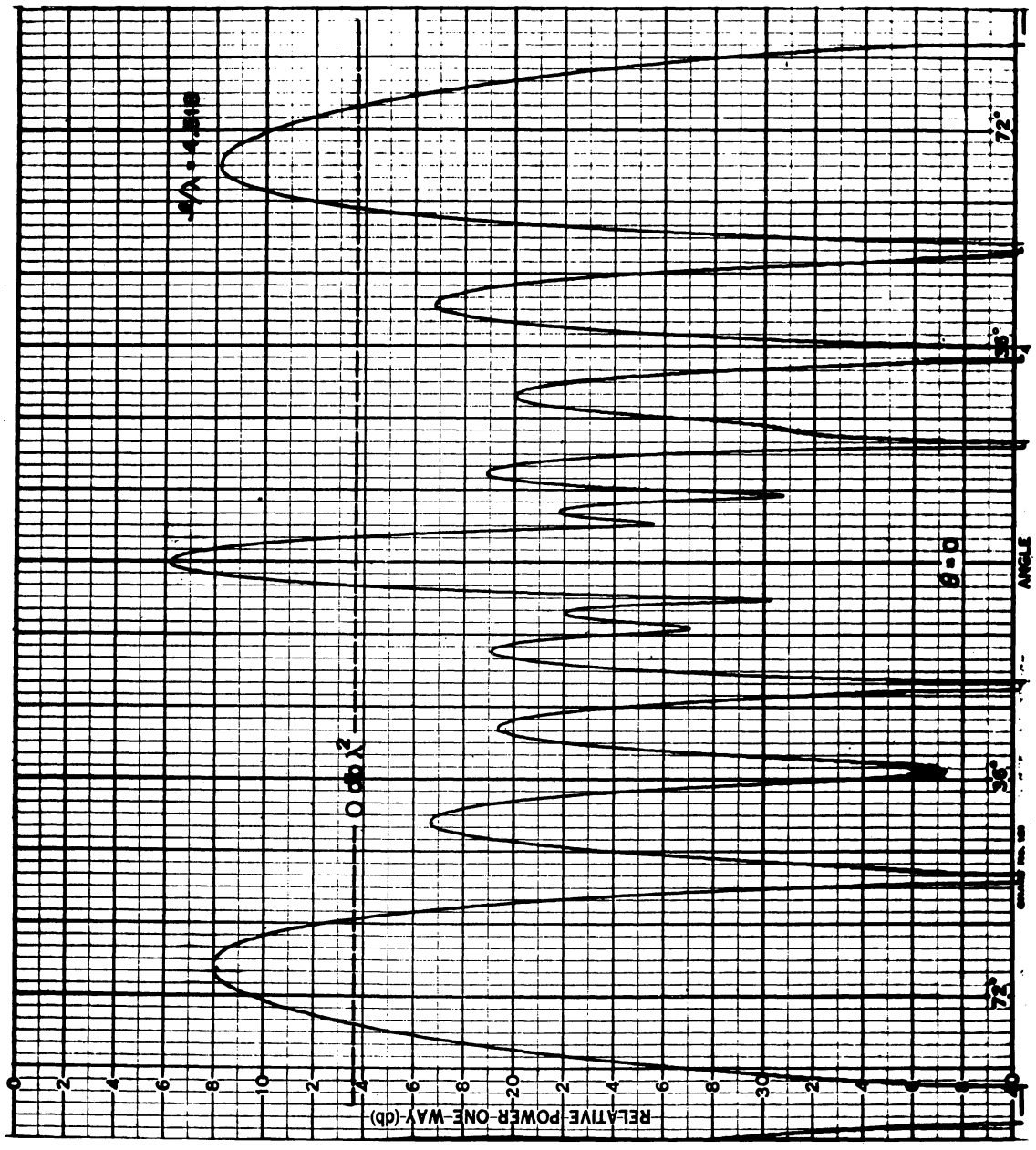
RELATIVE POWER ONE-WAY (db)
0
2
4
6
8
10
2
4
6
8
20
2
4
6
8
30
2
4
0
72°
36°
0°
36°
72°
ANGLE

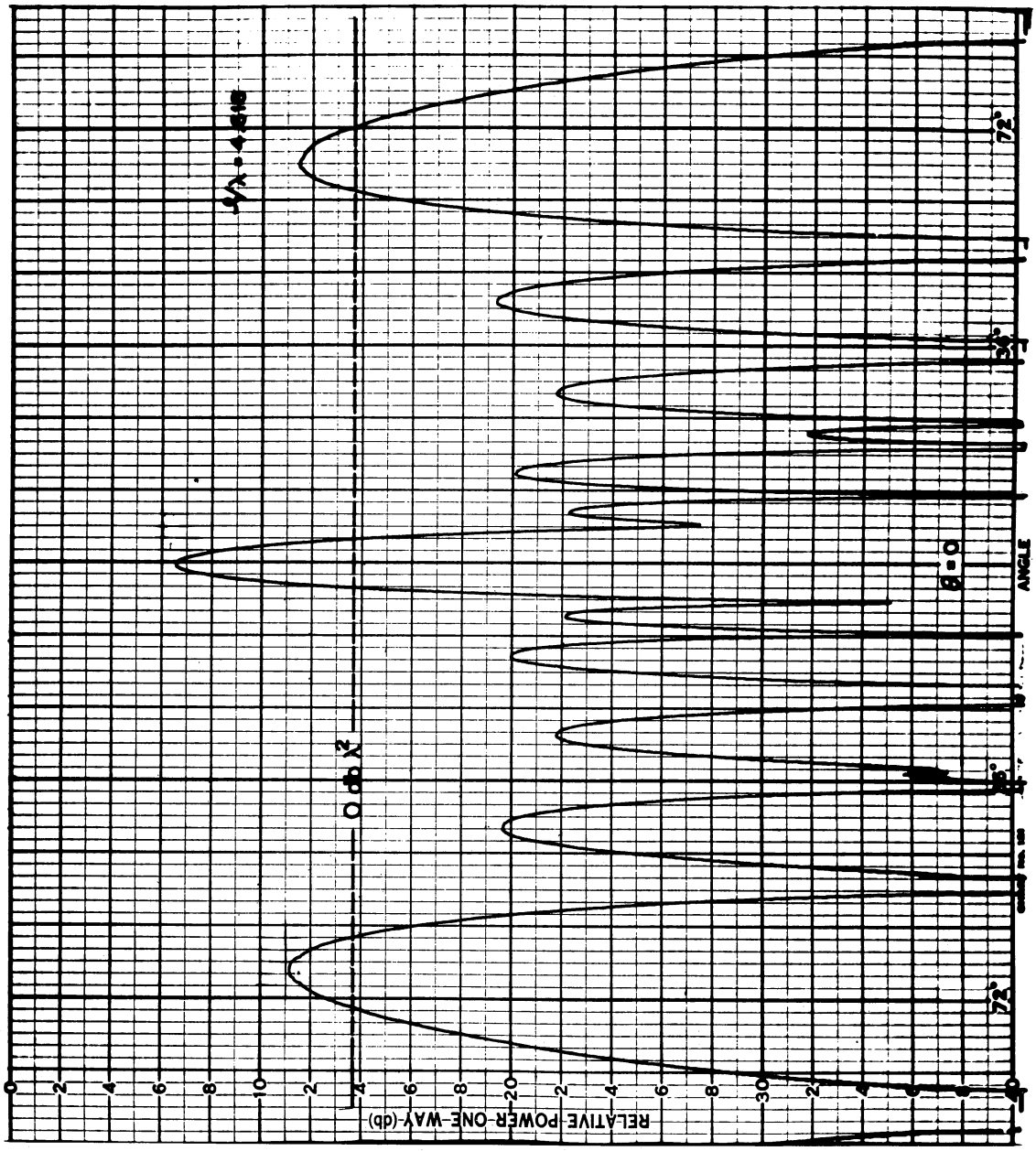
RELATIVE POWER-ONE-WAY-(db)
0 db
θ = 0
ANGLE
72°
24°
72°

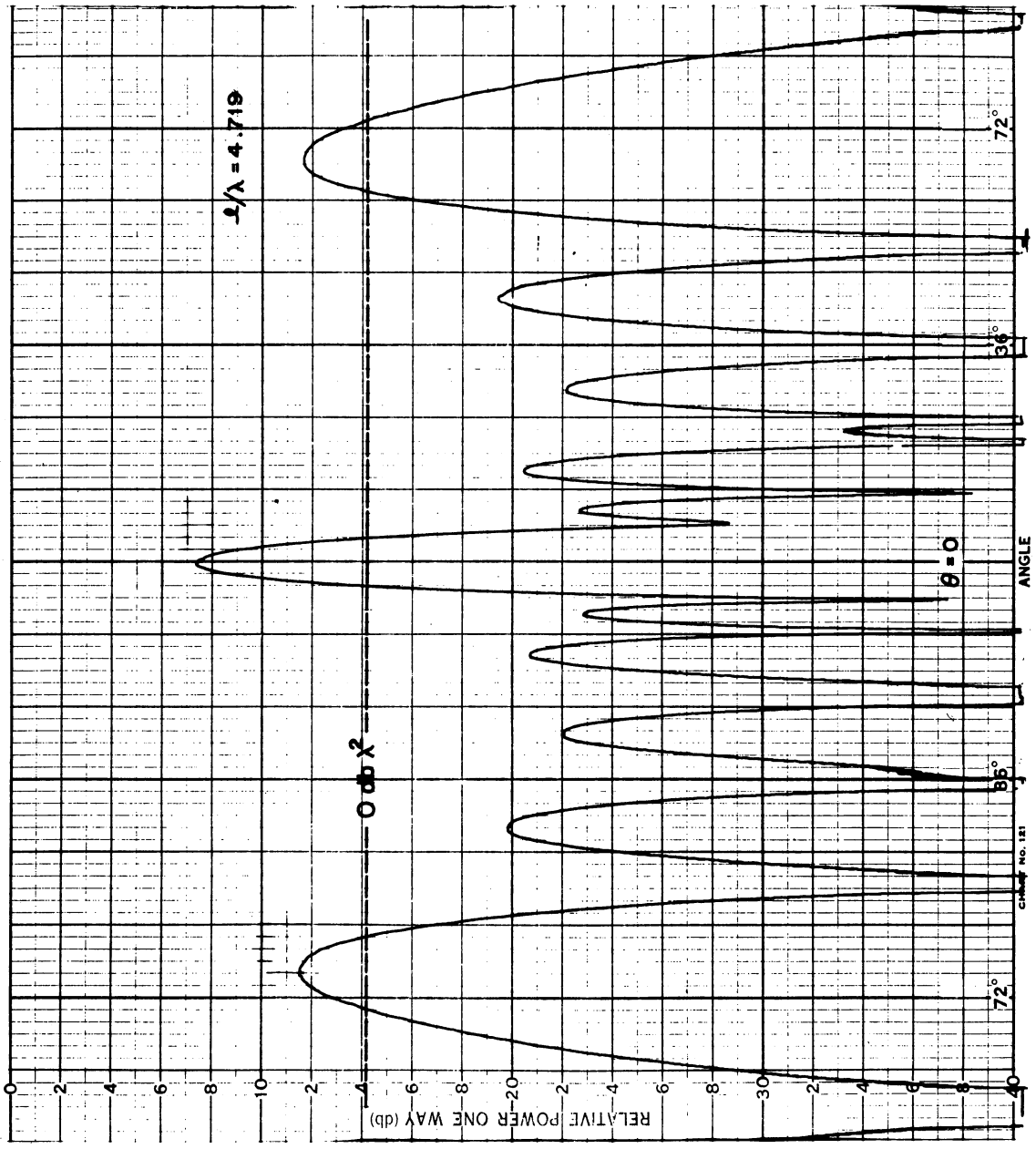
ℓ/λ = 4.719
0 db
θ = 0
ANGLE
72°
36°
36°
72°
RELATIVE POWER ONE WAY (db)
0
2
4
6
8
10
2
4
6
8
20
2
4
6
8
30
2
4
6
8
40

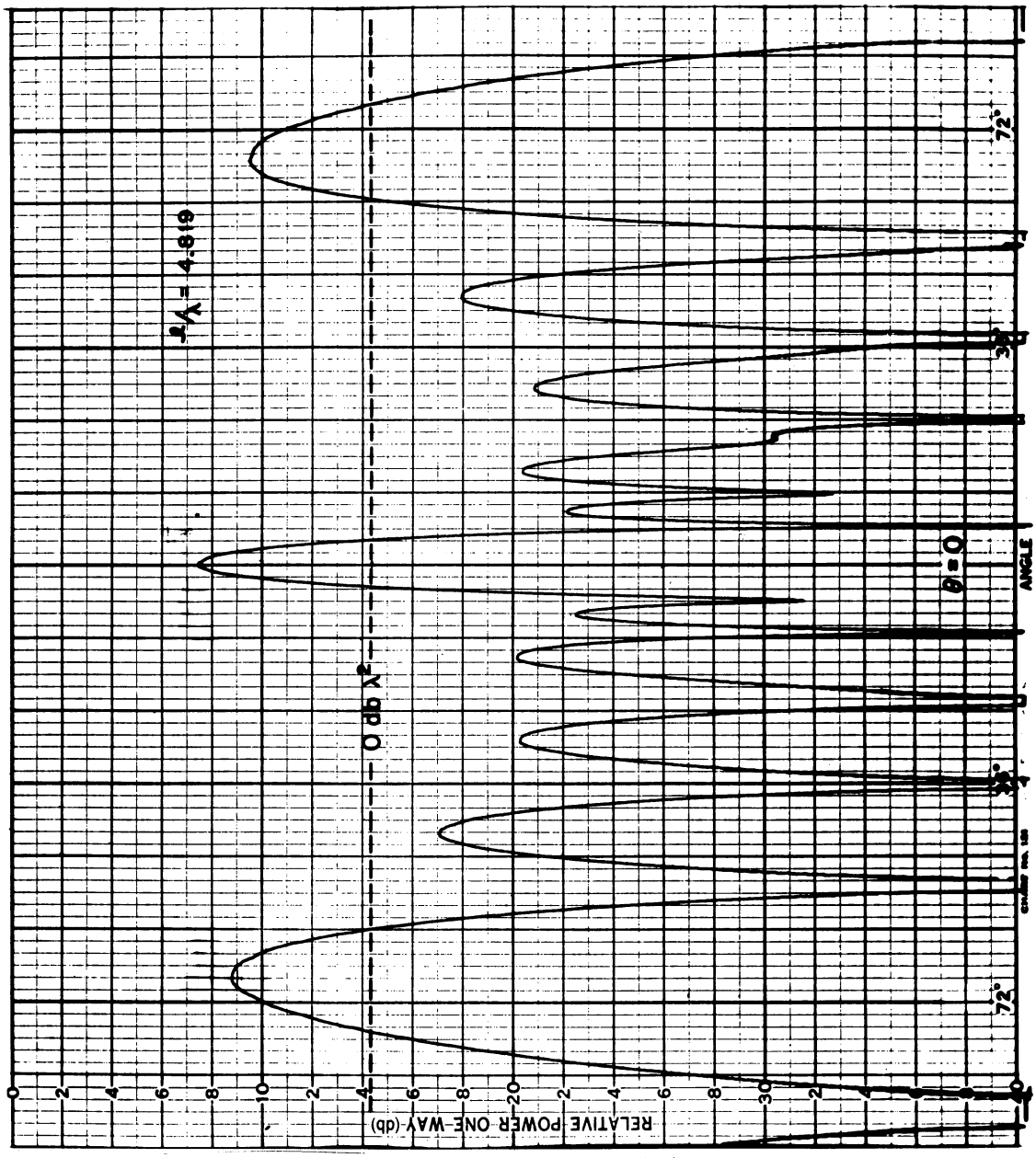
$\frac{1}{\sqrt{\lambda}} = 4.819$
0 db λ^2
$\theta = 0$
72°
36°
36°
72°
ANGLE
RELATIVE POWER ONE-WAY (db)
0
2
4
6
8
10
2
4
20
2
4
6
8
30
2
4
6
0

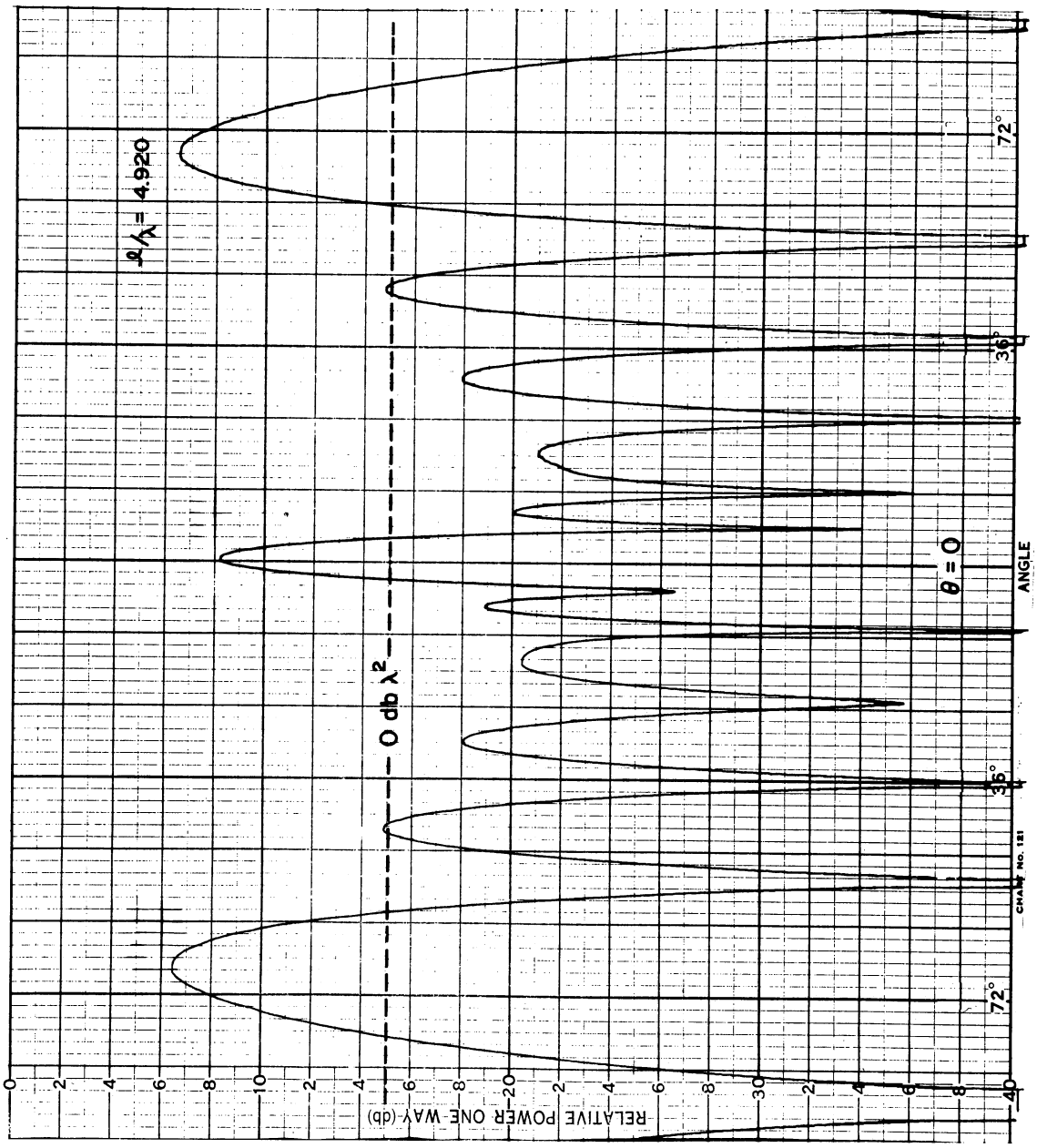
ℓ/λ = 4.920
0 db λ²
θ = 0
72°
36°
36°
72°
ANGLE
RELATIVE POWER ONE WAY (db)
0
2
4
6
8
10
2
4
6
8
20
2
4
6
8
30
2
4
6
8
40

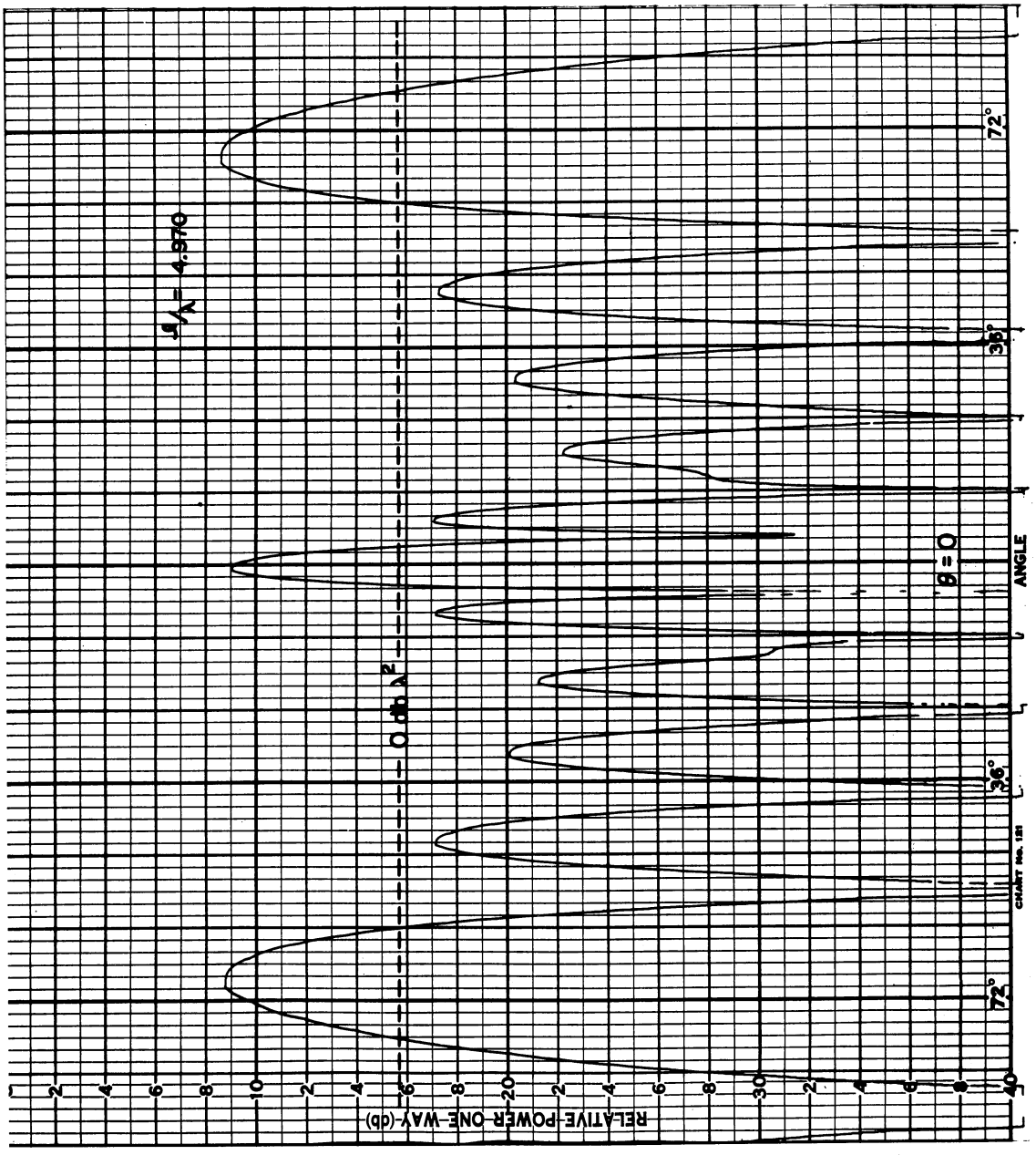
d/λ = 4.370
0 db
RELATIVE POWER ONE WAY (db)
72°
36°
θ = 0
ANGLE
36°
72°
CHART NO. 121

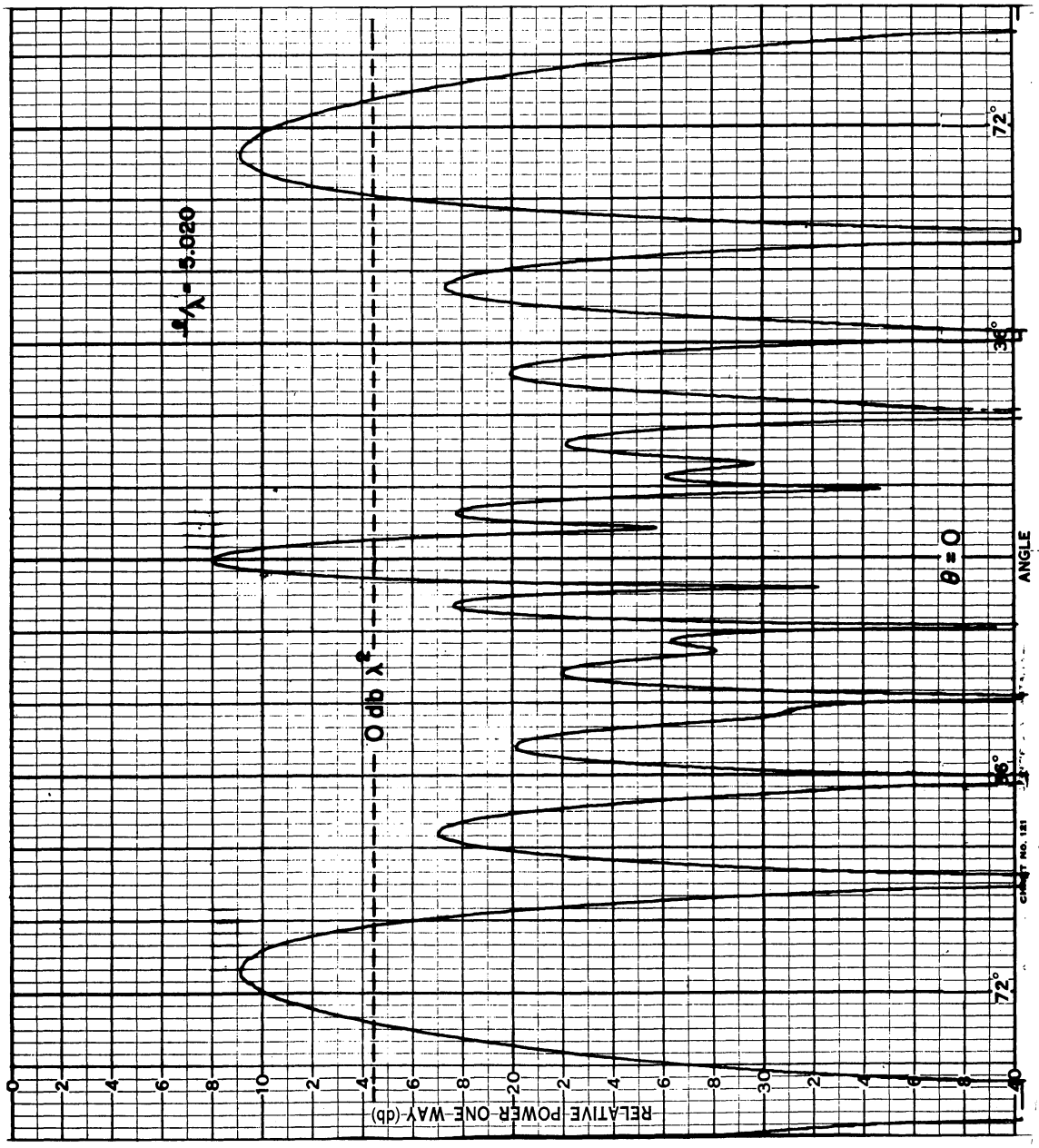
$\psi_1 - 5.020$
0 db
$\theta = 0$
72°
36°
36°
72°
ANGLE
RELATIVE POWER ONE-WAY-(db)
0 2 4 6 8 10 2 4 6 8 20 2 4 6 8 30 2 4 6 8 40

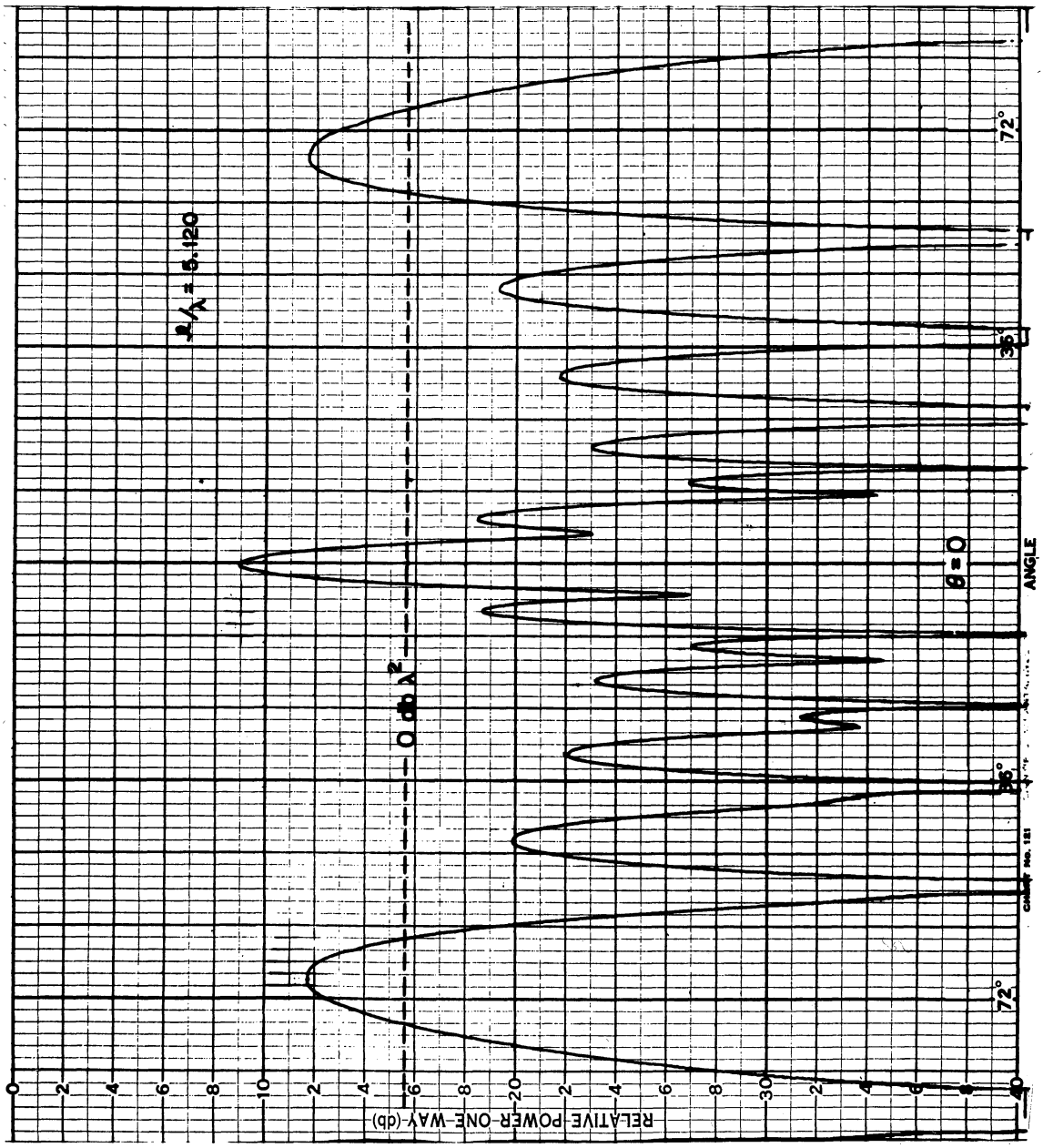
ℓ/λ = 6.120
0 db
θ = 0
72°
36°
36°
72°
ANGLE
RELATIVE POWER ONE-WAY (db)
0
2
4
6
8
10
2
4
6
8
20
2
4
6
8
30
2
4
6
8
40

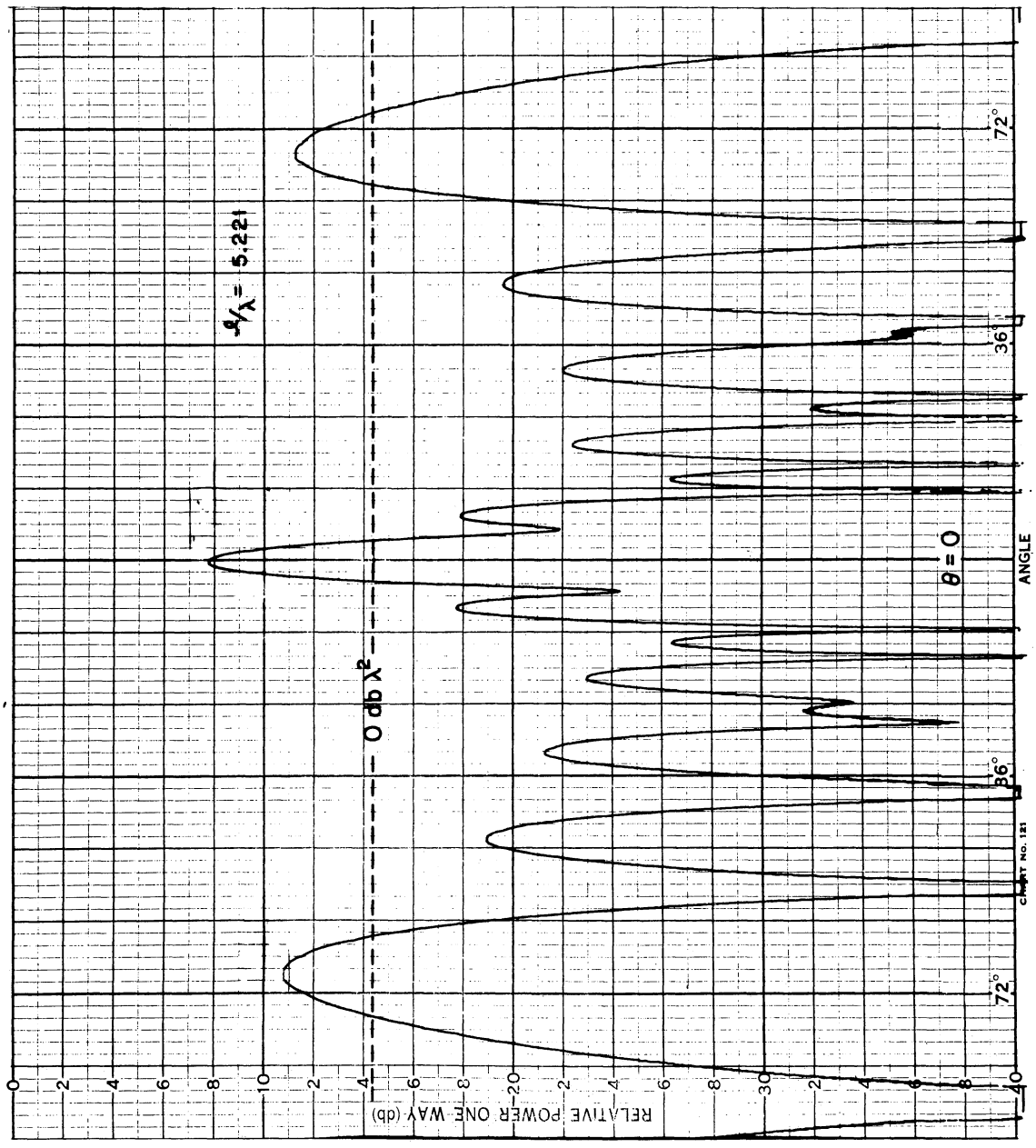
$\ell/\lambda = 5.221$
0 db λ^2
$\theta = 0$
72°
36°
36°
72°
ANGLE
RELATIVE POWER ONE WAY (db)
0
2
4
6
8
10
2
4
6
8
20
2
4
6
8
30
2
4
6
8
40

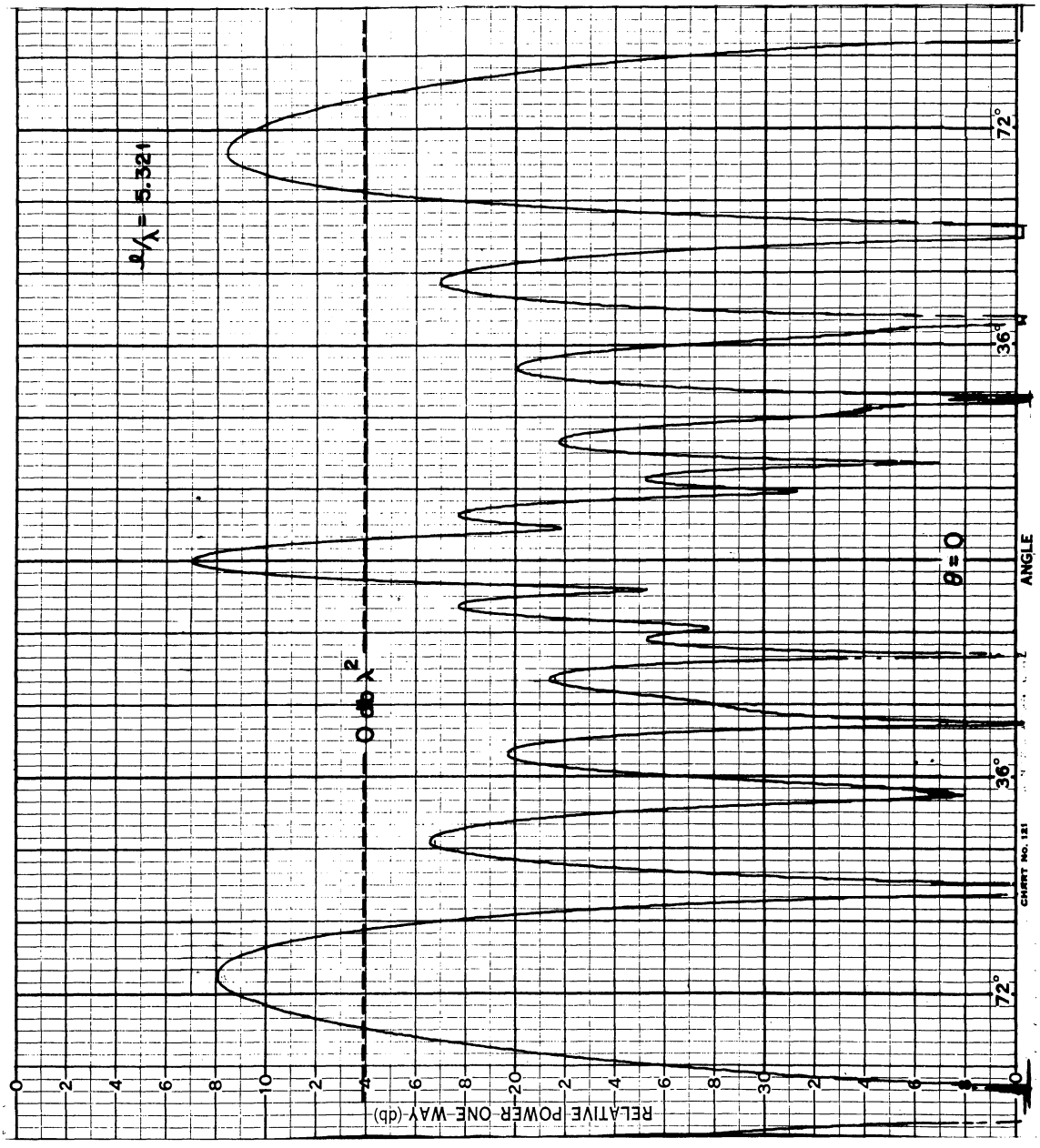
$\ell/\lambda = 5.321$
0 db
λ^2
$\theta = 0$
72°
36°
ANGLE
36°
72°
CHART NO. 121
RELATIVE POWER ONE-WAY (db)
0 2 4 6 8 10 2 4 6 8 20 2 4 6 8 30 2 4 6 0

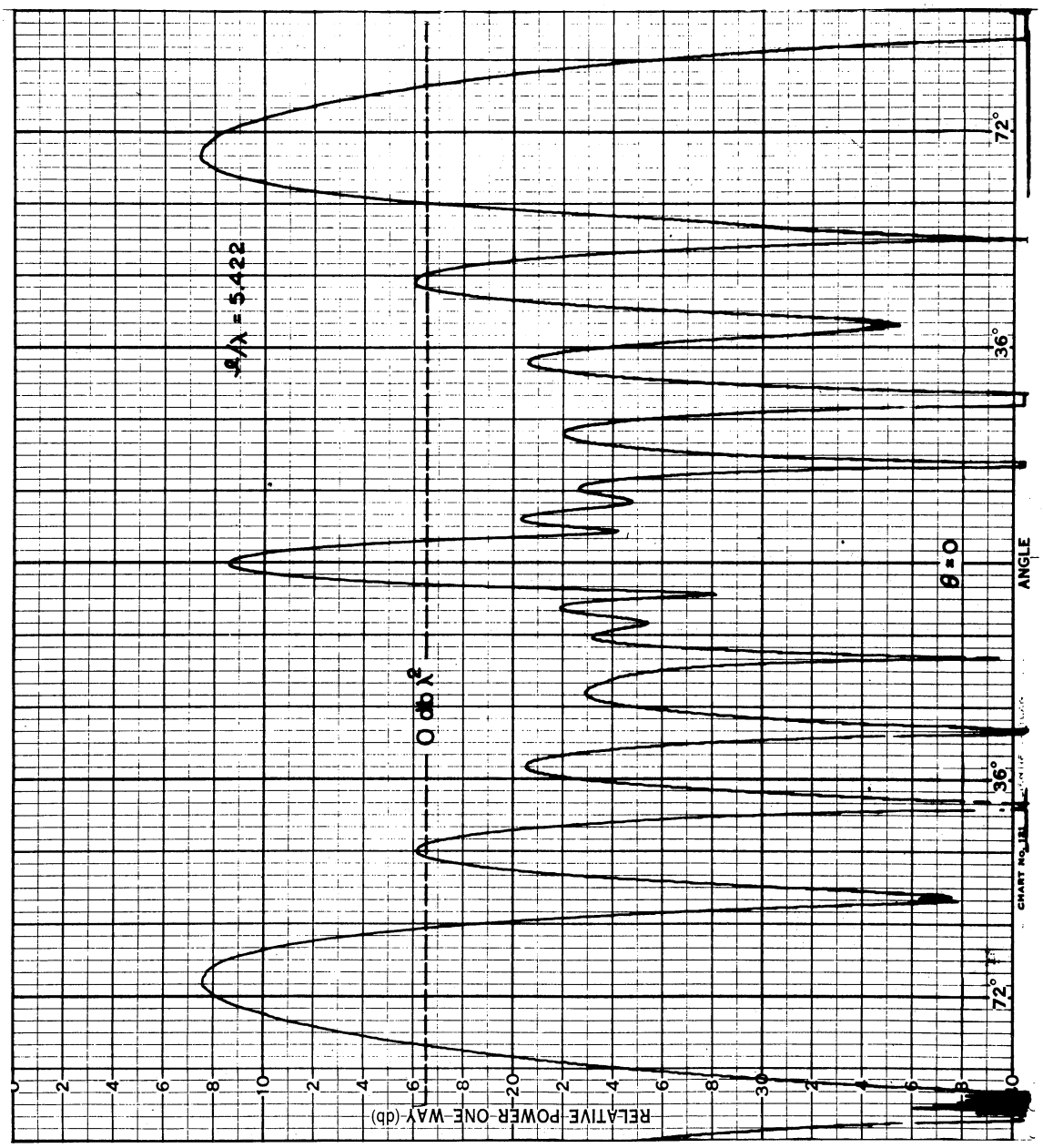
ℓ/λ = 5.422
0 db
θ = 0
72°
36°
36°
72°
ANGLE
RELATIVE POWER ONE WAY (db)

DISTRIBUTION LIST

Destination	Number of Copies
SEG (SEPIR) Wright-Patterson AFB, Ohio 45433	1
ASD (ASZB/C. Francus) Wright-Patterson AFB, Ohio 45433	1
AFAL (AVWE-2/William F. Bahret) Wright-Patterson AFB, Ohio 45433	2
AFML (MAYE/W. Frederick) Wright-Patterson AFB, Ohio 45433	1
HQ USAF (AFRDR/Colonel Lieber) Washington DC 20330	1
ADC (ADOAC-E) Ent AFB, Colorado 80912	1
ADC (ADOOA) Ent AFB, Colorado 80912	1
ADC (ADLPC) Ent AFB, Colorado 80912	1
AUL (9560) Maxwell AFB, Alabama 36112	1
Army Rocket and Guided Missile Agency ATTN: ORDXR-RF Redstone Arsenal, Alabama 35809	1
AFCRL (CRDG/R.B. Mack) L G Hanscom Field Bedford, Massachusetts 01730	1
ADC (AD4PL) L G Hanscom Field Bedford, Massachusetts 01730	1
U.S. Army Engineering Laboratories E.G. Linden, Materials Branch Electronic Parts and Materials Division Ft. Monmouth, N.J. 07703	1

Destination	Number of Copies
U.S. Electronics Command SIG-EL-RDR Ft. Monmouth, N.J. 07703	1
U.S. Army Engineering and Development Laboratories ATTN: E.J. York, Materials Branch Fort Belvoir, Virginia 22060	1
BSD Lt. J. Wheatley (BSD , BSYDP) Norton AFB, California 92409	1
Battelle Memorial Institute ATTN: G. Falkenbach, EE Division 505 King Avenue Columbus, Ohio 43201	1
Boeing Airplane Company ATTN: C.W. Mathis Jr. (3-7000) Wichita, Kansas 76210	1
Conductron Corporation Box 614 Ann Arbor, Michigan 48107	1
Cornell Aeronautical Laboratory ATTN: R.E. Kell 4455 Genesee Buffalo, New York 14221	1
DDC Cameron Station Alexandria, Virginia 22314	10
Harry Diamond Laboratories ATTN: ORDTL-012 Washington, D.C. 20438	1
ESD (ESLE) L G Hanscom Field Bedford, Massachusetts 01730	1
Emerson and Cuming, Inc. ATTN: E.F. Buckley 869 Washington Canton, Massachusetts 02021	1

Destination	Number of Copies
Evans Signal Laboratory ATTN: Orville C. Woodyard Belmar, New Jersey 07719	1
FTD (TDE-1a) Wright-Patterson AFB, Ohio 45433	2
General Dynamics/Fort Worth ATTN: Dr. C. Freeney Box 748 Fort Worth, Texas 76101	1
Goodyear Aerospace Corporation ATTN: F. Stimler 1210 Massillon Road Akron, Ohio 44315	1
Grumman Aircraft Engineering Department ATTN: J. Mockovciak Jr. Preliminary Design Bethpage, New York 11714	1
Jet Propulsion Laboratory - Technical Reports Sec. 4800 Oak Grove Drive Pasadena, California 91103	1
Lockheed Missiles and Space Company ATTN: D. Levine, Dept 65-50 P.O. Box 504 Sunnyvale, California 94088	1
A.D. Little, Inc. ATTN: J. Rothery 15 Acorn Park Cambridge, Massachusetts 02140	1
MIT - Lincoln Laboratory ATTN: J. Rheinstein Box 73 Lexington, Massachusetts 02173	1

Destination	Number of Copies
Whittaker Corporation Narmco R and D Division Security Office 3540 Aero Court San Diego, California 92123	1
U.S. Naval Research Laboratory ATTN: R. W. Wright Washington, D.C. 20390	1
NASA Scientific Technical Information Division Operations Section SAK/DL Box 33 College Park, Maryland 20740	1
NASA Headquarters (Code RV) Washington, D.C. 20546	1
Director NASA Ames Research Center Moffett Field, California 94035	1
Director NASA Flight Research Center P.O. Box 273 Edwards, California 93523	1
NASA Goddard Space Flight Center ATTN: F.O. Vonbun Greenbelt, Maryland 20771	1
NASA Manned Spacecraft Center ATTN: M. Kingsley, Apollo Project Office Box 1537 Houston, Texas 77058	1
Director NASA George C. Marshall Spaceflight Center Huntsville, Alabama 35812	1
NORAD (NPSD) Ent AFB, Colorado 80912	1
NORAD (NEEC) Ent AFB, Colorado 80912	1

Destination	Number of Copies
Office Assistant Secretary of Defense (R and D) Technical Library 3E1065 - Pentagon Washington, D.C. 20330	1
Ohio State University Research Foundation ATTN: Dr. L. Peters 1314 Kinnear Road Columbus, Ohio 43212	1
Rand Corporation ATTN: B. Potts 1700 Main Street Santa Monica, California 90406	1
RTD (RTTR) Bolling AFB, Washington 20332	1
A.S. Thomas, Incorporated ATTN: A.S. Thomas, President 355 Providence Highway Westwood, Massachusetts 02091	1
SAC (OA) Offutt AFB, Nebraska 68113	1
TAC (DORQ) Langley AFB, Virginia 23365	1
Ryan Aeronautical Company ATTN: Robert Giantvalley Lindbergh Field, Harbor Drive San Diego, California 92112	1
HQ USAF (AFCSA/Major Zetena) Washington, D.C. 20330	1
Northrup Corporation Norair Division ATTN: Mr. F. Oshiro 3901 W. Broadway Hawthorne, California 90250	1
SEG (SEAEP/Mr. Madden) Wright-Patterson Air Force Base, Ohio 45433	1

Destination	Number of Copies
Mitre Corporation ATTN: Dept D-82/Mr. Sussman Bedford, Massachusetts 01730	1
Advanced Research Projects Agency Ballistic Missile Defense ATTN: Mr. W.A. Van Zeeland Washington, D.C. 20330	1
HQ USAF (SAFRD/Mr. H. Davis) Washington, D.C. 20330	1
North American Aviation Inc. Space and Information Systems Division ATTN: Mr. S. Wozniak Hide Projects P.O. Box 8308 Tulsa, Oklahoma 74151	1
U.S. Army Aviation Material Laboratories ATTN: Mr. S. Pociluyko Fort Eustis, Virginia 23604	1
U.S. Army Electronics Research and Development Laboratory Combat Research Branch Fort Belvoir, Virginia 22060	1
NASA Manned Spacecraft Center ATTN: G. Gibson, Electrical Systems Branch Box 1537 Houston, Texas 77058	1
Goodyear Aerospace Corporation ATTN: G. H. Welsh, Dept. 474 (Wingfoot Lake) 1210 Massillon Road Akron, Ohio 44306	1
	74

UNCLASSIFIED
Security Classification

DOCUMENT CONTROL DATA - R&D

(Security classification of title, body of abstract and indexing annotation must be entered when the overall report is classified)

1. ORIGINATING ACTIVITY (Corporate author)	2a. REPORT SECURITY CLASSIFICATION
The University of Michigan Radiation Laboratory Department of Electrical Engineering Ann Arbor, Michigan 48108	UNCLASSIFIED 2b. GROUP

3. REPORT TITLE

MEASURED BACK SCATTERING CROSS SECTION OF THIN WIRES

4. DESCRIPTIVE NOTES (Type of report and inclusive dates)
Technical Report

5. AUTHOR(S) (Last name, first name, initial)

Seichoong Chang and Valdis V. Liepa

6. REPORT DATE	7a. TOTAL NO. OF PAGES	7b. NO. OF REFS
May 1967	102	10

8a. CONTRACT OR GRANT NO.	9a. ORIGINATOR'S REPORT NUMBER(S)
AF 33(615)-5170 b. PROJECT NO. 5546 c. Task 554601 d.	8077-4-T 9b. OTHER REPORT NO(S) (Any other numbers that may be assigned this report)

10. AVAILABILITY/LIMITATION NOTICES

Qualified requestors may obtain copies of this report from DDC, Cameron Station, Alexandria, Virginia 22314.

11. SUPPLEMENTARY NOTES	12. SPONSORING MILITARY ACTIVITY
	Air Force Avionics Laboratory Research and Technology Division AFSC Wright-Patterson Air Force Base, Ohio

13. ABSTRACT

A set of measured back scattering patterns is presented for a thin wire ($a/\lambda = 6.27 \times 10^{-3}$) for $\ell/\lambda = 0.3(0.025)0.55(0.05)1.60(0.10)5.42$, where a is the radius of the wire, ℓ is the length, and λ is the wavelength. The measurements were performed in our anechoic chamber at 2.370 GHz. From this set of patterns a number of curves has been extracted showing the amplitude and position of each back scattering lobe as a function of the wire length. These curves provide a convenient means of cross section estimation and may be used to reconstruct with reasonable accuracy the back scattering pattern for any value of $\ell/\lambda, \ell/\lambda \leq 5.42$.

DD FORM 1 JAN 64 1473

UNCLASSIFIED
Security Classification

14. KEY WORDS	LINK A		LINK B		LINK C	
	ROLE	WT	ROLE	WT	ROLE	WT
THIN WIRE BACK SCATTERING PATTERN RADAR CROSS SECTION EXPERIMENTAL DATA						

INSTRUCTIONS

1. ORIGINATING ACTIVITY: Enter the name and address of the contractor, subcontractor, grantee, Department of Defense activity or other organization *(corporate author)* issuing the report.

2*a*. REPORT SECURITY CLASSIFICATION: Enter the overall security classification of the report. Indicate whether "Restricted Data" is included. Marking is to be in accordance with appropriate security regulations.

2*b*. GROUP: Automatic downgrading is specified in DoD Directive 5200.10 and Armed Forces Industrial Manual. Enter the group number. Also, when applicable, show that optional markings have been used for Group 3 and Group 4 as authorized.

3. REPORT TITLE: Enter the complete report title in all capital letters. Titles in all cases should be unclassified. If a meaningful title cannot be selected without classification, show title classification in all capitals in parenthesis immediately following the title.

4. DESCRIPTIVE NOTES: If appropriate, enter the type of report, e.g., interim, progress, summary, annual, or final. Give the inclusive dates when a specific reporting period is covered.

5. AUTHOR(S): Enter the name(s) of author(s) as shown on or in the report. Enter last name, first name, middle initial. If military, show rank and branch of service. The name of the principal author is an absolute minimum requirement.

6. REPORT DATE: Enter the date of the report as day, month, year; or month, year. If more than one date appears on the report, use date of publication.

7*a*. TOTAL NUMBER OF PAGES: The total page count should follow normal pagination procedures, i.e., enter the number of pages containing information.

7*b*. NUMBER OF REFERENCES: Enter the total number of references cited in the report.

8*a*. CONTRACT OR GRANT NUMBER: If appropriate, enter the applicable number of the contract or grant under which the report was written.

8*b*, 8*c*, & 8*d*. PROJECT NUMBER: Enter the appropriate military department identification, such as project number, subproject number, system numbers, task number, etc.

9*a*. ORIGINATOR'S REPORT NUMBER(S): Enter the official report number by which the document will be identified and controlled by the originating activity. This number must be unique to this report.

9*b*. OTHER REPORT NUMBER(S): If the report has been assigned any other report numbers *(either by the originator or by the sponsor)*, also enter this number(s).

10. AVAILABILITY/LIMITATION NOTICES: Enter any limitations on further dissemination of the report, other than those imposed by security classification, using standard statements such as:

(1) "Qualified requesters may obtain copies of this report from DDC."

(2) "Foreign announcement and dissemination of this report by DDC is not authorized."

(3) "U. S. Government agencies may obtain copies of this report directly from DDC. Other qualified DDC users shall request through

_____."

(4) "U. S. military agencies may obtain copies of this report directly from DDC. Other qualified users shall request through

_____."

(5) "All distribution of this report is controlled. Qualified DDC users shall request through

_____."

If the report has been furnished to the Office of Technical Services, Department of Commerce, for sale to the public, indicate this fact and enter the price, if known.

11. SUPPLEMENTARY NOTES: Use for additional explanatory notes.

12. SPONSORING MILITARY ACTIVITY: Enter the name of the departmental project office or laboratory sponsoring *(paying for)* the research and development. Include address.

13. ABSTRACT: Enter an abstract giving a brief and factual summary of the document indicative of the report, even though it may also appear elsewhere in the body of the technical report. If additional space is required, a continuation sheet shall be attached.

It is highly desirable that the abstract of classified reports be unclassified. Each paragraph of the abstract shall end with an indication of the military security classification of the information in the paragraph, represented as *(TS)*, *(S)*, *(C)*, *or (U)*.

There is no limitation on the length of the abstract. However, the suggested length is from 150 to 225 words.

14. KEY WORDS: Key words are technically meaningful terms or short phrases that characterize a report and may be used as index entries for cataloging the report. Key words must be selected so that no security classification is required. Identifiers, such as equipment model designation, trade name, military project code name, geographic location, may be used as key words but will be followed by an indication of technical context. The assignment of links, rules, and weights is optional.